

Formation of PGE₂ in the tumor microenvironment and its impact on tumorigenesis

Dissertation

for attaining the PhD degree of Natural Sciences

submitted to the Faculty of Biochemistry, Chemistry and Pharmacy

of the Johann Wolfgang Goethe-University

in Frankfurt am Main

by

Weixiao Sha

from Beijing – PR China

Frankfurt am Main 2014

Accepted by the Faculty of Biochemistry, Chemistry and Pharmacy

Johann Wolfgang Goethe-University

Dean: Prof. Dr. Thomas Prisner

Referees:

Prof. Dr. Dieter Steinhilber

Prof. Dr. Bernhard Brüne

Date of the disputation:

“...There are known knowns; there are things we know that we know.

There are known unknowns: that is to say, there are things that we now know we don't know.

But there are also unknown unknowns – there are things we do not know we don't know.”

—Donald Rumsfeld, United States Secretary of Defense

Index

Index	1
List of figures	5
Abbreviations	7
1 Summary	11
2 Zusammenfassung	13
3 Introduction	18
3.1 Tumor development.....	18
3.1.1 Mutations generate abnormal cells.....	18
3.1.2 Immune escape fuels evolvement of cancers.....	20
3.1.3 Cancer as an immunological disease of ill-regulated inflammation	21
3.1.4 Experimental tumor models in vivo.....	22
3.1.5 Experimental tumor models in vitro	23
3.2 The anti-tumoral immune response	25
3.2.1 Phagocytes and their role in inflammation and anti-tumoral immunity	25
3.2.2 Immune cell crosstalk and anti-tumor T cell responses.....	26
3.2.3 Current aims and strategies in cancer therapies	29
3.3 Formation of PGE ₂	30
3.3.1 PGE ₂ synthesis.....	30
3.3.2 Stimulators of inducible PGE ₂	31
3.4 PGE ₂ down-stream signaling.....	32
3.4.1 EP receptor signaling.....	32
3.4.2 PGE ₂ supports tumor cell growth.....	32
3.4.3 PGE ₂ in the context of inflammation	33
3.4.4 Connection between PGE ₂ and tumor-associated mononuclear phagocytes	35
3.5 PGE ₂ and cancer	37

3.6	Aim of this study	40
4	Materials and Methods.....	41
4.1	Materials.....	41
4.1.1	Chemicals.....	41
4.1.2	Buffers and Solutions.....	41
4.1.3	Media and reagents for cell culture.....	41
4.1.4	Antibodies and cell dyes.....	42
4.1.5	Stimulants and Inhibitors	44
4.1.6	Cytokines.....	45
4.1.7	Kits and Ready-to-use solutions	45
4.1.8	Instruments.....	45
4.1.9	Software	46
4.1.10	shRNA plasmids	46
4.1.11	Oligonucleotides for qPCR	47
4.1.12	Cell lines.....	48
4.2	Methods.....	49
4.2.1	Cell Culture.....	49
4.2.2	Generation of stable mPGES-1 knockdown cells	49
4.2.3	Isolation of human PBMCs and culture of primary T cells	49
4.2.4	Cell proliferation assay	50
4.2.5	Generation and analysis of MCTS.....	50
4.2.6	Generation of necrotic cells	50
4.2.7	Quantitative PCR.....	50
4.2.8	Quantification of extracellular PGE ₂ via PGE ₂ EIA	51
4.2.9	Determination of prostanoids by Liquid Chromatography-Tandem Mass Spectrometry (LC-MS/MS).....	51
4.2.10	Flow Cytometry.....	51
4.2.11	MCF-7 tumor spheroid PBMC cocultures	53

4.2.12	T cell inhibition assay.....	53
4.2.13	Crossing and Genotyping of mice.....	54
4.2.14	Screening of PyMT tumors	55
4.2.15	Tissue isolation from PyMT mice and generation of single cell tumor suspensions.....	55
4.2.16	Statistical Analysis.....	55
5	Results.....	56
5.1	PGE ₂ and its role in prostate cancer cell spheroids.....	56
5.1.1	mPGES-1 supports MCTS formation of DU145 prostate cancer cells	56
5.1.2	COX-2 and mPGES-1 are both needed for spheroid formation-induced PGE ₂ production	57
5.1.3	Cell clustering induces COX-2 expression in prostate cancer cell lines.....	58
5.1.4	COX-2 and mPGES-1 inhibition impairs PGE ₂ production and MCTS growth.....	59
5.1.5	Glucose-deprivation, hypoxia and HIF-1 α accumulation fail to induce COX-2 mRNA in tumor spheroids	61
5.1.6	Necrotic cells induce COX-2 mRNA in DU145 cells	62
5.1.7	PGE ₂ impairs activation of cytotoxic T cells.....	65
5.2	Role of PGE ₂ in immunoediting.....	67
5.2.1	Human PBMCs cocultured with MCF-7 tumor spheroids require activation to maintain allogenic responses	67
5.2.2	LPS or LPS/IFN- γ upregulate CD80 expression of CD14 ⁺ CD11c ⁺ phagocytes to induce GrB ^{hi} CTLs	69
5.2.3	Activation of PBMCs with LPS triggers COX-2/mPGES-1-derived PGE ₂	71
5.2.4	PGE ₂ limits CD80 expression by activated CD14 ⁺ CD11c ⁺ phagocytes via EP2 signaling and accumulation of cAMP	74
5.2.5	mPGES-1-deficiency delays tumor development in vivo	76

5.2.6	Numbers of CD11c ⁺ TAMs are increased in tumors of mPGES-1 knockout PyMT mice	77
6	Discussion	81
6.1	Autologous PGE ₂ production by prostate cancer tumor spheroids	81
6.2	Pharmacological inhibition of PGE ₂ synthesis	81
6.3	Necrotic cells induced COX-2 expression in DU145 cells.....	82
6.4	Cell line-dependent PGE ₂ production	85
6.5	Therapy-induced PGE ₂	85
6.5.1	Phagocyte activation and prostanoid production	85
6.5.2	Shaping of phagocyte function by PGE ₂	86
6.6	Role of dead cells in immune activation.....	90
6.7	Therapeutic perspectives of PGE ₂ inhibition.....	91
7	Literature	95
8	Publications	104
9	Acknowledgements	105
10	Curriculum Vitae	106
11	Ehrenwörtliche Erklärung	107

List of figures

Figure 1:	Hallmarks of cancer.....	19
Figure 2:	Emerging hallmarks of cancer.	22
Figure 3:	Spheroids possesses features of avascular tumors.	24
Figure 4:	The B7 family and antigen presentation to T cells.....	27
Figure 5:	A scheme of a textbook anti-tumor response.	28
Figure 6:	PGE ₂ promotes cancer progression through the induction of tumor epithelial cell proliferation, survival, and migration and invasion.....	33
Figure 7:	Impact of PGE ₂ on cancer-associated mononuclear phagocytes.....	37
Figure 8:	shRNA targeting mPGES-1 mRNA efficiently reduced mPGES-1 mRNA levels.....	56
Figure 9:	mPGES-1 knockdown impaired tumor spheroid growth.	57
Figure 10:	COX-2 and mPGES-1 in tumor spheroids enables accumulation of PGE ₂	58
Figure 11:	Cell clustering induces COX-2 expression.....	59
Figure 12:	Celecoxib and DMC inhibited PGE ₂ production and growth of sh-control tumor spheroids.	60
Figure 13:	Spheroid formation does not affect expression of TNF- α or TGF- β 1 mRNA.....	61
Figure 14:	Glucose-deprivation, hypoxia and HIF-1 α stabilization fail to induce COX-2 mRNA expression.	62
Figure 15:	DU145 human prostate cancer cells were grown in monolayer cultures or as spheroids.	63
Figure 16:	NC but not NCM induces COX-2 expression and PGE ₂ synthesis.	64
Figure 17:	Necroptosis inhibitor necrostatin suppresses COX-2 induction during spheroid formation.....	65
Figure 18:	PGE ₂ in spheroid supernatants limits IFN- γ production by activated T cells.....	66
Figure 19:	PBMCs require activation to restrict tumor spheroid sizes and to induce GrB ^{hi} CTLs.	68
Figure 20:	Gating strategy for parallel discrimination of different T cell subsets and intracellular detection of their respective Granzyme B expression.	69

Figure 21:	Gating strategy to detect CD14 ⁺ CD11c ⁺ phagocytes.	70
Figure 22:	LPS or LPS/IFN- γ activation induces CD80 and inhibits CD206 expression on CD14 ⁺ CD11c ⁺ phagocytes.	70
Figure 23:	CD80 expression is needed for induction of GrB ^{hi} CTLs and tumor spheroid killing.	71
Figure 24:	MCF-7 cells do not upregulate COX-2 mRNA upon spheroid formation.	72
Figure 25:	LPS activation of PBMCs induces PGE ₂ production.	72
Figure 26:	C3 selectively inhibits synthesis of PGE ₂	73
Figure 27:	Inhibition of PGE ₂ production enhances CD80 expression on CD14 ⁺ CD11c ⁺ phagocytes.	74
Figure 28:	PGE ₂ inhibits CD80 and CD206 expression on CD14 ⁺ CD11c ⁺ phagocytes.	75
Figure 29:	EP2 signaling and upregulation of cAMP CD80 and CD206 expression on CD14 ⁺ CD11c ⁺ phagocytes.	75
Figure 30:	mPGES-1-deficiency impairs PyMT tumor growth.	76
Figure 31:	COX mRNA is expressed in PyMT tumors.	77
Figure 32:	mPGES-1-deficiency increases the abundance of F4/80 ⁺ CD11c ⁺ phagocytes in PyMT tumors.	78
Figure 33:	Gating strategy for discrimination of F4/80 ⁺ CD11c ⁺ phagocytes in PyMT breast tumors and detection of their respective polarization markers.	79
Figure 34:	Polarization markers of F4/80 ⁺ CD11c ⁺ macrophages in tumors and spleen of PyMT mice.	79
Figure 35:	mPGES-1-deficiency does not enhance CD80 expression of BMDM.	80
Figure 36:	BMDM shift prostaglandin profile.	80
Figure 37:	Overview: Stress-induced necrotic cells upregulate COX-2 and PGE ₂ in DU145 tumor spheroids.	84
Figure 38:	PGE ₂ suppresses CD80 expression of tumor-associated phagocytes to inhibit the anti-tumor response.	88
Figure 39:	PGE ₂ favors tumor growth by enforcing a chronic inflammatory microenvironment.	92

Abbreviations

15-PGDH	15-prostaglandin dehydrogenase
APC	adenomatous polyposis coli
APcells	antigen-presenting cells
AC	apoptotic cell
AA	arachidonic acid
BCG	<i>Bacillus Calmette-Guérin</i>
BMDM	bone marrow-derived macrophages
BSA	bovine serum albumin
CxB	celecoxib
CARs	chimeric antigen receptors
JNK	c-Jun N-terminal kinase
CD	cluster of differentiation
CM	conditioned medium
cDCs	conventional dendritic cells
cAMP	cyclic adenosine monophosphate
COX	cyclooxygenase
cPGES	cytosolic PGE synthase
CTL	cytotoxic T lymphocytes
CTLA-4	cytotoxic T-lymphocyte antigen 4
DAMPs	damage associated molecular patterns
DC	dendritic cells
DMSO	dimethylsulfoxide
DMEM	<i>Dulbecco's modified eagle medium</i>
ER	endoplasmatic reticulum
EIA	enzymatic immunosorbent assay
EGFR	epithelial growth factor receptor
EDTA	ethylene diamine tetra acetate
ERK	extracellular signal-regulated kinase

FCS	fetal calf serum
FMO	fluorescence minus one
FACS	fluorescence-activated cell sorting
GPCR	G-protein coupled receptors
GrB	granzyme B
GrB ^{hi}	GrB high
HMGB-1	high mobility box group 1
IDO	indoleamine 2,3-dioxygenase
ICER	inducible cAMP early repressor
IBD	Inflammatory bowel disease
IFN- α	interferon- α
IFN- γ	interferon- γ
LTB ₄	leukotriene B ₄
LLC	lewis lung carcinoma
LPS	lipopolysaccharide
M-CSF	macrophage colony-stimulating factor
M-CSFR	macrophage colony-stimulating factor receptor
MHC	major histocompatibility complex
MMTV	mammary tumor virus
mPGES-1	microsomal PGE synthase-1
mPGES-2	microsomal PGE synthase-2
MPL	monophosphoryl lipid A
sh-mPGES-1	mPGES-1 mRNA targeting small hairpin RNA
MUC-1	mucin-1
MCTS	multi-cellular tumor spheroids
MDSCs	myeloid-derived suppressor cells
Nec-1	necrostatin-1
NC	necrotic cells
NCM	necrotic cells conditioned medium

NSAIDs	non-steroidal anti-inflammatory drugs
NFκB	nuclear factor κ-light-chain-enhancer ¹ of activated B-cells
PRR	pattern-recognition receptors
PLA ₂	phospholipase A ₂
PMA	phorbol 12-myristate 13-acetate
PI3K	phosphatidylinositol 3-kinase
PS	phosphatidylserine
pDCs	plasmacytoid dendritic cells
PyMT	polyoma middle T antigen
PBS	potassium buffered saline
KCl	potassium chloride
PD-1	programmed cell death 1
PD-L1	programmed cell death 1 ligand 1
PGES	prostaglandin E synthase
PGE ₂	prostaglandin E2
EP	prostaglandin E2 receptor
PTGES	prostaglandin E2 synthase
PKA	protein kinase A
PKB	protein kinase B
PKC	protein kinase C
PSR	PS receptors
qPCR	quantitative real-time PCR
rVV	recombinant vaccinia virus
RPMI	<i>Roswell Park Memorial Institute</i>
sh-control	scrambled control shRNA
S1P	sphingosine-1-Phosphate
TCR	T cell receptor
T _H	T helper cells
TLR	toll-like receptors

TGF- β 1	transforming growth factor beta 1
TAA	tumor-associated antigens
TAMs	tumor-associated macrophages
TNF- α	tumor necrosis alpha
TiDC	tumor-induced DCs
VEGF	vascular endothelial growth factor

1 Summary

Tumor development usually follows predictable paths where tumor cells acquire common characteristics and features known as the hallmarks of cancer. Recently, additional characteristics have been added to these hallmarks since solid tumors are composed of a very heterogeneous population of transformed, formerly normal tissue cells and stromal cells, e.g. immune cells and fibroblasts. Compelling evidence suggests that stromal cells and tumor cells maintain a symbiotic relationship to build up the tumor microenvironment and to fuel tumor growth. In cancer therapies, common features of tumors such as unrestricted cell growth, suppression of immunological responses, and the ability to form new blood vessels (angiogenesis) have emerged as the main targets of interest. The lipid mediator prostaglandin E₂ (PGE₂) is known to promote all these features and thus, is connected to cancer progression in general. Its synthesis is triggered in response to stress factors or during inflammation. Inducible PGE₂ production relies on the enzymes cyclooxygenase 2 (COX-2) and microsomal prostaglandin E synthase 1 (mPGES-1), which are simultaneously expressed in response to a variety of different stimuli and are functionally coupled. Inhibition of COX-2 with non-steroidal anti-inflammatory drugs (NSAIDs) for cancer treatment is, however, limited by cardiovascular risks, since selective COX-2 inhibition disrupts the prostacyclin/thromboxane balance. Therefore targeting mPGES-1 downstream of COX-2 for PGE₂ inhibition was evaluated in this work in different steps of carcinogenesis. Knockdown of mPGES-1 in DU145 prostate cancer cells revealed that the mPGES-1 status did not affect growth of monolayer tumor cells, but significantly impaired 3D growth of multi-cellular tumor spheroids (MCTS). Spheroid formation induced COX-2 in DU145 and other prostate cancer spheroids. High levels of PGE₂ were detected in supernatants of DU145 MCTS as opposed to monolayer DU145 cells. Pharmacological inhibition of COX-2 and mPGES-1 confirmed the pivotal role of PGE₂ for DU145 MCTS growth. Besides promoting spheroid growth, MCTS-derived PGE₂ also inhibited cytotoxic T lymphocyte (CTL) activation. When investigating the mechanisms of COX-2 induction during spheroid formation, the typical tumor microenvironmental factors such as glucose deprivation, hypoxia or tumor cell apoptosis failed to enhance COX-2. Interestingly, when interfering with apoptosis in DU145 spheroids, the pan-caspase inhibitor Z-VAD-FMK triggered a

shift towards necrosis, thus enhancing COX-2 expression. Coculturing viable DU145 monolayer cells with isolated heat-shocked-treated necrotic DU145 cells, but not with necrotic cell supernatants, induced COX-2 and PGE₂, confirming the impact of necrosis for MCTS growth and CTL inhibition.

As mentioned, *in vivo* tumors are very heterogeneous mixtures of tumor cells and stromal cells e.g. immune cells. Hence, the interaction of the immune system with tumors was investigated in further experiments. When coculturing MCF-7 breast cancer spheroids with human peripheral blood mononuclear cells (PBMCs), only low levels of PGE₂ were detected, since MCF-7 cells did not upregulate COX-2 during spheroid formation and did not induce PGE₂ production by PBMCs. Under inflammatory conditions, by adding the toll-like receptor 4 (TLR4) agonist lipopolysaccharide (LPS) to cocultures, PGE₂ production was triggered, spheroid sizes were reduced, and numbers of high levels of granzyme B expressing (GrB^{hi}) CTLs were increased, while CD80 expression by tumor-associated phagocytes was also elevated. Inhibition of CD80 but not CD86 diminished numbers of GrB^{hi} CTLs and attenuated spheroid lysis. To determine the role of activation-induced PGE₂ production, use of the COX-2 inhibitor celecoxib and the experimental mPGES-1 inhibitor C3 further increased CD80 expression. Addition of PGE₂, the prostaglandin E2 (EP2) receptor agonist butaprost, and the phosphodiesterase 4 (PDE4) inhibitor rolipram reduced LPS/C3-triggered CD80 expression, confirming the impact of COX-2/mPGES-1-derived PGE₂ on shaping phagocyte phenotypes in an EP2/cAMP-dependent manner. In a spontaneous breast cancer model (MMTV-PyMT), mPGES-1-deficiency significantly delayed tumor growth in mice, confirming an overall pro-tumorigenic role of mPGES-1 in breast cancer development *in vivo*. However in tumors of mPGES-1^{-/-} mice, tumor-infiltrating phagocytes expressed low levels of CD80 similar to their wildtype counterparts. These data suggest that the immunosuppressive microenvironment does not allow for immunostimulatory effects by mPGES-1 inhibition without an activating stimulus. Evidences in this study recommend the application of mPGES-1 inhibitors for treating cancer diseases, since mPGES-1 promotes tumor growth in multiple steps of carcinogenesis, ranging from well-characterized effects of tumor cell growth to immune suppression of CTL activity and phagocyte polarization. Regarding the latter, blunting PGE₂ during immune activation may limit the tumor-favoring features of inflammation and improve the efficiency of TLR4 based immune therapies.

2 Zusammenfassung

Die klassische Onkologie beschäftigt sich mit der Fehlregulation von verschiedenen Signaltransduktionswegen in entarteten Zellen, sogenannten Tumorzellen, die zur Bildung von abnormalen Auswucherungen oder im engeren Sinne ‚Neoplasien‘ im Körper führen. Klassische chemotherapeutische Ansätze der neueren Generation sehen die spezifische Hemmung von fehlregulierten Signalwegen vor. Solide Tumore bestehen jedoch nicht nur aus entarteten Tumorzellen, sondern beinhalten eine Vielzahl nicht entarteter Stromazellen. Ein Großteil der Stromazellen besteht aus Immunzellen, die ursprünglich eingewandert sind um den Tumor zu bekämpfen, jedoch aufgrund vieler Faktoren die im Tumormikromilieu zugegen sind, eine symbiotische Beziehung zum Tumor eingehen und letztendlich das Wachstum des Gesamttumors fördern. Die mechanistischen Gründe zur Bildung von Tumorzellen wie z.B. genetische Prädisposition oder Umwelteinflüsse mögen somit vielfältig sein, jedoch besitzen sie sehr gleichartige charakteristische Kennzeichen, die sogenannten ‚Hallmarks of Cancer‘ (Merkmale/Kennzeichen von Krebs), welche den Weg ihrer Entwicklung erstaunlich präzise vorzeichnen. Die bedeutendsten therapeutisch relevanten Merkmale von Krebszellen sind die Fähigkeiten zur ungehemmten Zellteilung, Bildung von neuen Blutgefäßen (Angiogenese) und Hemmung des Immunsystems, das für die Abstoßung des Tumors verantwortlich ist. Vor allem Letzteres ist Fokuspunkt vieler neuartiger therapeutischer Ansätze, die das Ziel verfolgen, das Immunsystem zu reaktivieren und dazu anzuleiten Tumore effektiv zu bekämpfen. Das Lipid Prostaglandin E₂ (PGE₂) gehört mitunter zu den tumorrelevanten Faktoren, die die oben genannten Prozesse regulieren und wird auch mit Tumorerkrankungen in Verbindung gebracht. Die Synthese von induzierbarem PGE₂ in Entzündungsreaktionen erfolgt im ersten Schritt durch Cyclooxygenase 2 (COX-2), die aus Arachidonsäure PGH₂ bildet. Im folgenden Schritt sorgt die Isomerase mikrosomale Prostaglandin E₂ Synthase 1 (mPGES-1) für die Umwandlung von PGH₂ in PGE₂. Die Hemmung der COX mit nicht-steroidalen Anti-Rheumatika (NSAID) wird zur Behandlung von entzündungsvermittelten Krankheiten klinisch eingesetzt und zeigte auch Wirkung bei der Bekämpfung von Tumorerkrankungen, die oftmals aus entzündlichen Prozessen heraus entstehen oder Entzündungsreaktionen selbst induzieren. Leider führt die selektive COX-2 Hemmung zu einer Fehlregulierung der Balance zwischen Thromboxanen und

Prostazyklinen und somit zu Gerinnungsstörungen und damit verbundenen kardiovaskulären Nebenwirkungen, weswegen mPGES-1 zur selektiven Hemmung von PGE₂ pharmakologisch an Bedeutung gewonnen hat. In dieser Studie wird die Rolle der mPGES-1 in verschiedenen tumorrelevanten Prozessen evaluiert, um die Hypothese zu überprüfen ob eine therapeutische Anwendbarkeit von mPGES-1 Inhibitoren bei der Therapie von Tumorerkrankungen empfehlenswert ist. Neben klassischen etablierten Tumormodellen wie zum Beispiel der zweidimensionalen Kultivierung von humanen Tumorzelllinien in der Zellkulturschale und der Anwendung eines spontanen Brustkrebsmodells in der Maus, werden in der Arbeit auch dreidimensionale Experimentaltumore in der Zellkultur, sogenannte multizelluläre Tumorsphäroide (MCTS), beschrieben. Diese MCTS ähneln vom Aufbau her avaskulären Tumoren und stellen ein überlegeneres Mittel zur Untersuchung von Tumorerkrankungen im menschlichen System dar, da sie einen Kompromiss zwischen leicht einsetzbaren 2D Tumorzellkulturen und hochkomplexen Mausmodellen darstellen. Somit ist die MCTS Kultur auch die komplexeste und authentischste Methode, um die Tumorentwicklung im humanen System zu untersuchen. Überraschenderweise beeinflusste das Ausschalten der mPGES-1 in 2D-Kulturen von DU145 Prostatakrebszellen das Tumorzellwachstum nicht, aber signifikant das Wachstum dieser Zellen als 3D-Kultur. Dies hatte zur Ursache, dass bei der Aggregation von Zellen in Prostatakrebszelllinien COX-2 induziert wird und somit die Expression von mPGES-1 dann erst funktionell relevant wird. Während 2D-Kulturen von DU145 Zellen minimale Konzentrationen an PGE₂ akkumulierten, verzeichneten MCTS aus DU145 Kontrollzellen mit funktionalem mPGES-1 einen erhöhten Gehalt an PGE₂ im Überstand. Die effektive Ausschaltung von mPGES-1 wiederum verhinderte die PGE₂ Produktion fast komplett. Dies hatte zur Folge dass in mPGES-1-defizienten MCTS Kulturen gleich hohe PGE₂ Mengen wie in 2D-Kulturen gefunden wurden. Die pharmakologische Inhibition von COX-2 und mPGES-1 in MCTS führte in den Kontrollzellen ebenfalls zur Hemmung der PGE₂-Produktion und verlangsamte das Wachstum von MCTS. Um die zugrunde liegenden Mechanismen der COX-2 Induktion in DU145 MCTS zu ergründen, wurden die Einflüsse von bekannten Faktoren des Tumormikromilieus auf die COX-2 Expression untersucht. Es zeigte sich aber, dass Glukoseentzug, Hypoxie und auch die Tumorzellapoptose jeweils nicht die Ursache für das Phänomen darstellten. Interessanterweise konnte jedoch festgestellt werden, dass die Beeinflussung der

Apoptose in MCTS durch Einsatz des pan-caspase Inhibitors Z-VAD-FMK eine Verlagerung des Zelltodes von der Apoptose in Richtung Nekrose begünstigte, die mit einer gleichzeitigen Erhöhung der COX-2 Expression einherging. Die Kokultivierung von DU145 2D-Kulturen mit isolierten hitzeschock-behandelten nekrotischen Tumorzellen konnte dann schließlich bestätigen, dass die Anwesenheit von nekrotischen Zellen, nicht jedoch lösliche Faktoren aus deren Überstand, nötig war um die COX-2 Expression und PGE₂ Produktion zu induzieren. Zusätzlich konnte in dieser Studie noch nachgewiesen werden dass PGE₂ von MCTS Überständen die Aktivierung von cytotoxischen T Lymphozyten (CTL) hemmt. Damit hat die Nekrose in MCTS eine doppelte Wirkung: Durch die Induktion von PGE₂ fördert sie das Tumorwachstum und gleichzeitig schützt sie den Tumor vor der Zerstörung durch CTL.

Zellen des peripheren Blutes (PBMCs) wurden zusammen mit MCTS von MCF-7 Brustkrebszellen kokultiviert, um Interaktionen des Immunsystems mit dem Tumor zu untersuchen. Es konnte kein erhöhter Gehalt an PGE₂ in den Kokulturen gefunden werden, was darauf zurückzuschließen war dass MCF-7 Brustkrebszellen bei der Sphäroidbildung COX-2 nicht hochregulieren und ebenfalls keine PGE₂ Produktion durch PBMCs provozieren. Unter inflammatorischen Bedingungen nach Einsatz von Toll-like Rezeptor 4 (TLR4) Liganden Lipopolysaccharid (LPS) wurde die PGE₂ Produktion von PBMCs aktiviert und gleichzeitig war eine Verringerung des Sphäroiddurchmessers in diesen Kokulturen zu beobachten. Mit der LPS-Aktivierung wurde eine erhöhte Anzahl an Granzym B hoch exprimierenden (GrB^{hi}) CTL detektiert, während die CD80 Expression der tumor-assoziierten Phagozyten ebenfalls erhöht war. Die Inhibition von CD80, nicht jedoch CD86, wiederum reduzierte die Anzahl an GrB^{hi} CTL in aktivierten Kokulturen und verlangsamte die Zerstörung der Tumorsphäroide. Der Einsatz des COX-2 Inhibitors Celecoxib oder des experimentellen mPGES-1 Inhibitors C3 konnte die Expression des anti-tumoral relevanten CD80 Moleküls signifikant erhöhen. Trotz der unterschiedlichen Prostaglandin-Profile, bot die unspezifische Hemmung aller Prostaglandine mit Celecoxib der spezifischen Hemmung von PGE₂ mit C3 gegenüber keinerlei Vorteile, da die induzierte CD80 Expression zwischen beiden Vergleichsgruppen keinen signifikanten Unterschied zeigte. Durch die Zugabe von PGE₂ oder von Prostaglandin E2 Rezeptor (EP2) Agonisten Butaprost wurde die CD80 Expression nach LPS/C3-Aktivierung gehemmt. Die EP2 Aktivierung führt zur Erhöhung des

intrazellulären zyklischen Adenosinmonophosphat (cAMP)-Spiegels, dessen Abbau wiederum durch das Enzym Phosphodiesterase 4 (PDE4) erfolgt. Die Inhibition von PDE4 durch Rolipram führt zur Erhöhung des cAMP Spiegels und sorgte für eine Inhibition der CD80 Expression in LPS/C3 aktivierten PBMC MCTS Kokulturen. Zusammengefasst lassen die Erkenntnisse darauf schließen dass das durch die COX-2/mPGES-1 gebildete PGE₂ die CD80 Expression bei der Phagozytenaktivierung über EP2/cAMP hemmt. Dieser Mechanismus war jedoch nur im Kokulturmodell zu beobachten, während in aktivierten Knochenmarksmakrophagen mPGES-1 nicht die Expression von CD80 beeinflusste. Die Anwendung des Kokulturmodells ist somit für die Beschreibung von immunologischen Fragestellungen den der Makrophagenmonokultur überlegen, da sie komplexe Zellinteraktionen zwischen Phagozyten, T Zellen und Tumorzellen ermöglicht, die wiederum die Feinregulierung von immunologisch relevanten Vorgängen zulassen.

Im spontanen murinen Brustkrebsmodell (MMTV-PyMT) konnte dann festgestellt werden dass mPGES-1^{-/-} PyMT Mäuse eine verlangsamte Tumorentwicklung aufweisen. Interessanterweise wurde eine erhöhte Anzahl an tumor-assoziierten Phagozyten in mPGES-1^{-/-} PyMT Tumoren gefunden, die auch gleichzeitig die dominante Immunzellpopulation im Tumor darstellten. Eine weitere Unterteilung dieser F4/80⁺ Phagozyten in CD11c⁺ Dendritische Zellen-ähnliche sowie CD11c⁻ Makrophagen-ähnliche Subtypen stellte heraus dass verglichen zum Wildtyp auch diese Zellsubtypen jeweils in größerer Anzahl in Tumoren mPGES-1^{-/-} PyMT Mäuse vorzufinden waren. Tatsächlich ist die massive Einwanderung von Tumor-assoziierten Makrophagen ein vielbeobachtetes Phänomen in soliden Tumoren und wird bei Brustkrebspatienten in der Regel mit einer schlechten Prognose assoziiert. Die Korrelation eines verzögerten Tumorwachstums in mPGES-1^{-/-} PyMT Mäusen deckt sich also nicht mit einer erhöhten Infiltration Tumor-assoziiierter Phagozyten, was die Hypothese zuließ dass diese Phagozyten einen anderen Phänotyp besitzen als in Wildtyp Mäusen. In den Experimenten des Kokulturmodells wurde gezeigt dass die für die anti-tumorale Antwort notwendige Expression von CD80 durch mPGES-1/PGE₂ reguliert wird. Um die Stärke einer Immunantwort in den PyMT Mäusen zu ermitteln, wurde die CD80 Expression von Tumor-assoziierten Phagozyten in Tumorgewebe und der Milz untersucht. Interessanterweise exprimierten Tumor-assoziierte Phagozyten unabhängig vom mPGES-1 in etablierten PyMT Tumoren generell minimale Mengen an CD80- in etwa im gleichen Umfang

dem nicht-stimulierten Knochenmarksmakrophagen entsprechend. Ohne immunaktivierende Substanzen ist die Abwesenheit von mPGES-1 nicht ausreichend, um das stark immunhemmende Milieu in PyMT Tumoren zu überwinden. In fortführenden in vivo PyMT Studien sollte deshalb evaluiert werden, ob die mPGES-1-Defizienz im immunstimulierenden Kontext unter Einsatz von therapeutischen TLR-Agonisten Relevanz hat und die Kombination von mPGES-1-Inhibitoren mit TLR-Agonisten sollte in Wildtyp PyMT Mäusen diskutiert werden. Die Ergebnisse deuten daraufhin, dass mPGES-1 in diesem Model das Tumorwachstum eher durch klassische Parameter beeinflusst wie z.B. Tumorzellproliferation und Angiogenese. Nicht nur im Zusammenhang mit klassisch onkologischen Parametern kann die selektive Hemmung von PGE₂ wertvoll sein, sondern auch eine Kombination mit immunaktivierenden Substanzen wie z.B. TLR-Agonisten ist therapeutisch denkbar, um aktivierungsvermittelte Entzündungsreaktionen auszuschalten, die sonst tumorförderlich sein könnten und den Erfolg der Therapie beeinflussen würden. Die Anwendung von mPGES-1-Inhibitoren zur selektiven Hemmung von PGE₂ bei der Krebstherapie wird anhand der Daten dieser Studie empfohlen und würde eine risikominimierte Alternative zu nicht-steroidalen Anti-Rheumatika darstellen. Die Kontrolle von Entzündungsreaktionen ist somit der Schlüssel der zukünftigen Krebstherapie.

3 Introduction

Since 2008, more than 400,000 new cancer patients are registered annually in Germany. One half of these patients are destined to die from the disease, which is the fourth most common cause of death in the country and also worldwide in modern western nations (www.dkfz.de/krebsinformationsdienst). Many patients even harbor undiscovered not outgrowing tumors, so-called occult tumors, controlled by the immune system, which are accidentally discovered when these patients seek medical attention because of other diseases (1). High cancer incidents in the western countries have many origins: genetic predisposition, bad life style choices, and high life expectancy. The mechanisms how cancers arise are manifold and depend on the affected entity, the original cell type of cancerous cells, and the environmental niche where the original tumor can prosper. Modern chemotherapy deals with specific inhibition of characteristic cancer-related signaling pathways. However, outgrown cancers are highly heterogeneous in their composition, making it difficult to find specific targets for the whole population. Some investigators even suggested abandoning of the traditional view of tumors as clonal monocultures of cancer cells but rather seeing them as developing organs, which enables classification and treatment of cancers by their microenvironmental composition (2). The immune system is fairly capable of restricting tumors, but fails to do so due to the interplay of different tumor microenvironmental factors causing ineffective immunological control of tumors. Out of the same reasons, reactivation of the immune system has emerged as one of the most challenging tasks of modern cancer therapy, since immune therapeutics often lack efficiency in vivo or trigger autoimmune reactions. Hence, understanding how the tumor microenvironment affects the immune system will help to find treatments for effective reactivation of the immune system.

3.1 Tumor development

3.1.1 Mutations generate abnormal cells

When referring to tumors, often solid tumors are meant, neglecting the existence of 'wet' tumors such as leukemia without localized tissue structures. Tumors or neoplasms are tissues consisting of abnormal cells and can be divided into two major

subclasses- the benign and malignant tumors. While the former is localized and not transformed to a cancer yet, the latter is able to invade and destroy surrounding tissues, and is also commonly called cancer. Tumor cells of different entities possess characteristic mutational signatures or share common ones, which originate from age, UV-exposure or tobacco smoke (3). The majority of mutations is of somatic nature, widely random, and regularly leads to loss of function- the so-called non-sense mutations. With few exceptions, random nonsense mutations result in loss of function, increased overall cell entropy, and forces mutated cells into programmed cell death. Occasionally, mutations result in gain of functions, which is also one of the driving factors of the evolutionary development of organisms (4-5). However, a gain of function does not necessarily imply a newly acquired functionality benefitting surrounding cells besides the mutated cell. Usually, these new cell features are exclusively beneficial for the mutated cell itself but prove to be highly detrimental for the whole organism. As a matter of fact, abnormal cells are usually depleted by the immune system. Therefore, these cells have to compensate more drawbacks by selectively developing traits such as resistance to cell death and growth suppressors, unrestricted proliferation, induction of angiogenesis and metastasis (Figure 1).

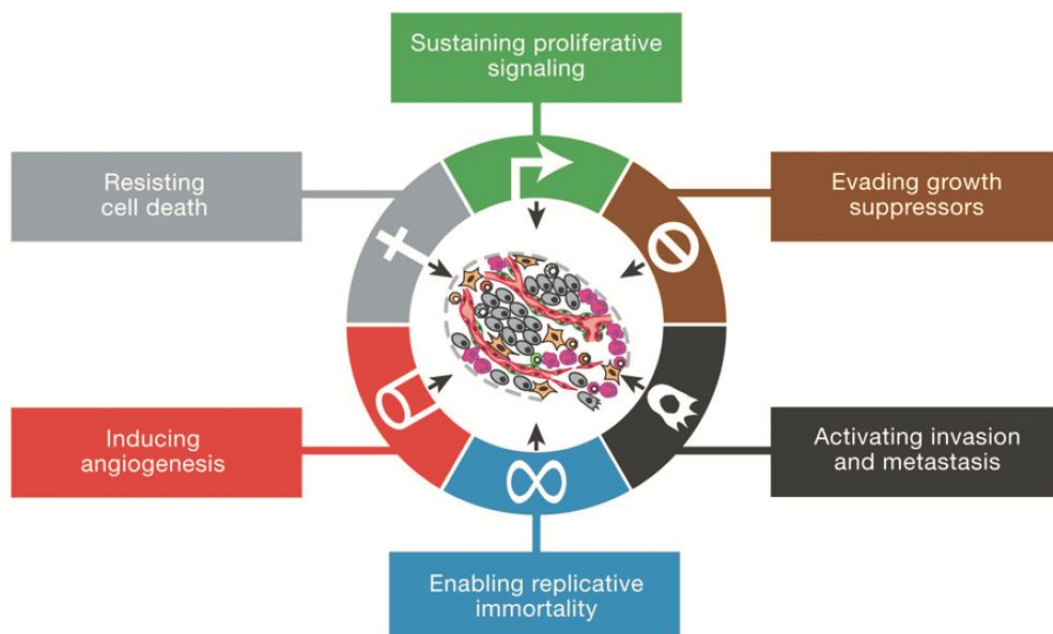


Figure 1: Hallmarks of cancer. Classical cancer traits known as hallmarks of cancer include unrestricted proliferation, immortality, induction of angiogenesis, resistance to cell death and growth suppressors, and activation of metastasis (6).

These specific features/traits are defined as hallmarks of cancer, as reviewed by Weinberg and Hanahan (6). It seems to be an irony of life that mutated tumor cells with their truncated, doubled, incomplete, and/or rearranged genetic materials are not more vulnerable but paradoxically more adapted to the environmental cues than their normal counterparts (4). The traditional darwinistic explanation of tumor development does not suffice considering that cancers are able to acquire their hallmarks within months. However, non-traditional views claim that cancer cells built-up their microenvironment e.g. their stromal cell composition and characteristic microenvironmental factors, which vice-versa shapes the tumor cell itself constructing a mutual relationship. Indeed, breast cancer cells transferred into normal mammary glands are able to proliferate and contribute to mammary gland development without forming tumors (7). In principle, both views do not exclude each other and may be complementally applied for the understanding of cancer development.

3.1.2 Immune escape fuels evolvement of cancers

Tumors are not only built out of mutated tumor cells, but are highly heterogenic structures composed of tumor cells and non-mutated stromal cells, e.g. immune cells. Besides protection of the host from 'non-self' and otherwise harmful pathogens, one of the main tasks of the immune system is to detect and to destroy mutated cells, which are declared as 'altered-self' (8). As mentioned, escape of abnormal cells from the immunological control requires effort, because eluding the restrictive chains of the collective demands mutated cells to acquire additional hallmarks through mutations and natural selection, which they do not possess in the first place (6). By more and more giving up their original form, tumor cells are more prone to be detected by the immune system due to these 'altered-self' changes. This additional evolutionary pressure provided by the immune system constantly creates a vicious circle, when tumor cells have to evolve in an even faster pace in order to escape immunological control (5). In fact, cancers may arise out of many random reasons, but once transformed, the development of abnormal cells into cancers follows a frighteningly predictable path with the acquisition of different hallmarks of cancer and ending with metastasis formation, which in most cases is lethal for the patient.

3.1.3 Cancer as an immunological disease of ill-regulated inflammation

Traditional oncology concentrates on abnormal behavior and unconstrained signaling of tumor cells. In the past decade, oncology has moved one step closer towards immunology, since the paradigm has shifted from treating the roots of cancer e.g. abnormal cell signaling to more macroscopic immunological approaches, which focuses on how to activate the natural ability of the immune system to restrict tumors. Besides abnormal tumor cells, stromal cells play an important role in the development of cancers (9). Among them, tumor-infiltrating immune cells, migrated towards the tumor site and designated to mediate anti-tumoral effects, are reprogrammed by tumor environmental factors to promote wound-healing responses such as angiogenesis, thus favoring tumor growth (10). The traditional tumor staging and prediction of clinical outcomes includes the parameters tumor burden (T), presence of cancer cells in draining lymph nodes (N) and evidence for metastasis (M)- the so-called 'TNM-parameters'. However, the classical TNM-classification has limited prognostic value and does not predict response to therapy. Recently, a new classification parameter for scoring cancer disease severity was suggested, claiming that immunophenotyping of tumors may provide more accurate prognostic informations and therapy strategies (11). A crucial parameter known to regulate immune cell features is immune cell activation-induced inflammation. The lack of fine-tuning during inflammatory responses is disastrous for the patients, since chronic inflammation is known to favor tumor growth, whereas anti-inflammatory signaling terminates immune activation (8,12). Therefore, additional cancer features added to the classical hallmarks of cancer include tumor-promoting inflammation and evasion of immune destruction (Figure 2) (6). The word tumor per se means swelling in latin, which is also described as a feature of inflammation (rubor-redness, tumor-swelling, calor-heat, dolor-pain) and the early development of tumors can be described as a process of unresolved chronic inflammation apparent in all tumors (8,13). The inflammatory environment in the inflammatory bowel disease (IBD) for example promotes colorectal cancer formation (14), whereas autoimmunity and inflammation in females seem to increase cervical but reduce ovarian and breast cancer risks (15). Inflammation itself implicates two processes. Early on, acute inflammation is needed for destruction of harmful structures invading the host organism. When pathogens

elude immunologic control, a state of chronic inflammation is established, activating pro-tumorigenic processes such as wound-healing conditions. The balance of these two processes also defines the outcome of an immunological response. While tumors exploit this system by shifting the balance to the latter, therapy approaches should focus on redirecting the balance to the former. Thus, cancer diseases can be seen as ill-regulated immune/inflammatory responses and careless dealing with the ‘double-edged sword’ inflammation, especially in the context of immunotherapies, will not only result in non-responsiveness of the therapy itself, but may also be highly detrimental for the patient, when therapy-inflicted inflammation backfires to induce tumor promoting features (16).

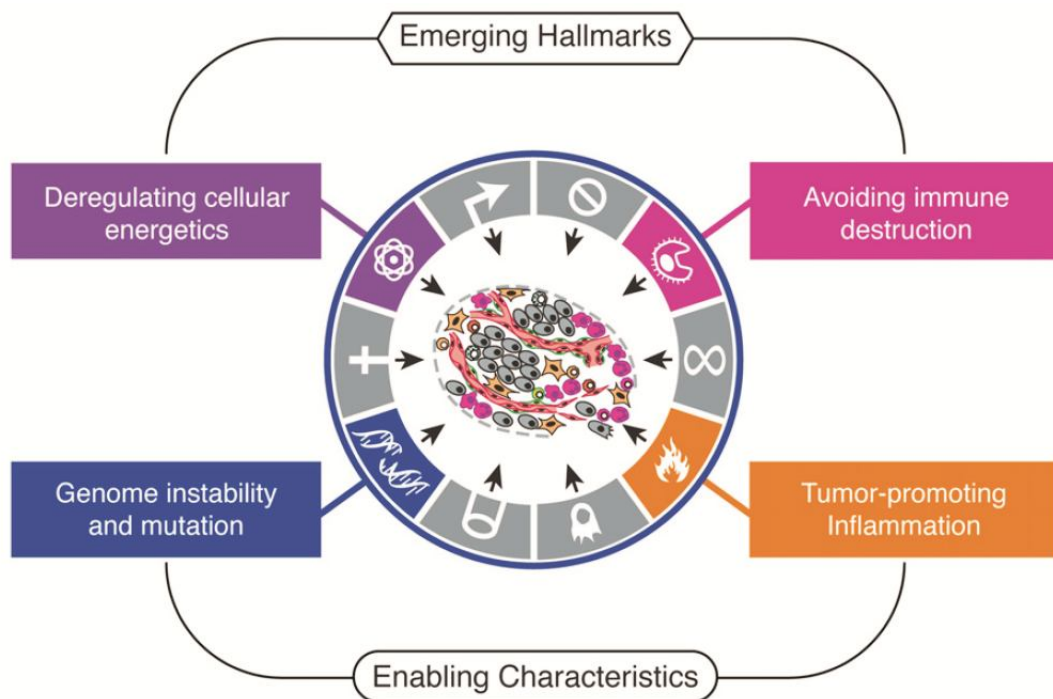


Figure 2: Emerging hallmarks of cancer. Newly added hallmarks involve impaired metabolism, genome instability, resistance to immune destruction and tumor-promoting inflammation (6).

3.1.4 Experimental tumor models in vivo

The need for studying cancer as a disease has prompted investigators to use experimental tumor models. Preclinical research starts with the use of authentic tumor models to discuss problems emerging in cancer diseases. Use of animal models is still the gold standard and a plethora of different animal models exist to study tumor growth in vivo. By far the most prominent one is the use of mouse models (17). Common techniques to generate tumors in mice are tumor grafts,

(chemically) induced tumor models or spontaneous transgenic tumor models. Grafts are tissues of e.g. murine or human cells transplanted into mice to differentiate tumorigenic effects of grafted cells from their host environment. Chemically induced tumors involve use of tumorigenic substances such as polycondensated aromatic structures acting as carcinogens. Both methods give the investigator a high degree of freedom in terms of their experimental planning, but suffer from their artificial nature, whereas spontaneous tumor models reflect more accurately authentic tumor development, but face greater handling and timing problems. The choice of the right animal model for different study approaches highly depends on the aim of the respective project- their advantages and drawbacks are reviewed by Richmond et al. in 2008 (17). One spontaneous tumor model used in my thesis is the mammary tumor virus (MMTV)-polyoma middle T antigen (PyMT) model, where mice express the PyMT oncogene under the control of the MMTV-promotor, which provokes formation of mammary carcinoma in female PyMT mice (18). PyMT mice undergo four distinct stages in tumor progression ranging from premalignant to malignant stages followed by a high frequency of metastasis, making the model a good fit to study human breast cancer development in vivo (19).

3.1.5 Experimental tumor models in vitro

Besides in vivo studies, in vitro models are financially more feasible for many laboratories. Immortalized cell lines have been easy accessible tools for cancer research in the past decades. They derive from primary tumor cells isolated out of cancer patients and can be maintained in the cell culture. The most common tool in oncology is to culture tumor cell lines as monolayers in cell culture flasks. With the evolution of advanced flow cytometric techniques, use of complex tumor models has become more feasible. Next generation tumor models include generation of three-dimensional experimental tumors out of tumor cell lines, so-called multi-cellular tumor spheroids (MCTS) or spheroids for short (20). Spheroids possess characteristic features of avascular solid tumors, with a high proliferating outer border and an inner core consisting of anergic and dead cells due to hypoxia or nutrient deficiency (Figure 3). These conditions highly reflect in vivo solid tumor growth and make tumor spheroids a suitable tool to study authentic tumor development in vitro (21). Not every cell line is spheroid-compatible and the underlying mechanisms how tumor

cells form spheroids is still elusive. Important to know is that cadherins are required for tumor cell adhesion, but the type of cadherins needed for cell aggregation is highly cell line-specific (22). A common technique to generate spheroids is to use the liquid overlay method to culture suspension cells on non-adherent agar plates (23) or by aggregating suspension cells in small droplets using the hanging-drop method (24). Due to their spherical structures and the resulting diffusion barriers, which protect cells of the inner layers, spheroids are more resistant to chemotherapy than ordinary monolayer cell cultures (25).

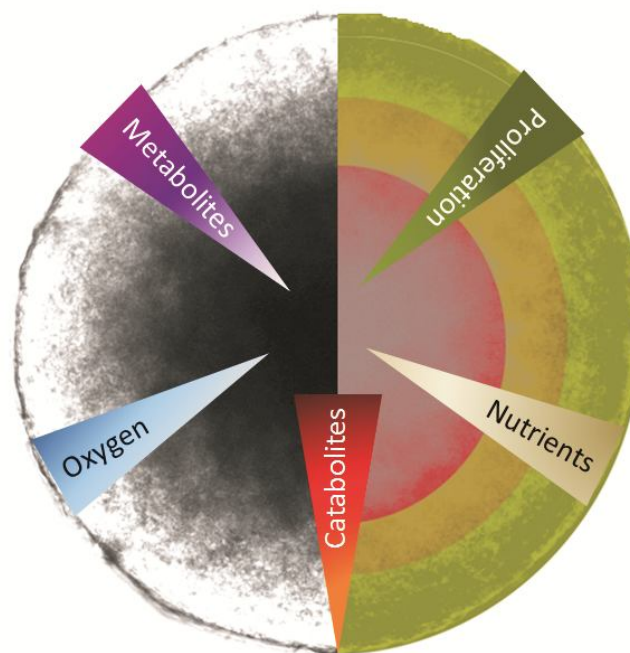


Figure 3: Spheroids possess features of avascular tumors. Physical parameters such as diffusion barriers restrict equal contribution of nutrients, oxygen and metabolites to all areas of the tumor, which forms an outer high proliferating (green) tumor periphery, while quality of support with oxygen and nutrients declines in the inner core of the spheroids, which drives tumor cells into the anergic state (yellow) and finally forces them into programmed cell death (red).

3.2 The anti-tumoral immune response

3.2.1 Phagocytes and their role in inflammation and anti-tumoral immunity

Phagocytes as the dominant part of the antigen-presenting cells (APcells) population and the innate immune system stand as the first line of defense, responsible for inducing specific immune responses dependent on how they interpret their local environments. Phagocytes constantly take up antigens as 'fingerprints' of their surrounding cells and in order to interpret the pathogenic potential of these antigens, phagocytes are programmed to 'sense' immunological 'non-self' molecules with pattern-recognition receptors (PRR) on their surfaces (26). This process is crucial for the initiation of an immune response and pivotal in the protection of the host against potentially harmful pathogens or foreign organisms. Toll-like receptors (TLRs) are a dominant subset of PRRs and upon recognition of their respective ligands, they activate the transcription factor 'nuclear factor kappa-light-chain-enhancer' of activated B-cells' (NF κ B) and enable the transcription of numerous genes encoding mediators for inflammation, a process which is also heavily linked to cancer diseases in general (27-29). Tumors may activate TLRs of phagocytes through damage associated molecular patterns (DAMPs), but, however, they may avoid detection by T cells, partly by expressing TAAs with a low immunogenic potential or by abandoning expression of major histocompatibility complex (MHC)-molecules capable of presenting TAAs (30). Another strategy of tumors to thrive in a hostile environment is to overload their proximity with DAMPs and desensitize phagocytes through continuous activation (31-32). Inflammation triggered by tumor-derived DAMPs can be maintained in the absence or strengthened in the presence of exogenous inflammatory stimuli and evokes immune-suppressive anti-inflammatory signaling as negative feedback (8,10). Additionally, tumor environmental factors present at the tumor site such as dead tumor cells, chronic cell stress and suppressive factors drive phagocytes to sense and interpret the tumor microenvironment as a site of severe tissue damage to boost their anti-inflammatory features (10). Thus, during the early development of tumors, a mix of both inflammatory and anti-inflammatory signals exists to create a state of 'smoldering' inflammation, which does not efficiently trigger immune responses, but features a continuous pro-tumorigenic, wound-healing

phenotype of phagocytes, which eventually develops into a highly anti-inflammatory tumor environment in late stage tumor development (29). High numbers of tumor-induced DCs (TiDCs) or tumor-associated macrophages (TAMs) correlate with bad prognosis because of their impotency to promote immune responses (33). Depletion of phagocytic myeloid cells (e.g. TAMs) triggered spontaneous anti-tumor activity (34). Thus, re-activation of these phagocyte subsets to kick-start immune responses against tumors open up new opportunities for therapy, but also bears risks since insufficient control of activation-induced inflammation promotes tumor favoring mechanisms and thus relapse of the disease, or may even feature acquirement of autoimmunity.

3.2.2 Immune cell crosstalk and anti-tumor T cell responses

In order to reject tumors, APcells such as dendritic cells (DCs) have to acquire TAAs (16) and migrate towards nearby lymph nodes to present TAAs to resting naïve T cells. The process of antigen presentation is pivotal for communication between the innate and the adaptive immune system to build a sensible network needed for reacting to intruding pathogens and abnormal tissue cells. Upon antigen recognition, naïve CD4⁺ T cells differentiate into various types of T helper cells (T_H) in a context-dependent manner, though the mechanisms are still not fully understood. The general consensus is that T_H-differentiation depends on the local cytokine profile at the site where the antigen is taken up by APcells, polarizing APcells to drive differentiation of naïve CD4⁺ T cells into the respective T_H cells (35). In contrast, naïve CD8⁺ T cells are already destined to differentiate into cytotoxic T lymphocytes (CTLs) (36). In principle, differentiation of naïve T cells into effector T cells works in the same manner for both CD4⁺ and CD8⁺ T cells. The anti-tumoral response per se depends on the induction of T_H1 cells and activation of CTLs and relies on a so-called 'two-signal' process. TAAs presented by the MHC complex on APcells have to be recognized by antigen-specific T cell receptors (TCRs) and activating costimulatory molecules e.g. CD80/CD86 (B7.1/B7.2) expressed on APcells need to ligate to their cognate receptors (e.g. CD28) on T cells (37). These two signals are sufficient to induce expression of signature cytokines needed for the differentiation of respective TAA-sensitive T_H cells, whereas CD8⁺ T cells upregulate expression of granzyme B (GrB) and interferon- γ (IFN- γ) and differentiate into TAA-recognizing

CTLs (36,38). Chamberlain et al demonstrated that the costimulatory molecules CD80/CD86 were required to induce an anti-tumoral response and enhance survival of mice by vaccination of CT26 tumor-bearing mice with recombinant vaccinia virus (rVV) expressing CD8, CD86, or model antigen (39). Blocking CD80/CD86 in combination with the CD40-CD40L-interaction fully abrogated an immune response in C57Bl/6 mice (40). However, binding of CD80/CD86 to cytotoxic T lymphocyte antigen (CTLA-4) expressed by regulatory T cells (T_{reg}) counteracts the initial activation of CD28 and prevents activating costimulatory molecules from undermining the peripheral suppression mediated by regulatory T cells (41-42). Alternatively, AP cells may also turn off T cell activation by inhibitory costimulatory molecules of the B7 family, e.g. B7-H1 binding to programmed cell death 1 (PD-1) on T cells (Figure 4). This imbalance between the expression of stimulatory and inhibitory B7 molecules might help tumors to elude immune control in the tumour microenvironment (43).

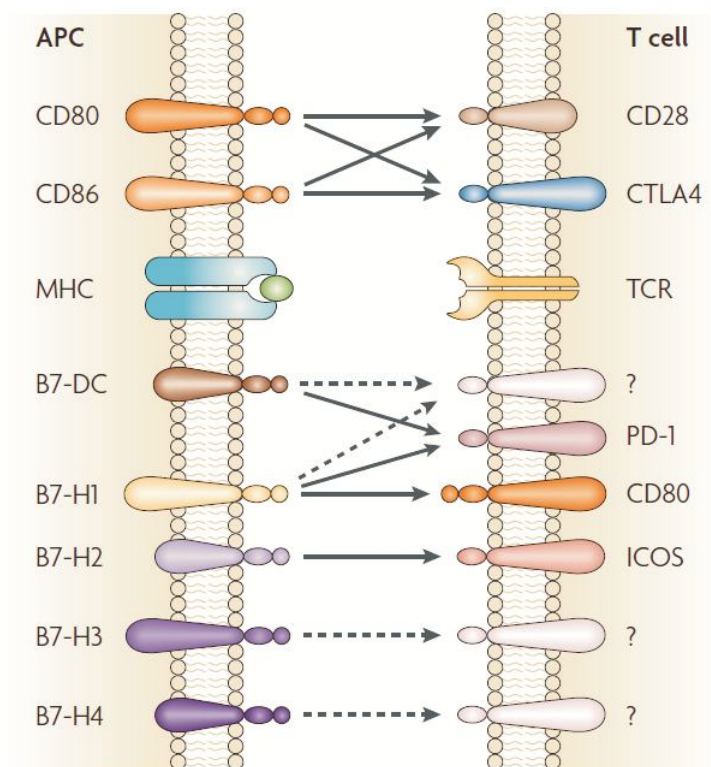


Figure 4: The B7 family and antigen presentation to T cells.

Antigens complexed by MHC molecules on AP cells are recognized by the TCRs of T cells. Members of the B7 family and other co-stimulatory molecules regulate the type of response of the antigen-sensitive T cell. The newly identified B7-H1 and B7-H4 molecules provide negative signals that control and suppress T cell responses. Human tumor cells and tumor-associated AP cells express limited levels of the stimulatory B7-family members CD80 and CD86, and high levels of the inhibitory B7-family members B7-H1 and B7-H4 (43).

In contrast, self-antigens are ‘silently’ recognized under anti-inflammatory conditions and presentation of self-antigens occurs in the absence of costimulatory molecules, which drives T cells into anergy. Upon successful priming of TAA-sensitive T cells, CTLs migrate out of lymph nodes and are recruited to the proximal tumor site to kill tumor cells expressing TAA, while TAA-specific T_H1 cells direct activation of macrophages. At the end, which also marks the beginning of the circle, activated CTLs consistently kill tumor cells and generate new TAAs, which can be again taken up by phagocyte subsets (Figure 5) (16).

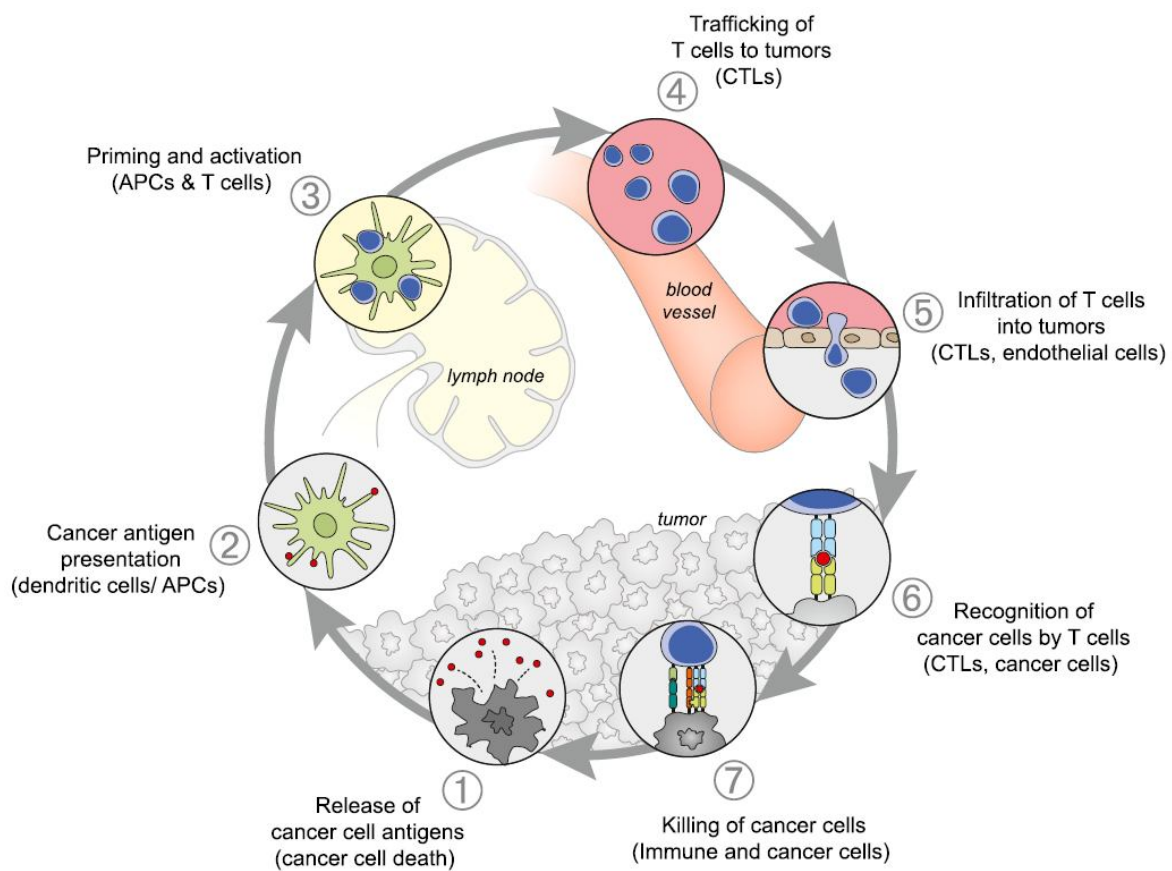


Figure 5: A scheme of a textbook anti-tumor response. DCs take up TAAs, migrate to lymph nodes to prime T cells eg. naïve $CD8^+$ T cells, which expand and differentiate to TAA-specific CTLs. CTLs migrate back to the tumor site to track down tumor cells expressing TAA (16).

As a fundamental process, the immune system itself is highly capable of recognizing and destroying abnormal cells such as tumor cells and its failure in doing so results in tumor outgrowth and cancer progression (16). Every anti-tumoral response also triggers massive cell stress and tissue damage setting free dead tumor cells and danger signals (31). This in part alerts the immune system to proceed in a more cautious manner, therefore activating immune suppressive mechanisms, which halt

further recruitment and cytotoxicity of CTLs. In addition to the aforementioned positive APcells T cell interaction provided by B7-CD28 interaction, there exists various negative regulators of T cell activation, which control the intensity of immune responses and are triggered as a negative feedback loop upon activation, hence the name 'immunological checkpoints' (44). The most important checkpoints are cytotoxic T-lymphocyte antigen 4 (CTLA-4) and programmed cell death 1 (PD-1) known to interfere with the priming of T cells in the lymph node and restricts cytotoxicity of CTLs at the proximal tumor site (16,44-45).

3.2.3 Current aims and strategies in cancer therapies

Current cancer therapy strategies still rely on the standard procedures chemotherapy, radiation and surgery. Classical oncologic approaches suggest use of inhibitors targeting specific cancer related signaling pathways. This approach faces severe challenges, as tumors per se compose of very heterogenic cell populations, complicating therapies and limiting the potential of these agents for broad applications. Immune therapies involve induction/reactivation of the anti-tumoral capacity of the immune system in particular T cell responses in patients. Direct CD28 activation leads to uncontrolled activation of the immune system. One well known case of how immune therapeutics can miserably fail is the early Phase I trial of the CD28 superagonist TGN1412, causing massive cytokine storms and multiple organ failure in test subjects (46). As an option to CD28 activation, checkpoint inhibition releases the restrictive immunological brakes. The antibody ipilimumab directed against CTLA-4 is already clinically approved for broad applications, whereas antibodies targeting PD-1 are currently undergoing Phase III trials (10,16). A more tumor specific strategy is to inhibit the PD-1 ligand B7-H1 (also PD-L1) expressed by tumor cells or tumor-associated phagocytes, disrupting the ability of these cells to inactivate TAA-sensitive CTLs (16). However, antigen-unspecific T cell activation is always coupled to auto-immunity. Therefore, antigen-specific T cells are created by grafting chimeric antigen receptors (CARs) recognizing TAA-expressing cells (16,45,47). Even though first generation CARs lack efficacy, caution is needed for the use of second and third generation CARs carrying additional costimulatory adapters, since these CARs possessed increased autoreactivity against normal tissue cells (48). Opposed to the artificial nature of CARs, phagocyte-based cancer vaccines

have emerged as attractive alternatives to induce TAA-specific T cell responses. Sipuleucel-T[®] was recently FDA approved as the first DC-based vaccine and uses GM-CSF-stimulated ex-vivo DCs to sensitize T cells for the prostate tumor antigen PA2024 (49). To further increase specificity, next generation DC vaccines include multiple tumor peptides such as the IMA901 vaccine discovered by using a multiple antigen discovery platform (50). However, these vaccination protocols are impotent to overcome suppression of regulatory T cells and still require low-dose cyclophosphamide to break the tumor-induced tolerance (51). Stimulation of phagocyte populations with toll like receptor (TLR) agonists is regularly required for vaccination strategies and lead to development and FDA approval of several drugs such as using bacterial components agonists *Bacillus Calmette-Guérin* (BCG) and monophosphoryl lipid A (MPL) activating TLR2/4, or the TLR9 ligand imiquimod (52). The tumor vaccine Stimuvax[®] couples MPL-based TLR2/4 activation with the tumor antigen Mucin-1 (MUC-1), stimulating T cell responses against MUC-1 expressing tumor cells (53). The therapeutically desired effect of TLR activation, the induction of a T_H1 response, is restricted by the tumor promoting feedback of activation-inflicted inflammation, which is often overlooked during the design of new immunotherapy, since immunotherapy-aroused inflammation is primarily seen as a response feature of successful immune activation. Thus, inflammation modulating agents are natural combinational therapy partners for TLR agonists. In this regard, inflammatory mediators, which affect type, strength, and duration of an immune response, require further attention, since their inhibition may be decisive in improving specific anti-tumoral immunity without promoting tumor favoring features. One of these inflammatory mediators relevant for cancer diseases is prostaglandin E₂ (PGE₂).

3.3 Formation of PGE₂

3.3.1 PGE₂ synthesis

PGE₂ synthesis is basically a three step process and its kinetics is determined by the presence of enzymes, which process each step of this procedure. In the first step, phospholipase A₂ (PLA₂) cleaves arachidonic acid (AA) from phospholipids of the plasma membrane (54). In the following second step, AA is metabolized to PGH₂ by cyclooxygenases (COX). Two COX-isoforms exist, the constitutively expressed

COX-1 and the inducible COX-2 (55). In a third step, PGH₂ is converted into the specific prostanoids by prostanoid isomerases, e.g. into PGE₂ by prostaglandin E2 synthases (PGES). The cytosolic PGE synthase (cPGES) (56) is localized in the cytoplasmic compartment, whereas microsomal PGE synthase-1 (mPGES-1) (57), and microsomal PGE synthase-2 (mPGES-2) (58) are integral membrane proteins and can be found in microsomes derived from the endoplasmatic reticulum (ER) and the perinuclear membrane (59). COX and PGES are functionally coupled. While cPGES is mainly associated with COX-1 (56), mPGES-1 is functionally linked to the inducible COX-2 (60). By way of exception mPGES-2 utilizes both COX-1 and COX-2 products to produce PGE₂ (61). Extracellular PGE₂ levels are tightly controlled by PGE₂ degrading enzyme 15-prostaglandin dehydrogenase (15-PGDH), which catalyses the oxidation of PGE₂ into the inactive 15-keto PGE₂ (62).

3.3.2 Stimulators of inducible PGE₂

PGE₂ secretion in phagocytes and tumor cells can be induced by pro-inflammatory stimuli such as LPS (32,63), TNF-alpha and IL-1 β signaling, as well as DAMPs (64). Under inflammatory conditions, production of PGE₂ strictly relies on the COX-2/mPGES-1 axis but neither cPGES nor mPGES-2 and involves c-Jun N-terminal kinase (JNK), phosphatidylinositol 3-kinase (PI3K), protein kinase C (PKC), and NF κ B (65). COX-2 and mPGES-1 expression are functionality coupled, however there is evidence that both enzymes can be unlinked, since inhibition of PI3K decreased mPGES-1 but enhanced COX-2 expression (66). Besides inflammatory mediators, anti-inflammatory transforming growth factor beta (TGF- β) and microenvironmental cues may also orchestrate COX-2 induction. However, PGE₂ production commonly occurs in response to cell stress factors such as hypoxia, glucose deprivation or the presence of apoptotic cells (67-70). Since all these conditions are also abundant in the tumor, it is not surprising that PGE₂ has been described as one of the most characteristic tumor microenvironmental factors (71).

3.4 PGE₂ down-stream signaling

3.4.1 EP receptor signaling

Prostaglandin E2 receptors (EP) 1-4 are G-protein coupled receptors (GPCR) (72). The interpretation of PGE₂-dependent signaling relies on the tissue-dependent expression of EP receptors (73) and their collective recognition of PGE₂. EP1 activates G_q, induces the flux of free Ca²⁺ into the cytosol and activates protein kinase C (PKC) (74). EP2 and EP4 couple to G_s and raise formation of intracellular cyclic adenosine monophosphate (cAMP), which results in protein kinase A (PKA) activation (75). EP3 exists in several different splice variants, which is unique for EP receptors. In this context, the original consensus regarding EP3 to activate G_i and decrease cAMP levels should be reviewed, since variable isoform expression may affect the specificity of EP3 mediated signaling (76).

3.4.2 PGE₂ supports tumor cell growth

PGE₂ supports tumor cell growth by acting on several pathways to concomitantly activate cell proliferation and support tumor cell survival and cell migration in cancers deriving from different entities, which is extensively reviewed by Wang et al. (77) and illustrated in Figure 6. On tumor cells EP1 induces cell proliferation by extracellular signal-regulated kinase (ERK) 1/2-mediated transactivation of epithelial growth factor receptor (EGFR), while EP3 is also a prerequisite for vascular endothelial growth factor (VEGF) expression needed for the induction of angiogenesis. EP2 signaling triggers the β -catenin pathway and EP4 mainly induces the phosphatidylinositide-3-kinase (PI3K)/protein kinase B (PKB)/Akt pathway (71,76). However, EP2/EP4 signaling has also been linked to inducing EGFR and VEGF so far (71,77). Hence, it is not surprising that EP signaling favors wound-healing signaling pathways and promotes tumor growth, since PGE₂ is secreted in response to cell stress. In tumors of different entities, all four receptors are relevant, but expression of EP2 and EP4 receptors is much more dominant on immune cells rather than tissue-resident cells (www.biogps.org) (77-78). Regarding the former, PGE₂ signaling on immune cells may promote their polarization/differentiation into tumor promoting cells, which will be discussed in following chapters.

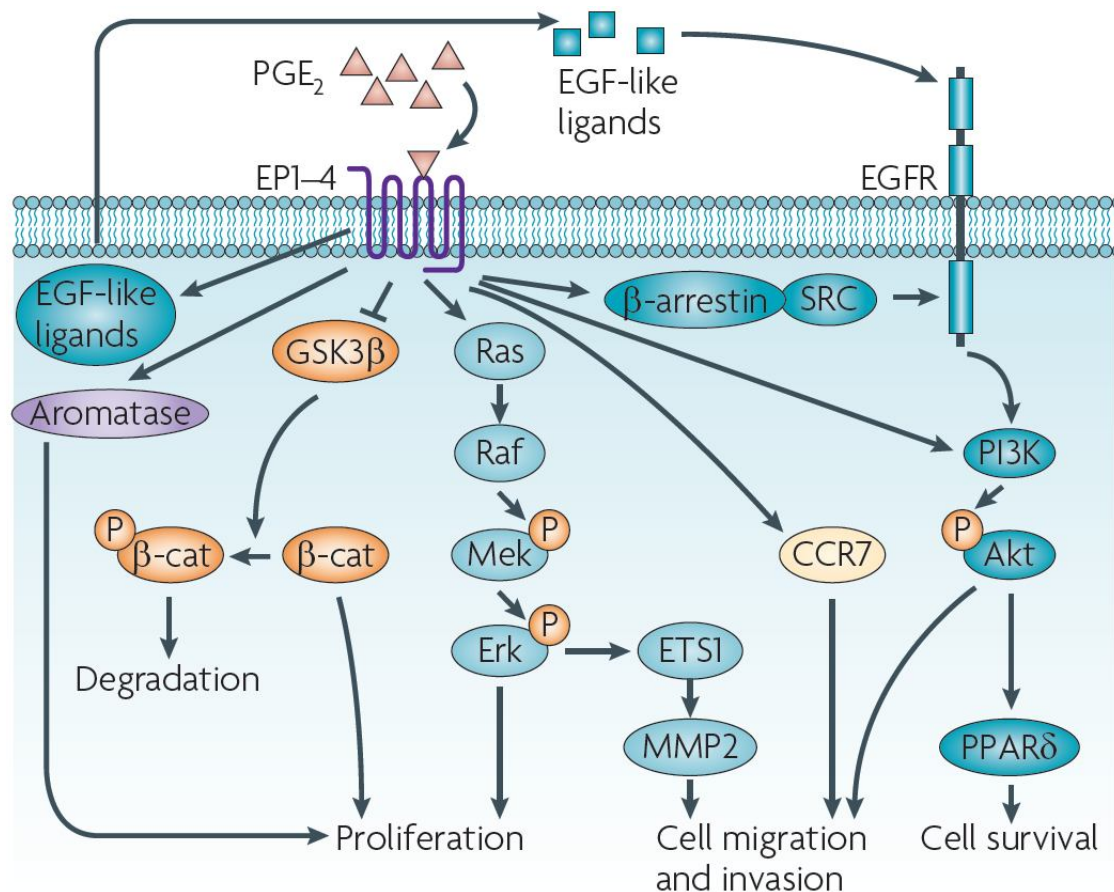


Figure 6: PGE₂ promotes cancer progression through the induction of tumor epithelial cell proliferation, survival, and migration and invasion. Multiple cellular signalling pathways mediate the effects of PGE₂ on the regulation of epithelial tumor cell proliferation, survival, and migration and invasion (77).

3.4.3 PGE₂ in the context of inflammation

Sensing of extracellular pathogenic epitopes, such as LPS, is mediated by PRRs. Upon recognition of pathogens, signalling downstream of PRRs leads to activation of the transcription factor NF- κ B and initiates the expression of inflammatory genes, including those coding for the enzymes COX-2 and mPGES-1. Termination of mPGES-1 expression can be achieved in LPS-activated macrophages by glucocorticoids (65), which is relevant for treating inflammatory diseases given the profound inflammatory potential of PGE₂ with regard to inducing vasodilatation, enhancing chemotaxis of immune cells and promoting DC maturation (79). Mice deficient of mPGES-1 develop normally, but have impaired inflammatory and pain responses (80). Hence, development of new mPGES-1 inhibitors targeting inducible PGE₂ downstream of COX-2 is highly promising for the treatment of inflammation-associated autoimmune diseases, but however excess PGE₂ again has anti-

inflammatory properties at the local site of inflammation (81). Extracellular PGE₂ can serve as a dampening signal for inflammatory mediator production, by activating EP2 and EP4 on macrophages, thus inhibiting LPS-mediated cytokine release (82). This principle might be relevant for conditions of overshooting inflammation as transfer of mesenchymal stem cells into septic mice reduced mortality by PGE₂ release from these cells, which enhanced IL-10 secretion from host macrophages in an EP2- and EP4-dependent manner (83). Furthermore, in a model of LPS-induced spinal neuroinflammation, mPGES-1-derived PGE₂ coupling to EP2 on microglia reduced the synthesis of inflammatory mediators including prostaglandins themselves (84). As mentioned, EP2 and EP4 ligation upregulates cAMP levels. It was shown that cAMP may be a master negative regulator of inflammatory macrophage function (85) by inhibiting NF-κB activation, interfering with ROS formation, and suppressing the generation of inflammatory cytokines such as TNF-α (86-88). Furthermore, PGE₂ has the potential to impair macrophage maturation through EP2/cAMP/PKA signalling, resulting in a lower percentage of F4/80^{high}/CD11b^{high} cells and reduced expression of macrophage colony-stimulating factor receptor (M-CSFR) (89). In line, macrophages present in the resolution-phase of inflammation exhibit a unique phenotype that is controlled by cAMP (90). These data together indicate an anti-inflammatory function of PGE₂ favoring the resolution of inflammation through the elevation of cAMP in macrophages in an EP2/EP4-dependent manner. These findings are puzzling given our daily life experience that non-steroidal anti-inflammatory drugs (NSAIDs), which inhibit COX enzymes, are effective in treating inflammatory conditions. Thus, one would assume that COX-derived PGE₂ solely affects the maintenance of inflammation, while an anti-inflammatory role of PGE₂ would appear as highly counter-intuitive. This is due to the ability of PGE₂ to induce vasodilatation and recruit phagocytes, which again amplifies the initial inflammatory stimuli already present at the inflammation site, whereas an imbalance of excess PGE₂ is rather immune suppressive (79). Hence, it would be more reasonable to interpret PGE₂ concentrations in a context-specific manner, i.e. in terms of the abundance of additional inflammatory stimuli. This interpretation justifies the different roles of PGE₂ in inflammation being on the one hand a pro-inflammatory mediator as originally hypothesized but also fitting to the refashioned anti-inflammatory role, which is apparent during cancer progression.

3.4.4 Connection between PGE₂ and tumor-associated mononuclear phagocytes

PGE₂ overproduction fuels the growth of tumors (3.4.2) and is a common feature in most cancer diseases, associated with expression of COX-2 and mPGES-1 by cancer and stromal cells. Furthermore, PGE₂ as part of a negative feedback mechanism during inflammation leads to spatial and temporal suppression of phagocyte functions at the site of inflammation or tissue damage (81). Therefore it seems rational to assume that tumor-associated PGE₂ may act as an autocrine or paracrine stop signal for inflammatory phagocyte function in cancer. Although PGE₂ is part of the protocol for generating mature conventional dendritic cells (cDCs) for tumor therapy, its suppressive effect on mature DCs or tumor-modulated DC maturation is well characterized (79). Culture supernatants from isolated solid human tumors impaired the differentiation of cDCs from human monocytes in a PGE₂, IL-6-dependent manner (91). In line with these observations, PGE₂ inhibited interferon- α (IFN- α) secretion of plasmacytoid dendritic cells (pDCs) during maturation via activation of both EP2 and EP4 (92). Apart from that, PGE₂ drives differentiation of DCs into suppressive cell types such as myeloid-derived suppressor cells (MDSCs) through PGE₂/EP2 signaling (93-94), and impairs both macrophages and DCs in their ability to induce T_H1 responses and thus, generation of anti-tumoral CTLs (79,95). Likewise, EP2-deficiency in mice injected with colon or lung cancer cell lines attenuated tumor growth and prolonged survival times, correlating with enhanced abundance of cDCs and T cells in tumor-draining lymph nodes and enhanced anti-tumor cytotoxic T cell responses (96). TAMs may constitute up to 40% of the tumor mass and are thus the most abundant immune cells in non-leukemic tumors (97). Depletion of TAMs using clodronate triggers spontaneous T cell and NK cell responses against the tumor, pointing out the suppressive capacity of TAMs to control peripheral tolerance at the tumor site (34). The degree of their accumulation predicts poor patient prognosis in most tumors, especially in later stages of tumor progression (33). TAMs may support virtually all stages of oncogenesis including tumor initiation of inflammation-induced tumors, tumor progression by producing tumor growth/survival factors and by recruiting blood vessels to the tumor, as well as metastasis to distant organs (98). Just as in DCs, PGE₂ restrains macrophage maturation via EP2 signaling (89), participates in deactivation of macrophages

through the PGE₂/EP2/cAMP-axis and is a negative regulator of TNF- α and a positive regulator of IL-6 (84,99). C-26 colon cancer cell conditioned medium suppressed macrophage TNF- α production through autocrine IL-10, which was produced downstream of PGE₂ (100). Also co-cultures with melanoma cells triggered COX-2 and PGE₂ release from macrophages (101). Upon melanoma cell interaction, PGE₂ reduced macrophage cytotoxicity, which was restored by inhibiting COX-2 (102). In this context, it was reported that COX-2 expression by TAMs correlates with disease progression in melanoma patients (103). The question that remains is how tumors program macrophages to overproduce PGE₂. Soluble factors derived from tumor cells have been suggested to induce mPGES-1 and COX-2 expression in human and mouse macrophages, thereby limiting IL-12 production and associated CTL priming, which was suppressed with indomethacin or in mPGES-1-deficient macrophages (104). However, the nature of these factors is presently unclear. Tumor cell death and the release of apoptosis-dependent soluble mediators are of relevance (105). Being forced into a harsh and competitive environment, which is rapidly depleted of oxygen and nutrients, tumor cells frequently undergo cell death, which provokes resident phagocytes to ill-interpret the terms of tumor cell death (106). The direct outcome is an overflow of dying cell and phagocyte-derived signalling molecules, which lead to a distracting mix of both maintenance and dampening mediators of inflammation- the so called 'injury- and death-induced inflammation' (29). A profound PGE₂ production of phagocytes during the clearance process of apoptotic cells was reported and dying tumor cells upregulated the expression of COX-2 and mPGES-1 but repressed 15-PGDH in human macrophages to accumulate PGE₂ (107-108). This was at least partly dependent on the sphingolipid sphingosine-1-phosphate (S1P), which is released from dying tumor cells (109-110). It is important to note that at least in mice, apoptotic tumor cells might produce PGE₂ themselves as a result of apoptotic protease activation (111). Taken together, there is compelling evidence suggesting that TAMs are programmed by tumors to provide high levels of PGE₂, which in turn suppresses the anti-tumoral capacity of a variety of different phagocyte subtypes (summarized in Figure 7).

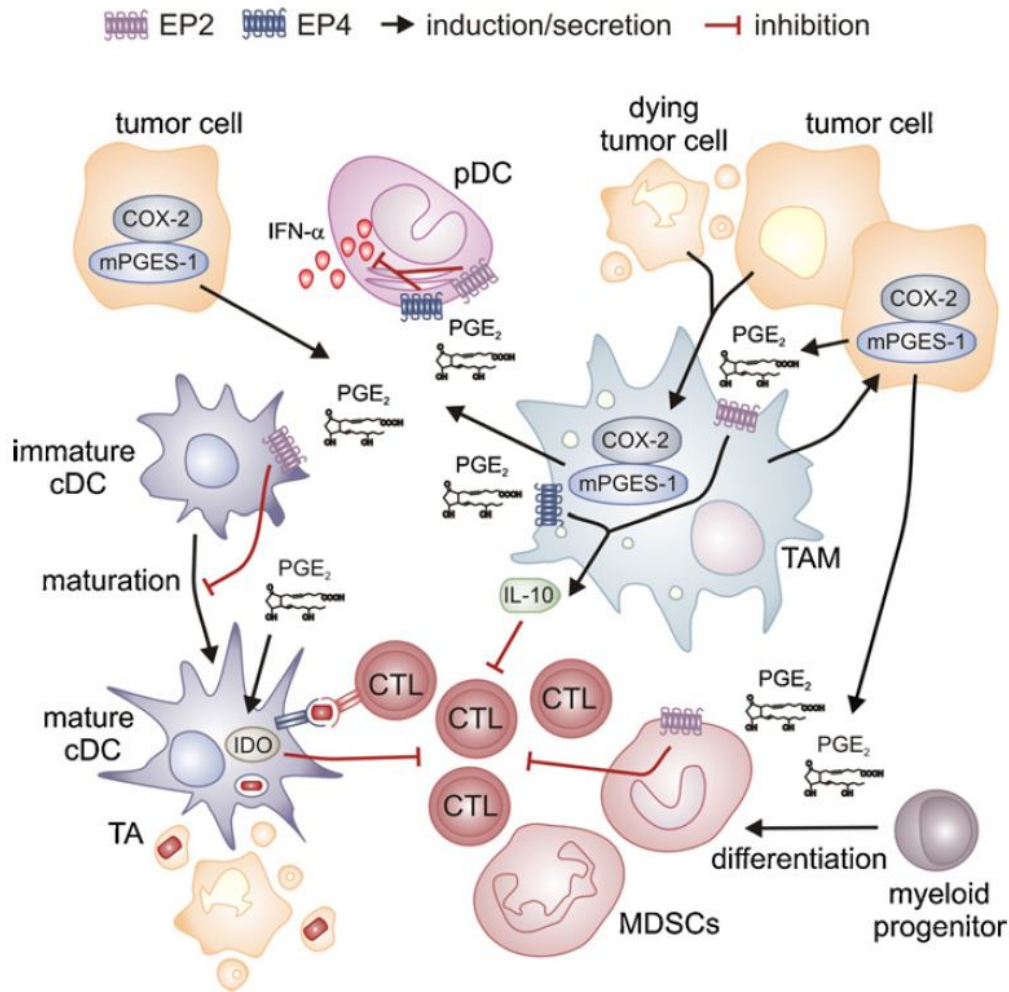


Figure 7: Impact of PGE₂ on cancer-associated mononuclear phagocytes. Cyclooxygenase-2 (COX-2) and microsomal PGE synthase-1 (mPGES-1) are upregulated in tumor cells and tumor-associated macrophages (TAMs), which enables secretion of PGE₂. PGE₂ couples to Prostaglandin E2 receptors 2 and 4 (EP2/4) on pDCs to inhibit interferon-α (IFN-α) production and to EP2 on immature cDCs to prevent maturation. In mature cDCs, PGE₂ prevents the priming of tumor antigen (TA)-specific cytotoxic lymphocytes (CTL), partly through induction of indolamine 2,3-dioxygenase (IDO). Generation of myeloid-derived suppressor cells (MDSCs) from bone marrow-derived myeloid progenitors is enhanced by PGE₂ through EP2, as is MDSC function (suppression of CTL). Finally, PGE₂ enhances the secretion of immunosuppressive mediators such as interleukin 10 (IL-10) from TAM (112).

3.5 PGE₂ and cancer

The role of PGE₂ in tumorigenesis has been outlined in various cancer models and entities (77). Overproduction of PGE₂ in many tumors has been associated with COX-2/mPGES-1-derived PGE₂ and favors hallmarks of cancer such as increased angiogenesis, metastasis, survival responses and cell cycle regulation (71,77,113).

Many cancer types arise as a consequence of chronic inflammation (98), suggesting NF- κ B activation to be critically involved in the early stages of tumorigenesis (29). Inflammatory environments foster PGE₂ production, which was first described in colorectal adenomas and cancers. The use of NSAIDs inhibiting COX isoenzymes had cancer preventive effects in a large number of clinical trials and not only in colorectal cancer (114-115), highlighting the tumor-promoting properties of prostaglandins per se. However, not all prostaglandins possess pro-tumorigenic tendencies. In fact PGE₂ may be dominant in these terms, which would attribute a major pro-tumorigenic function for PGES isoenzymes. Indeed, a very recent study highlighted the shunting of tumor-associated prostaglandin metabolism towards PGD₂ due to deletion of mPGES-1 in colorectal cancer (116). This study emphasized the observed absence of pro-tumorigenic PGE₂ favoring synthesis of anti-tumorigenic PGD₂ through its metabolite 15-deoxy- $\Delta^{12,14}$ -PGJ₂ that acts as a PPAR- γ activator to inhibit pro-tumorigenic NF- κ B (117-118). The shunting of prostaglandins towards anti-tumorigenic metabolites appears, from a therapeutic view, as highly desirable. However, the immune-suppressive role of PGD₂ raises the question whether prostanoid shunting from PGE₂ towards PGD₂ may be detrimental in immune therapeutic approaches (117,119). Overexpression of mPGES-1 has been found in various cancers, including lung, colorectal and breast cancer as well as hepatocellular carcinoma (120). Knockdown of mPGES-1 by siRNA significantly reduced tumorigenicity of prostate DU145 cells, human lung cancer A549 cells (121) in nude mice, which was attributed to the effect of PGE₂ on tumor cell proliferation. The finding that PGE₂ accelerates intestinal adenoma growth in adenomatous polyposis coli (APC)^{min} mice led to a focus on investigating mPGES-1 function in colorectal cancer (122). However, two studies investigating mPGES-1-deletion in intestinal tumorigenesis, reported controversial outcomes. Elander and co-workers observed that mPGES-1-deletion rendered APC^{min/+} mice more susceptible to developing intestinal tumors (123-124), whereas APC ^{$\Delta^{14/+}$} mPGES-1^{-/-} mice were less prone to developing intestinal tumors than WT mice (125). Despite this paradox, other reports investigating the impact of PGE₂ on cancer progression using genetic mouse models frequently underlined the pro-tumorigenic role of PGE₂. Severe hyperplastic gastric tumors can be induced by helicobacter pylori-activated macrophages in COX-2/mPGES-1 transgenic mice (126). In this study the investigators established the connection between h.pylori-mediated inflammation,

PGE₂ synthesis, macrophage recruitment and their impact on gastric hyperplasia. To complicate matters further, COX isoenzymes and mPGES1 are also expressed by tumor-associated stromal cells. Recently, efforts were made to identify principal sources of PGE₂ in the tumor microenvironment to determine the significance of tumor-derived versus stromal-derived PGE₂ with regard to cancer progression. In a xenograft approach, mPGES-1-silenced lewis lung carcinoma (LLC) cells grew slower than wildtype LLC tumors after transplantation. Additionally, LLC WT cells grafted into mPGES-1 deficient mice developed smaller tumors than in WT mice (127), underlining the relevance of both graft and host derived PGE₂. Furthermore, in a mouse BM transplantation model, BM-derived mPGES-1 expressing cells enhanced tumor growth and angiogenesis, while mPGES-1-deleted BM-derived cells were less efficient in promoting tumor growth, pointing out the importance of mPGES-1-expressing stromal cells in tumorigenesis (128). It is important to stress that in tumors that do not arise from pre-existing inflammation the PGE₂-producing machinery may not exist or may not be active in cancer cells. This was e.g. observed in human and murine glioma cells that did not produce significant amounts of PGE₂ (104). Thus, understanding which circumstance provokes PGE₂ synthesis by tumor or cancer-associated phagocytes and how accumulated PGE₂ participates in establishing an immunosuppressive pro-tumorigenic milieu is highly desirable.

3.6 Aim of this study

COX-2-derived PGE₂ is associated with cancer progression under inflammatory or anti-inflammatory conditions in cancer diseases of different entities (71,114). However, inhibition of COX-2 for treatment of cancer diseases may increase cardiovascular risks as discussed in previous chapters. Hence, mPGES-1 downstream of COX-2 may serve as an alternative target for cancer therapies. The purpose of this study was to determine the emerging role of COX-2/mPGES-1-derived PGE₂ in chosen aspects of the tumor development. In spheroid cultures, the role of mPGES-1 for tumor spheroid growth was evaluated, excluding an involvement of tumor-promoting stromal cells. Immune cells were cocultured with tumor spheroids to investigate the interaction of different immune cell subsets with a live three-dimensional tumor, helping to assess the role of mPGES-1-derived PGE₂ in different steps of the anti-tumoral response based on key parameters e.g. phagocyte polarization, T cell activation and tumor killing. The sum of these single parameters among others was expanded to a more complex tumor model using PyMT mice, which develop spontaneous breast cancers, to determine the overall tumorigenic potential of mPGES-1. The relation between tumor growth and tumor infiltrating immune cells was evaluated, especially how phagocyte polarization was affected in mPGES-1-deficient and wild-type PyMT mice. In this regard, the phenotype of tumor-associated phagocytes was compared with those in the *in vitro* coculture system and the overall feasibility of both tumor models was evaluated. This is necessary from a technical point of view, considering the fact that translation of *in vitro* findings to more complex tumor models such as murine tumor models has been termed as highly problematic or even failed miserably, and demands the establishment of new alternative tumor models, which more accurately reflect authentic tumor growth *in vivo*. In this thesis, the use of tumor spheroids as an *in vitro* tumor model is evaluated as a replacement for common monolayer tumor models and may enable a better transition of basic findings *in vitro* to more complex *in vivo* situations.

4 Materials and Methods

4.1 Materials

4.1.1 Chemicals

Absolute ethanol	Roth GmbH, Karlsruhe
Agarose	PeqLab, Erlangen
Bovine serum albumin (BSA)	Sigma-Aldrich, Deisenhofen
Dimethylsulfoxide (DMSO)	Roth, Karlsruhe
Ethylene diamine tetra acetate (EDTA)	Sigma-Aldrich, Deisenhofen
Potassium chloride (KCl)	Sigma-Aldrich, Deisenhofen

4.1.2 Buffers and Solutions

BD Cytotfix/Cytoperm	BD Biosciences, Heidelberg
BD Perm/Wash	BD Biosciences, Heidelberg
FACSflow	BD Biosciences, Heidelberg
Ultra-Pure Water	PAA, Cölbe

4.1.3 Media and reagents for cell culture

Accutase	PAA Laboratories, Cölbe
DMEM (high glucose)	Gibco, Carlsbad
DMEM (without glucose)	Gibco, Carlsbad
Fetal calf serum (FCS)	PAA, Cölbe
JetPrime	Peqlab, Erlangen

Penicillin/Streptomycin	PAA, Cölbe
Potassium buffered saline (PBS)	Sigma-Aldrich, Deisenhofen
RPMI 1640	PAA, Cölbe
Trypsin	PAA, Cölbe

4.1.4 Antibodies and cell dyes

7-AAD	BD Biosciences, Heidelberg
AnnexinV FITC	Imunotools, Friesoythe
anti-human active caspase3 FITC	BD Biosciences, Heidelberg
anti-human CD11c V450	BD Biosciences, Heidelberg
anti-human CD14 APC-H7	BD Biosciences, Heidelberg
anti-human CD206 PE-Cy5	BD Biosciences, Heidelberg
anti-human CD3 V450	BD Biosciences, Heidelberg
anti-human CD4 FITC	Imunotools, Friesoythe
anti-human CD45 APC	Imunotools, Friesoythe
anti-human CD45 PE	BD Biosciences, Heidelberg
anti-human CD68 APC	Biolegend, San Diego
anti-human CD8 APC-H7	BD Biosciences, Heidelberg
anti-human CD80	eBioscience, Frankfurt
anti-human CD80 APC	eBioscience, Frankfurt
anti-human CD86	R&D Systems, Minneapolis
anti-human CD86 FITC	BD Biosciences, Heidelberg
anti-human COX-1/COX-2 Mix	BD Biosciences, Heidelberg

anti-human GrB PE	Imunotools, Friesoythe
anti-human HLA-DR PE-Cy7	BD Biosciences, Heidelberg
anti-human IFN-gamma PE-Cy7	BD Biosciences, Heidelberg
anti-human IL-4 APC	BD Biosciences, Heidelberg
anti-mouse CD11b eFluor605NC	eBioscience, Frankfurt
anti-mouse CD11c Alexafluor700	BD Biosciences, Heidelberg
anti-mouse CD11c PerCP-Cy5.5	Biolegend, San Diego
anti-mouse CD16/CD32 FC blocking reagent	Miltenyi, Bergisch Gladbach
anti-mouse CD19 APC-H7	BD Biosciences, Heidelberg
anti-mouse CD206 FITC	Biolegend, San Diego
anti-mouse CD3 PE-CF594	BD Biosciences, Heidelberg
anti-mouse CD4 V500	BD Biosciences, Heidelberg
anti-mouse CD45 VioBlue	Miltenyi, Bergisch Gladbach
anti-mouse CD49b PE	Miltenyi, Bergisch Gladbach
anti-mouse CD8 eFluor605NC	eBioscience, Frankfurt
anti-mouse CD80 APC	Biolegend, San Diego
anti-mouse CD86 PE	BD Biosciences, Heidelberg
anti-mouse F4/80 PE-Cy7	Biolegend, San Diego
anti-human FC blocking reagent	eBioscience, Frankfurt
anti-mouse Ly6C PerCP-Cy5.5	Biolegend, San Diego
anti-mouse Ly6G APC-Cy7	Biolegend, San Diego
anti-mouse MHC-II APC	Miltenyi, Bergisch Gladbach
IgG1 isotype control	R&D Systems, Minneapolis

4.1.5 Stimulants and Inhibitors

2,5-Dimethylcelecoxib	Sigma-Aldrich, Deisenhofen
Aspirin	Sigma-Aldrich, Deisenhofen
Brefeldin A	Sigma-Aldrich, Deisenhofen
Butaprost	Cayman Chemicals, Ann Arbor
Cay10580	Cayman Chemicals, Ann Arbor
Celecoxib	Sigma-Aldrich, Deisenhofen
Cell stimulation cocktail	eBioscience, Frankfurt
Dimethyloxalyglycin	Sigma-Aldrich, Deisenhofen
Dynabeads human T-cell Activator anti-CD3/anti-CD28	inVitrogen, Carlsbad
Forskolin	Cayman Chemicals, Ann Arbor
Golgistop	BD Biosciences, Heidelberg
Lipopolysacharide	Sigma-Aldrich, Deisenhofen
Prostaglandin E2 synthetic powder	Sigma-Aldrich, Deisenhofen
Rolipram	Sigma-Aldrich, Deisenhofen
SC-560	Cayman Chemicals, Ann Arbor
Sulprostone	Cayman Chemicals, Ann Arbor
TPA/Ionomycin	Sigma-Aldrich, Deisenhofen
Z-VAD-Fmk	BD Biosciences, Heidelberg
Necrostatin -1	Sigma-Aldrich, Deisenhofen

4.1.6 Cytokines

Human interferon- γ	Peprotech, Hamburg
Human interleukin-2	Peprotech, Hamburg
Murine interferon- γ	Peprotech, Hamburg

4.1.7 Kits and Ready-to-use solutions

Anti-mouse compensation particles set	BD Biosciences, Heidelberg
GentleMACS tumor dissociation kit	Miltenyi, Bergisch Gladbach
Kapa2G hotstart genotyping	PeqLab, Erlangen
PEQgold	PeqLab, Erlangen
PGE2 EIA kit monoclonal	Cayman Chemicals, Ann Arbor
PureExtreme cDNA kit	Fermentas, St.Leon-Rot
SYBR green fluorescein mix	Thermo Scientific, Karlsruhe

4.1.8 Instruments

Apollo multiplate reader	Berthold Tech., Bad Wildbad
CASY® cell counter	Schärfe System, Reutlingen
Centrifuge 5415 R	Eppendorf, Hamburg
Centrifuge 5810 R	Eppendorf, Hamburg
CFX cycler system	Biorad, München
FACS LSR II Fortessa	BD Biosciences, Heidelberg
Fluorescence Axiovert microscope	Carl Zeiss, Göttingen
GentleMACS	Miltenyi, Bergisch Gladbach

Handystep electronic	Brand, Wertheim
HERAcell incubator	Heraeus, Hanau
HERAsafe clean bench	Heraeus, Hanau
In Vivo 400 hypoxia workstation	IUL Instruments, Königswinter
NanoDrop ND-1000	Peqlab, Erlangen
PCR mastercycler	Eppendorf, Hamburg
Pipettes (10 μ l, 100 μ l, 1.000 μ l)	Eppendorf, Hamburg
Plastibrand PD tip	Brand, Wertheim
Plastic material (cell culture)	Greiner Bio-One, Frickenhausen
Thermomixer 5436	Eppendorf, Hamburg
TipOne filter tip	StarLab, Ahrensburg
UV-Transilluminator gel documentation	Raytest, Straubenhardt

4.1.9 Software

AxioVision software	Carl Zeiss, Göttingen
FACSDiva software	BD Biosciences, Heidelberg
FlowJo	Tree Star, Ashland
Graphpad PRISM	Graphpad Software, La Jolla
Bio-Rad CFX manager	Biorad, München

4.1.10 shRNA plasmids

Sh-mission plasmids encoding mPGES-1 targeting shRNA or non-coding controls were obtained from Sigma-Aldrich, containing a pLKO.1-puro base vector and allow for transient or stable transfection of the shRNA as well as production of lentiviral particles.

4.1.11 Oligonucleotides for qPCR

Gene	Official Name		Sequence
Human COX-1	PTGS1	forward	ACCTCGGCCACATTTATGGAGACA
		reverse	AGCACCTGGTACTTGAGTTTCCCA
Human cPGES	PTGES3	forward	GCCAGTCATGGCCAAGGTTAACAA
		reverse	ACATCCTCATCACCACCCATGTTG
Human mPGES-2	PTGES2	forward	ACCTCATCAGCAAGCGACTCAAGA
		reverse	CATACACCGCCAAATCAGCGAGAT
Human COX-2	PTGS2	forward	CTTGCTGTTCCCACCCATGTCAA
		reverse	TGCACTGTGTTTGGAGTGGGTTTC
Human mPGES-1	PTGES1	Quantitect	Hs_PTGES_1_SG QT00208607
Human TNF- α	TNF	Quantitect	Hs_TNF_3_SG QT01079561
Human TGF- β 1	TGFB1	forward	ACAATTCCTGGCGATACCTCAGCA
		reverse	CGCTAAGGCGAAAGCCCTCAATTT
Human Bcl-2	BCL2	Quantitect	Hs_BCL2_1_SG QT00025011
Human Ki67	MKI67	Quantitect	Hs_MKI67_1_SG QT00014203

4.1.12 Cell lines

Primary PBMCs:

Primary human peripheral blood mononuclear cells were isolated from human buffy coats of healthy donors obtained from DRK-Blutspendedienst Baden-Württemberg-Hessen, Frankfurt.

MCF-7 cells:

MCF-7 cells originate from a human invasive breast ductal carcinoma and were established from the pleural effusion of a 69-year-old Caucasian woman with metastatic mammary carcinoma in 1970.

DU145 cells:

DU145 cells were isolated from a brain metastatic site, but originate from a prostate carcinoma of a 69-year old Caucasian man and established by Stone et al. in 1978.

PC3 cells:

PC3 cell lines were established in 1979 from bone metastasis of a 62-year-old Caucasian male prostate cancer patient.

LNCap cells:

LNCap was established from a lymph node metastatic lesion of a 50-year-old Caucasian male, who developed human prostatic adenocarcinoma in 1977.

HEK293 cells:

HEK 293 cells were generated by transformation of human embryonic kidney cell cultures with sheared adenovirus 5 DNA in the early 1970s.

4.2 Methods

4.2.1 Cell Culture

DU145, LNCap and PC3 prostate cancer cells and MCF-7 breast carcinoma cells were cultured in *Roswell Park Memorial Institute* (RPMI) 1640. HEK293T embryonal kidney cells were kept in *Dulbecco's Modified Eagle Medium* (DMEM). All media were supplemented with 5 mM glutamine, 100 U/ml penicillin, 100 µg/ml streptomycin and 10% heat-inactivated FCS. Cells were maintained at 37° C in a humidified atmosphere of 5 % CO₂ and 95 % air (normoxic conditions) or 5% O₂ (hypoxic conditions) using In Vivo₂ hypoxia workstation. To transfer cells, cells were washed with PBS/EDTA and detached using 1 unit Trypsin/EDTA. Digestion by trypsin was stopped with 4 units of complete media and cells were centrifuged (500 x g, 5 min, 20 °C). Supernatants were discarded and cells resuspended in fresh media before further use.

4.2.2 Generation of stable mPGES-1 knockdown cells

Sh-control transfected (sh-control) and sh-mPGES-1 transfected (sh-mPGES-1) DU145 human prostate cancer cells were generated as described (121). Cells were maintained and knockdown efficiency was controlled by Quantitative real-time PCR (qPCR).

4.2.3 Isolation of human PBMCs and culture of primary T cells

PBMCs were isolated from human buffy coats of healthy donors obtained from DRK Blutspendedienst (Frankfurt, Germany) using a ficoll gradient by centrifuging at 440 x g, 45 min with turned off centrifuge rotor brakes. Due to centrifugation, different fractions of the buffy coat were separated by their respective densities with the plasma fraction sitting on top, followed by a thin middle layer composed by mononuclear cells and erythrocytes and granulocytes sitting at the bottom. The middle layer mostly composing of leukocytes without granulocytes was separated and cells were either directly seeded for coculture experiments or transferred to adhesive cell culture dishes. Non-adherent cells were harvested for primary human T cell enrichment and cultured with IL-2 containing RPMI as described recently (129).

4.2.4 Cell proliferation assay

1×10^4 cells were seeded into 6 well plates, cultured for three days and were then harvested consecutively each day over a period of at least five days using trypsin/EDTA. Cell numbers were determined by CASY TT flow cytometric cell counting. Doubling time was calculated using exponential regression.

4.2.5 Generation and analysis of MCTS

Spheroids were generated using the liquid overlay technique by plating 2.5×10^4 cells/ml onto non-adherent 1% agarose-coated 96 well plates. Plates with cells in suspension were centrifuged at $500 \times g$ for 5 min and cells maintained in the incubator. MCTS size was acquired with a Carl Zeiss Axiovert microscope and diameters were determined using AxioVision 40 software.

4.2.6 Generation of necrotic cells

1×10^6 DU145 cells/ml were heat-killed at $60 \text{ }^\circ\text{C}$ and centrifuged at $1000 \times g$ for 5 min at $4 \text{ }^\circ\text{C}$. Supernatant and cell pellet were separated to obtain necrotic cells conditioned medium (NCM) or necrotic cells (NC).

4.2.7 Quantitative PCR

MCTS (10 spheroids each) were extracted, washed two times with PBS and disintegrated with accutase at $37 \text{ }^\circ\text{C}$ for 45 min. Total RNA out of single cell suspensions or monolayer cells was prepared using PEQgold. RNA pellets were washed with 75 % ethanol and total RNA amounts determined using Nanodrop ND-1000. RNA was transcribed with the PureExtreme cDNA synthesis kit to yield cDNA. Quantitative real-time PCR was performed using qPCR SYBR green fluorescein mix and the CFX96 Real Time PCR Detection System. Quantification of gene expression was performed with the Bio-Rad CFX Manager. 18S rRNA was used as the internal control. Primer sequences and predesigned QuantiTect Primer Assays are listed in 4.1.11.

4.2.8 Quantification of extracellular PGE₂ via PGE₂ EIA

PGE₂ concentrations in supernatants of monolayer cultures or MCTS were quantified using the Prostaglandin E2 enzymatic immunosorbent assay (EIA) kit-monoclonal. Supernatants were generally harvested after two or three days of culture in fresh medium.

4.2.9 Determination of prostanoids by Liquid Chromatography-Tandem Mass Spectrometry (LC-MS/MS)

LC-MS/MS analysis of PGF_{2α}, PGE₂, PGD₂, TXB₂, and 6-keto-PGF₁ from coculture supernatants were extracted using solid-phase extraction and analysis was performed as described in Linke et al. 2009 (130). Measurements were carried out by the cooperation partner Carlo Angioni of the Institute of Clinical Pharmacology (Prof. G. Geisslinger).

4.2.10 Flow Cytometry

Samples were acquired with a LSRII/Fortessa flow cytometer and analyzed using FlowJo software 7.6.1 or FACSDiva. All antibodies and secondary reagents were titrated to determine optimal concentrations. Antibody-capturing CompBeads were used for single-color compensation to create multi-color compensation matrices. For gating, fluorescence minus one (FMO) controls were used. The instrument calibration was controlled daily using Cytometer Setup and Tracking beads.

4.2.10.1 Annexin-PI staining

For fluorescence-activated cell sorting (FACS), single cells suspensions were generated from detached monolayer cell cultures or disintegrated spheroids by digestion with accutase (PAA) for 30 min at 37°C. 1×10^6 cells were transferred to FACS tubes for further treatment. To discriminate viable cells from apoptotic and necrotic cells, samples were stained as described recently (110). Briefly, AnnexinV⁻PI⁻ cells were classified as viable cells, whereas single positive AnnexinV cells were early apoptotic cells and double positive cells were declared as late apoptotic or necrotic cells.

4.2.10.2 Intracellular staining of COX-1/COX-2

For intracellular detection of protein expression, cells were harvested by centrifugation, fixed with Cytotfix/Cytoperm buffer, followed by washing and permeabilization with Perm/Wash buffer using standard protocols. Before staining, non-specific antibody binding to FC- γ receptors was blocked with FC Receptor Binding Inhibitor for 15 min on ice. For intracellular detection of COX-1/COX-2, samples were treated with an anti-COX-1-FITC/anti-COX-2-PE combined antibody mix for 30 min on ice.

4.2.10.3 Intracellular staining of IFN- γ

For intracellular detection of IFN- γ ⁺ cells were treated as described in 4.2.10.2, and stained with anti-CD3-eFluor605NC, anti-CD4-FITC, anti-CD8-APC-H7, anti-IL-4-APC and anti-IFN- γ -PE-Cy7 for at least 15 min on ice.

4.2.10.4 Staining of human CD14⁺ CD11c⁺ phagocytes

MCF-7 spheroid PBMC cocultures were harvested and spheroids washed with PBS twice. Supernatants and PBS were mixed and centrifuged at 500 xg for 5 min to yield a pellet with non-spheroid cells. These cells were again resuspended, blocked with FC Receptor Binding Inhibitor for 15 min on ice and stained with anti-CD45-PE, anti-CD11c-V450, anti-CD14-APC-H7, anti-CD80-APC, anti-CD86-PE, anti-CD206-PE-Cy5 for at least 15 min on ice.

4.2.10.5 Staining of GrB in CTLs

For intracellular staining of GrB in CTLs, PBMCs were isolated out of MCF-7 spheroid PBMCs cocultures as described in 4.2.10.4, fixed with Cytotfix/Cytoperm buffer for a maximum of 5 min on ice, followed by washing and permeabilization with Perm/Wash buffer. Permeabilized cells were blocked with FC Receptor Binding Inhibitor for 15 min on ice, using standard protocols. For intracellular detection of GrB, samples were stained with anti-CD45-APC, anti-CD3-V450, anti-CD4-FITC, anti-CD8-APC-Cy7, anti-GrB-PE for at least 15 min on ice.

4.2.10.6 Characterization of PyMT tumor infiltrating leukocytes

PyMT tumors were isolated out of sacrificed PyMT mice. For detection of different leukocyte subsets, cells were blocked with FC Receptor Binding Inhibitor for 15 min on ice and stained with anti-CD3-PE-CF594, anti-CD4-V500, anti-CD8-eFluor650, anti-CD11b-eFluor605NC, anti-CD11c-AlexaFluor700, anti-CD19-APC-H7, anti-CD45-VioBlue, anti-CD49b-PE, anti-F4/80-PE-Cy7, anti-MHC-II-APC, anti-Ly6C-PerCP-Cy5.5, anti-Ly6G-APC-Cy7, anti-SiglecH-FITC for at least 15 min on ice.

4.2.10.7 Characterization of F4/80⁺ CD11c⁺ phagocytes

For characterization of F4/80⁺ CD11c⁺ phagocytes, cells were isolated as described in 4.2.10.6 and stained with anti-CD45-VioBlue, anti-F4/80-PE-Cy7, anti-CD11c-PerCP-Cy5.5, anti-Ly6G-APC-Cy7, anti-CD80-APC, anti-CD86-PE, anti-CD206-PE-Cy5 for at least 15 min on ice.

4.2.11 MCF-7 tumor spheroid PBMC cocultures

MCF-7 tumor spheroids were generated as described in 4.2.5. PBMCs were isolated using standard protocols as indicated in 4.2.3. Media of MCF-7 spheroids were changed prior to starting the experiment. PBMCs were either left untreated or stimulated with 50 ng/ml LPS or LPS and 100 U/ml IFN- γ . Neutralizing antibodies or chemical agents such as inhibitors were added directly after activation of PBMCs. PBMCs were cocultured with MCF-7 tumor spheroids at 37 °C in the incubator.

4.2.12 T cell inhibition assay

2×10^6 purified T cells/ml were seeded into 24 well plates. Cells were pre-activated with 1:10 Dynabeads[®] Human T-Activator CD3/CD28 in the presence of 10 ng/ml IL-2 for 1 h and pulsed with 100 μ l RPMI or spheroid supernatants every day over a time course of five days. Before staining, T cell samples were treated with cell stimulator containing phorbol 12-myristate 13-acetate (PMA) and ionomycin for 4 h and brefeldin A added for additional 2 h. Cells were fixed, permeabilized and analyzed by FACS as described in 4.2.10.

4.2.13 Crossing and Genotyping of mice

Wildtype and mPGES-1 knockout PyMT mice were generated by crossing male PyMT^{+/-} mice with female mPGES1^{-/-} PyMT^{-/-} mice. Heterozygous male mPGES-1^{+/-} PyMT^{+/-} mice were crossed with female mPGES-1^{+/-} PyMT^{-/-} mice to either yield male mPGES-1^{+/+} PyMT^{+/-} and female mPGES-1^{+/+} PyMT^{-/-} for generation of a wildtype strain or male mPGES-1^{-/-} PyMT^{+/-} and female mPGES-1^{-/-} PyMT^{-/-} to create a mPGES-1 knockout PyMT strain. Genotypes of mice were determined by PCR of tail genomic DNA. To prepare DNA samples, tail-tips were cooked in 100µl of KAPA Genotyping lysis buffer. 1µl of lysed DNA solution was used for PCR and amplified using KAPA Hotstart Genotyping Reaction mix.

Setup of genotyping PCR reaction:

- | | |
|-------------------------|-------------|
| 1) Initial denaturation | 95 °C 3 min |
| 2) Denaturation | 95 °C 15 s |
| 3) Annealing | 55 °C 15 s |
| 4) Extension | 72 °C 30 s |

Step 2-4 were repeated for 35 cycles

- | | |
|--------------------|--------------|
| 5) Final extension | 72 °C 10 min |
|--------------------|--------------|

4.2.13.1 Discrimination of wild-type and mPGES-1 knockout mice

Primers a and b were used for wild-type allele and primers b and c used for the mutated allele.

'a': 5'-CAG TAT TAC AGG AGT GAC CCA GAT GTG-3'

(specific for targeted mPGES-1 gene)

'b': 5'-GGA AAA CCT CCC GGA CTT GGT TTT CAG-3'

(specific for the mPGES-1 gene downstream of the targeting construct)

'c': 5'-ATC GCC TTC TAT CGC CTT CTT GAC GAG-3'

(specific for the neo resistance gene)

4.2.13.2 Discrimination of wild-type and PyMT mice

Primer used for PyMT genotyping include

PyMT forward: 5'-CTA GGC CAC AGA ATT GAA AGA TCT-3'

PyMT reverse: 5'-GTA GGT GGA AAT TCT AGC ATC ATC C-3'

Internal control forward: 5'-GGA AGC AAG TAC TTC ACA AGG G-3'

Internal control reverse: 5'-GGA AAG TCA CTA GGA GCA GGG-3'

4.2.14 Screening of PyMT tumors

Female PyMT^{+/-} were screened 6 weeks after birth for breast tumors. Tumor burden of breast glands was scored for size and position of emerging tumors.

4.2.15 Tissue isolation from PyMT mice and generation of single cell tumor suspensions

20 weeks after birth, PyMT mice were sacrificed and perfused with PBS. After perfusion, PyMT tumors and lungs were isolated and their respective weight measured. Tissues were lysed with Miltenyi Tumor dissociation kit and GentleMACS using standard protocols. Generated single cell suspensions were counted and 3×10^6 cells used for further staining.

4.2.16 Statistical Analysis

All data represented in graphs are, unless otherwise stated, means \pm SEM. If not stated otherwise, statistically significant differences between groups were calculated using student's t-test (two groups) or ANOVA (multiple groups) with Bonferroni's post-correction for analysis of parametric data. Non-parametric data sets were analyzed with the Mann-Whitney U-test. Data between two groups were considered significant if *, $p \leq 0.05$, **, $p \leq 0.01$, ***, $p \leq 0.001$. Significance between normalized values and the control group were analyzed with the one-sample t-test against the hypothetical value 1 of the control group. Data were considered significant if #, $p \leq 0.05$, ##, $p \leq 0.01$, ###, $p \leq 0.001$.

5 Results

5.1 PGE₂ and its role in prostate cancer cell spheroids

A first goal was to establish tumor spheroids as an in vitro tumor model that closely mimics tumor growth in vivo. For this purpose, the liquid overlay method was chosen to generate tumor cell clusters out of monolayer-cultured cells. The aim was to use a feasible model, that allows to grow tumors as three-dimensional structures in vitro, to assess the impact of mPGES-1 expressed in cancer cells on the growth of tumor spheroids.

5.1.1 mPGES-1 supports MCTS formation of DU145 prostate cancer cells

The expression of mPGES-1 was knocked down by lipofection of mPGES-1 mRNA targeting small hairpin RNA (sh-mPGES-1) into wildtype DU145 prostate cancer cells as described by Hanaka et al. in 2009 (121). DU145 cells transfected with scrambled control shRNA (sh-control) were generated as control cells and mPGES-1 mRNA expression of monolayer DU145 cells was analyzed by qPCR (Figure 8).

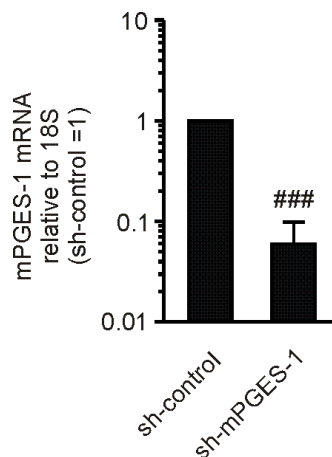


Figure 8: shRNA targeting mPGES-1 mRNA efficiently reduced mPGES-1 mRNA levels. Knockdown of mPGES-1 was performed via lipofection as described (121). Data are means \pm SD of at least three independent experiments. Diamonds indicate significant differences between experimental groups and the control group in a one-sample t-test ($^{\#}$, $p \leq 0.05$, $^{\#\#}$, $p \leq 0.01$, $^{\#\#\#}$, $p \leq 0.001$).

Surprisingly, the mPGES-1 knockdown did not affect tumor cell growth in monolayer cultures as equal doubling rates were determined for sh-control and sh-mPGES-1 monolayer DU145 cells (Figure 9a). Instead, the mPGES-1 knockdown significantly impacted size development of tumor spheroids (Figure 9b), when DU145 cells were seeded to form tumor spheroids using the liquid overlay method. Compared with sh-control spheroids, knockdown of mPGES-1 impaired spheroid growth as displayed in the growth curve shown in Figure 9b and also resulted in a decreased spheroid size of 10 days old tumor spheroids (Figure 9c).

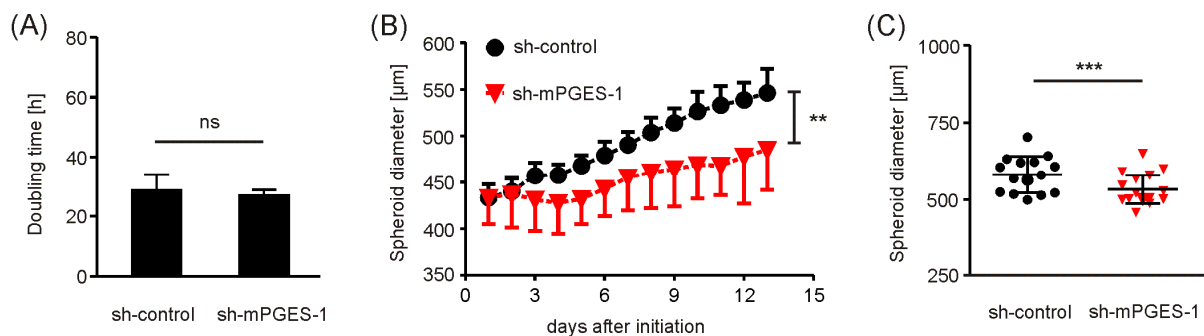


Figure 9: mPGES-1 knockdown impaired tumor spheroid growth. (A-C) Control (sh-control) or mPGES-1 knockdown (sh-mPGES-1) DU145 human prostate cancer cells were grown in monolayer cultures or seeded on agarose to induce spheroid formation. (A) Doubling time of monolayer cells was determined by CASY cell counting. (B) A representative growth curve of three independent experiments is displayed. (C) Spheroid sizes after 10 days of cultivation are displayed. Each data point corresponds to the mean diameter of 10 spheroids. Data are means \pm SD of at least 15 independent experiments. Asterisks indicate significant differences between experimental groups (*, $p \leq 0.05$, **, $p \leq 0.01$, ***, $p \leq 0.001$).

5.1.2 COX-2 and mPGES-1 are both needed for spheroid formation-induced PGE₂ production

At first, it was surprising that mPGES-1 knockdown only hampered growth of tumor spheroids, but did not affect cells grown in monolayer cultures. A possible explanation for this phenomenon was quickly found when intracellular staining of COX-2 protein expression revealed that COX-2 was induced in both sh-control and sh-mPGES-1 cell lines, leading to accumulation of PGE₂ in control DU145 spheroids. In parallel, knockdown of mPGES-1 efficiently limited PGE₂ levels (Figure 10) of sh-mPGES-1 spheroid cultures to the minimal amounts usually found in monolayer cultures. The difference in secreted PGE₂ positively correlated with the growth rate of

the sh-control and sh-mPGES-1 spheroid cultures, whereas in monolayer cultures equal levels of secreted PGE₂ correlated with equal growth rates of these two cell lines. Put together, spheroid formation-induced elevation of COX-2 expression only promoted synthesis of PGE₂ in sh-control DU145 cells, since the knockdown of mPGES-1 completely diminished PGE₂ production in sh-mPGES-1 spheroid cultures. In monolayer cells, COX-2 expression levels were not sufficient for effective PGE₂ accumulation and thus, knockdown of mPGES-1 appeared to be irrelevant for PGE₂ synthesis.

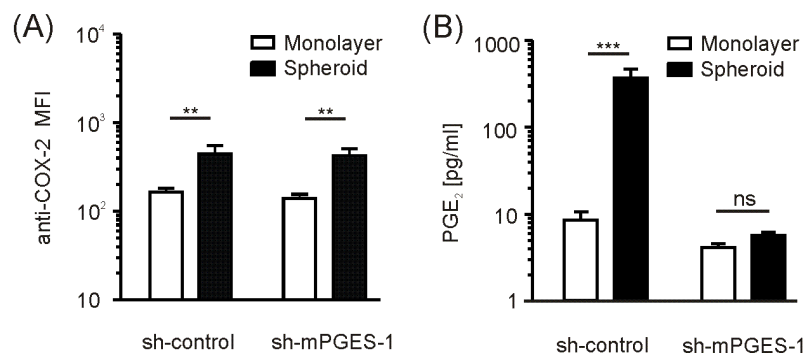


Figure 10: COX-2 and mPGES-1 in tumor spheroids enables accumulation of PGE₂. (A-B) Control (sh-control) or mPGES-1 knockdown (sh-mPGES-1) DU145 human prostate cancer cells were grown in monolayer cultures or seeded on agarose to induce spheroid formation. (A) Intracellular staining of COX-2 protein and extracellular levels of (B) PGE₂ of monolayer and spheroid cultures measured by PGE₂ EIA are displayed. Asterisks indicate significant differences between experimental groups (*, $p \leq 0.05$, **, $p \leq 0.01$, ***, $p \leq 0.001$).

5.1.3 Cell clustering induces COX-2 expression in prostate cancer cell lines

Several prostate cancer cell lines were analyzed with regard to their COX-2 mRNA expression to exclude that COX-2 elevation in tumor spheroids was a cell line-exclusive effect of DU145 cells. Among the three available prostate cancer cell lines, only DU145 cells formed spheroids, while LNCap and PC3 cells aggregated as cell clusters. Cells were harvested and the mRNA expression of PGE₂ synthesizing enzymes was detected by qPCR. COX-2 mRNA expression was significantly enhanced in tumor spheroids of DU145 cells and PC3 cell clusters, confirming that COX-2 was not exclusively elevated in aggregating DU145 cells (Figure 11). In contrast, COX-1 mRNA was not significantly upregulated in all three prostate cancer

cell lines as a result of cell clustering, whereas mPGES-1 mRNA expression was only enhanced in LNCap clusters (Figure 11).

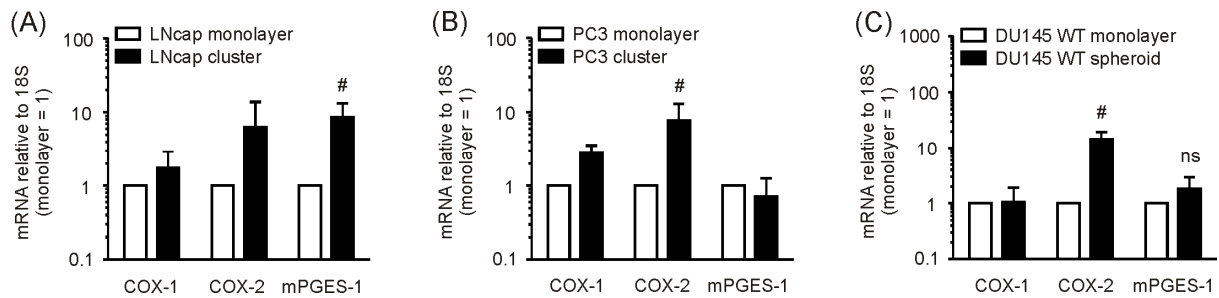


Figure 11: Cell clustering induces COX-2 expression. (A) LNCaP, (B) PC3 or (C) WT DU145 human prostate cancer cells were grown in monolayer cultures or were seeded on agarose to induce spheroid formation. mRNA expression of COX-2 in monolayer cells or spheroids was analyzed using qPCR. Data are means \pm SD of four independent experiments. Diamonds indicate significant differences between experimental groups and the control group in a one-sample t-test (#, $p \leq 0.05$, ##, $p \leq 0.01$, ###, $p \leq 0.001$).

5.1.4 COX-2 and mPGES-1 inhibition impairs PGE₂ production and MCTS growth

Reduced PGE₂ production was arguably the reason for limited growth of mPGES-1-deficient MCTS and to prove this concept, application of the COX-2 inhibitor celecoxib (Cxb) and the mPGES-1 inhibitor 2,5-dimethylcelecoxib (DMC) served as tools to blunt PGE₂ production in monolayer and MCTS cultures of DU145 cells. As expected, it was observed that inhibition of either COX-2 or mPGES-1 blocked PGE₂ production in MCTS cultures, but did not significantly affect minimal levels of PGE₂ produced in monolayer cell supernatants (Figure 12). The COX-2 inhibitor celecoxib, but not the mPGES-1 inhibitor DMC reduced the growth of sh-control transfected DU145 monolayer cells, whereas both inhibitors had no effects on sh-mPGES-1 transfected DU145 monolayer cells (Figure 12b). In contrast, application of Cxb or DMC markedly impaired growth of control DU145 MCTS at 10 μ M, which correlated with the significantly reduced PGE₂ levels measured in respective supernatants, while using 1 μ M of Cxb or DMC failed to significantly reduce tumor growth and restrict PGE₂ synthesis of sh-control MCTS (Figure 12a, c). In accordance with the initial hypothesis, Cxb did not affect growth of mPGES-1-deficient MCTS, whereas DMC slightly enhanced MCTS growth (Figure 12d).

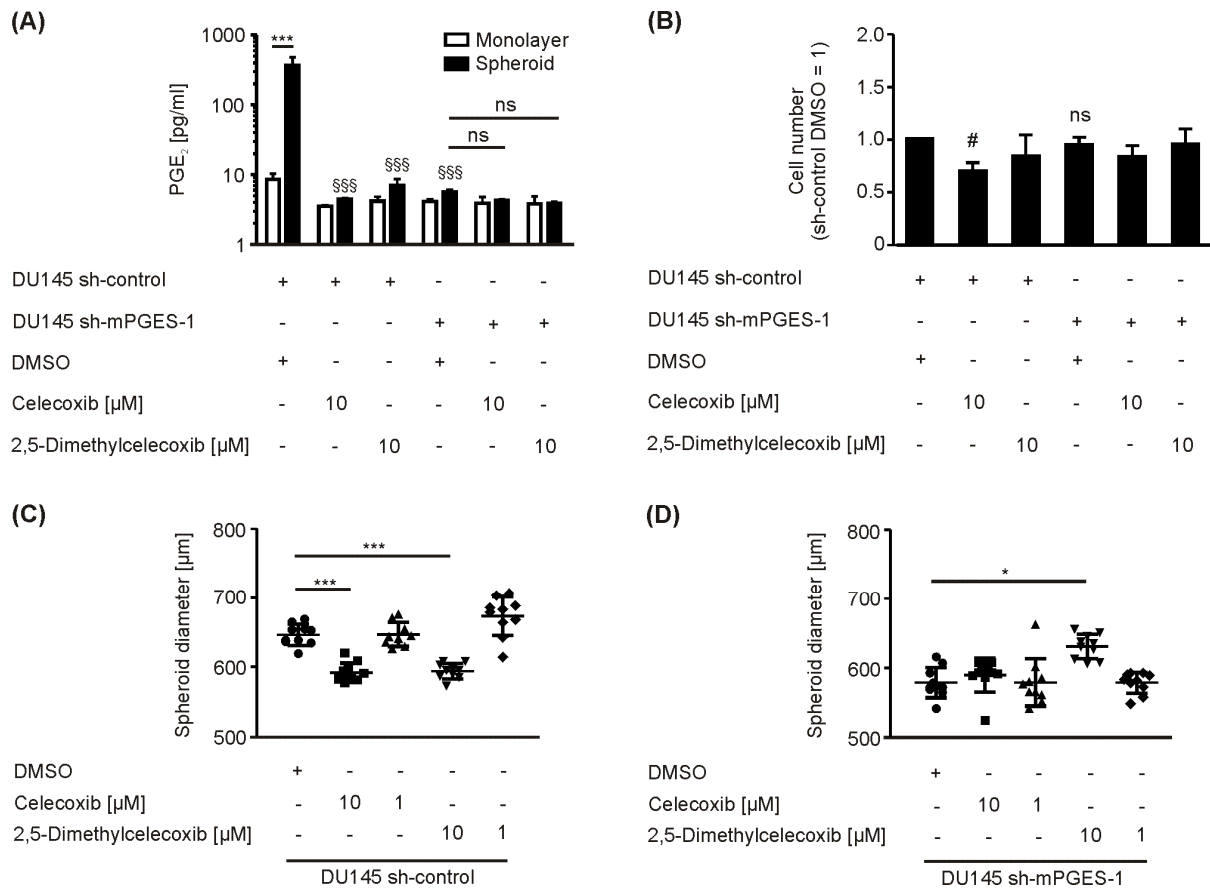


Figure 12: Celecoxib and DMC inhibited PGE₂ production and growth of sh-control tumor spheroids. Control (sh-control) or mPGES-1 knockdown (sh-mPGES-1) DU145 human prostate cancer cells were grown in monolayer cultures or seeded on agarose to induce spheroid formation. (A) PGE₂ levels measured by PGE₂ EIA are displayed. Section signs indicate significant differences between experimental groups and the sh-control spheroid group ([§], $p \leq 0.05$, ^{§§}, $p \leq 0.01$, ^{§§§}, $p \leq 0.001$). (B) Cell numbers three days after plating were determined. (C and D) A representative experiment, out of two, showing spheroid size after the addition of PGE₂ synthesis inhibitors is displayed. Data are means \pm SD of 10 spheroids. Data are means \pm SD of at least three independent experiments. Asterisks indicate significant differences between experimental groups (*, $p \leq 0.05$, **, $p \leq 0.01$, ***, $p \leq 0.001$). Diamonds indicate significant differences between experimental groups and the control group in a one-sample t-test ([#], $p \leq 0.05$, ^{##}, $p \leq 0.01$, ^{###}, $p \leq 0.001$).

In conclusion, application of the COX-2 inhibitor Cxb and the mPGES-1 inhibitor DMC abrogated PGE₂ accumulation in sh-control transfected MCTS cultures, thereby significantly impairing the growth of these high PGE₂ level-producing experimental tumors. Taken together, these findings suggest that COX-2 and mPGES-1 are both needed for accumulation of PGE₂ in tumor cell cultures, revealing that spheroid formation-dependent COX-2 induction is required for PGE₂ production.

5.1.5 Glucose-deprivation, hypoxia and HIF-1 α accumulation fail to induce COX-2 mRNA in tumor spheroids

Spheroid formation and thus, cell clustering induced COX-2, raising the question which environmental cues would be responsible for such changes. Hence, the task was to mimic defined conditions in MCTS spheroids that would affect COX-2 expression. The first approach was to analyze whether expression of soluble factors, which induce PGE₂ production, were altered during spheroid formation, since cells tend to release so-called ‘attention-factors’ during chronic cell stress (Figure 13).

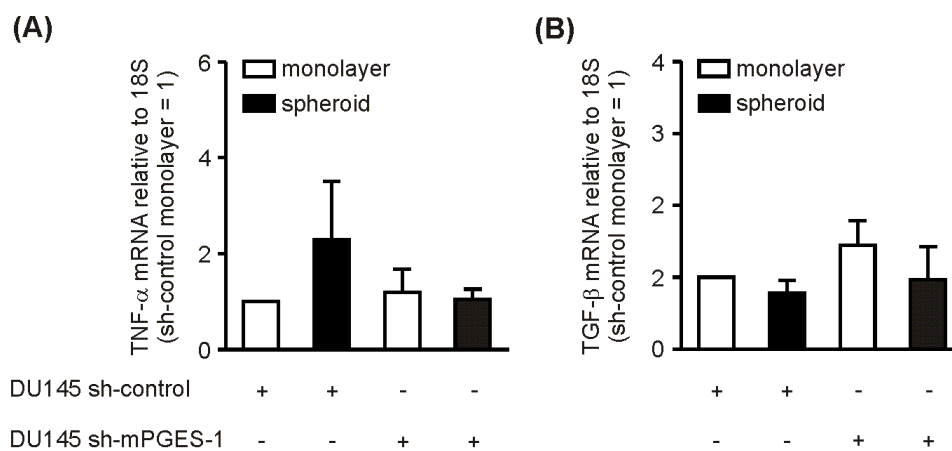


Figure 13: Spheroid formation does not affect expression of TNF- α or TGF- β 1 mRNA. Control (sh-control) or mPGES-1 knockdown (sh-mPGES-1) DU145 human prostate cancer cells were grown in monolayer cultures or seeded on agarose to induce spheroid formation. mRNA expression of TNF- α and TGF- β 1 are analyzed by qPCR. Data are means \pm SD of four independent experiments. Asterisks indicate significant differences between experimental groups (*, $p \leq 0.05$, **, $p \leq 0.01$, ***, $p \leq 0.001$). Diamonds indicate significant differences between experimental groups and the control group in a one-sample t-test (#, $p \leq 0.05$, ##, $p \leq 0.01$, ###, $p \leq 0.001$).

Interestingly, spheroid formation did not impact the expression of tumor necrosis factor alpha (TNF- α) or transforming growth factor beta 1 (TGF- β 1) mRNA (Figure 13), which were connected to COX-2 induction before (67-68,131). Besides soluble mediators, microenvironmental cues may also orchestrate gene expression of tumor cells. Among others, COX-2 levels can be enhanced by hypoxia/HIF-1 α (68) or glucose deprivation (69). Cell aggregation during spheroid formation results in high cell densities, forming an environment with nutrient deficiency and chronic hypoxia as direct consequences. Hence, monolayer sh-control DU145 cells were cultured under glucose-free conditions, but no elevation of COX-2 mRNA levels was observed in this setting (Figure 14). Also, hypoxic conditions or application of the prolyl hydroxylase

inhibitor DMOG as a HIF-1 α stabilizer under normoxia failed to significantly induce COX-2 mRNA in DU145 monolayers (Figure 14).

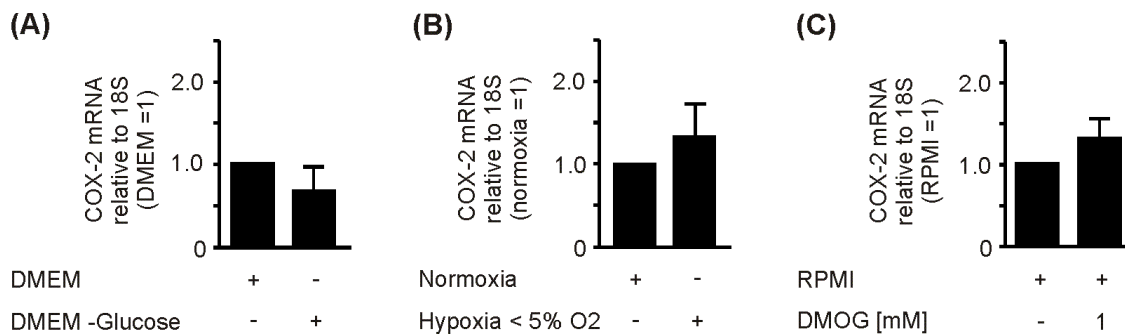


Figure 14: Glucose-deprivation, hypoxia and HIF-1 α stabilization fail to induce COX-2 mRNA expression. COX-2 mRNA expression in sh-control transfected DU145 cells was analyzed via qPCR after 24 h. (A) DU145 cells were cultured in DMEM/high glucose or DMEM without glucose. Values were normalized to cells cultured in DMEM/high glucose. Data are means \pm SD of four independent experiments. (B) DU145 cells were cultured in RPMI under normoxia or \leq 5% hypoxia. Values were normalized to cells cultured under normoxic conditions. Data are means \pm SD of three independent experiments. (C) DU145 cells were treated with the solvent control (DMSO) or the HIF-1 α stabilizer DMOG. Values are normalized to cells treated with DMSO. Diamonds indicate significant differences between experimental groups and the control group in a one-sample t-test ([#], $p \leq 0.05$, ^{##}, $p \leq 0.01$, ^{###}, $p \leq 0.001$).

5.1.6 Necrotic cells induce COX-2 mRNA in DU145 cells

Recently, evidence accumulated that apoptotic cells may participate in inducing PGE₂ in an active caspase3/7- and iPLA₂-dependent manner (70,111). In line with these reports, investigators previously observed that apoptotic cells induced COX-2 expression in macrophages, which was tracked back to sphingosine-1-phosphate (S1P) or TGF- β 1-dependent mechanisms (107,132). Since the increase of active caspase3⁺ cells correlated with COX-2 mRNA induction in MCTS as compared to monolayer cells (Figure 15), it was hypothesized that apoptotic cells in MCTS may play a potential role to induce COX-2 mRNA in living bystander cells. By using the pan-caspase inhibitor Z-VAD-FMK, the percentage of active caspase3⁺ and early apoptotic (annexin V⁺ PI⁻) cells was repressed in MCTS cultures. However, contrary to the original hypothesis, application of Z-VAD-FMK further increased COX-2 mRNA and PGE₂ synthesis in sh-control transfected DU145 MCTS (Figure 15d, e).

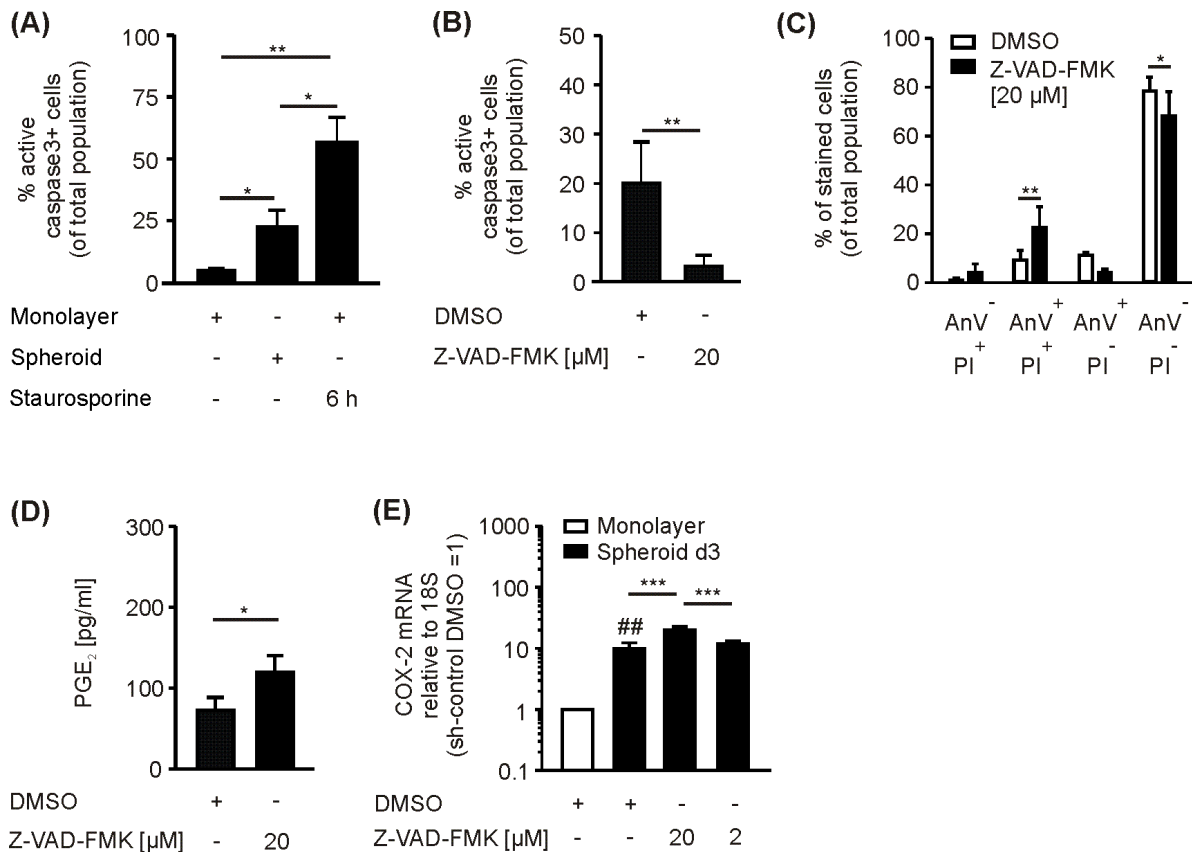


Figure 15: DU145 human prostate cancer cells were grown in monolayer cultures or as spheroids. (A) Percentage of active caspase3⁺ cells of 10 day old spheroids, control monolayer and 0.5 µg/ml staurosporine-treated monolayer cells was determined by intracellular staining and flow cytometry. Data are means ± SD of four independent experiments. (B-D) DU145 cells were pre-treated with the apoptosis inhibitor Z-VAD-FMK for 30 min before seeding for spheroid generation. 5 days after initiation, spheroids were disintegrated for further analysis. Data are means ± SD of four independent experiments. (B) Percentage of active caspase3⁺ cells was analyzed by intracellular staining and flow cytometry. (C) Spheroid single cell suspensions were stained with annexinV and propidium iodide to discriminate viable cells (AnV⁻ PI⁻) from apoptotic (AnV⁺ PI⁻) and necrotic cells (AnV⁻ PI⁺). Data are means ± SD of four independent experiments. (D) Extracellular PGE₂ was determined by PGE₂ EIA. (E) Relative COX-2 mRNA of three day old DU145 spheroid cells was analyzed by qPCR. Values are normalized to sh-control monolayer cells pre-treated with DMSO. Data are means ± SD of four independent experiments. Asterisks indicate significant differences between experimental groups (*, p ≤ 0.05, **, p ≤ 0.01, ***, p ≤ 0.001). Diamonds indicate significant differences between experimental groups and the control group in a one-sample t-test (#, p ≤ 0.05, ##, p ≤ 0.01, ###, p ≤ 0.001).

By applying Z-VAD-FMK on sh-control transfected DU145 MCTS, a decrease in annexinV⁻/PI⁻ viable cells and annexinV⁺/PI⁻ apoptotic cells correlated with an increase in annexinV⁺/PI⁺ necrotic cells (Figure 15c). These observations raised the question whether necrotic cells provoked induction of COX-2 expression in viable MCTS bystander cells. To deal with this issue, heat-treated necrotic DU145 cells

(NC) or their respective supernatants (NCM) were cocultured with monolayer sh-control DU145 cells. By using isolated necrotic cells, a significant increase in COX-2 mRNA expression and extracellular PGE₂ was indeed observed in these cultures (Figure 16), supporting a role of necrotic cells for COX-2 mRNA induction in surrounding tumor cells. Interestingly, necrotic cell supernatants failed to induce COX-2 mRNA and PGE₂ production to the same extent as it was observed earlier in macrophages (107).

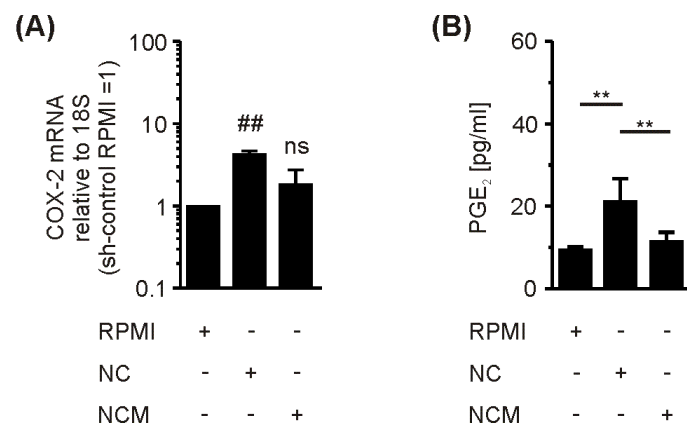


Figure 16: NC but not NCM induces COX-2 expression and PGE₂ synthesis. DU145 cells were treated with equivalent amounts of NC (1:1) and/or NCM derived from equivalent amounts of NC. (A) COX-2 expression was analyzed via qPCR after 24 h. Values are normalized to cells cultured in RPMI. Data are means \pm SD of four independent experiments. (B) PGE₂ levels in DU145 culture supernatants were measured via PGE₂ EIA. Data are means \pm SD of four independent experiments. Asterisks indicate significant differences between experimental groups (*, $p \leq 0.05$, **, $p \leq 0.01$, ***, $p \leq 0.001$). Diamonds indicate significant differences between experimental groups and the control group in a one-sample t-test (#, $p \leq 0.05$, ##, $p \leq 0.01$, ###, $p \leq 0.001$).

It was reported that inhibition of apoptosis with the pan-caspase inhibitor Z-VAD-FMK evokes an alternative cell death, described as programmed necrosis or necroptosis (133). Hence necroptosis in spheroids was inhibited with necrostatin-1 (Nec-1) to determine the relevance of necroptosis for COX-2 mRNA induction. In contrast to Z-VAD-FMK, which enhanced COX-2 mRNA (Figure 15), application of Nec-1 significantly reduced COX-2 mRNA in DU145 sh-control spheroids (Figure 17), suggesting that programmed necrosis may regulate COX-2 mRNA induction during spheroid formation. In conclusion, among the various microenvironmental factors in MCTS only necrotic DU145 cells showed the potency to induce COX-2 and PGE₂ production. This might be a mechanism to adapt to increased environmental stress found in MCTS and in early tumors in vivo. These data underline the role of necrotic

cells in altering gene expression of neighboring cells, generating a growth advantage to heterogeneous tumor cell populations.

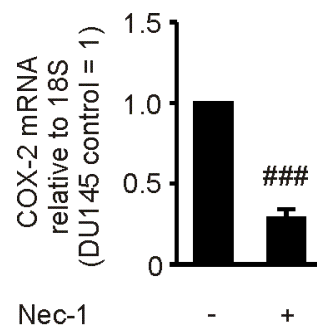


Figure 17: Necroptosis inhibitor necrostatin suppresses COX-2 induction during spheroid formation. DU145 cells were pre-treated with the necroptosis inhibitor necrostatin-1 for 30 min before seeding for spheroid generation. COX-2 mRNA expression in sh-control transfected DU145 spheroids was analyzed via qPCR after 24 h. Diamonds indicate significant differences between experimental groups and the control group in a one-sample t-test ([#], $p \leq 0.05$, ^{##}, $p \leq 0.01$, ^{###}, $p \leq 0.001$).

5.1.7 PGE₂ impairs activation of cytotoxic T cells

Beyond pure tumor growth, PGE₂ was also described as an immune suppressor in the literature (79). To prove this principle, the physiological relevance of tumor spheroid-produced PGE₂ in terminating activation of isolated T cells was tested. To mimic T cell activation, purified T cells were pre-activated with anti-CD3/anti-CD28 beads and pulsed with supernatants from sh-control or sh-mPGES-1 tumor spheroids every day for a time course of five days. Initially, it was observed that supernatants of sh-control (PGE₂ high) DU145 spheroids possessed a higher capacity to reduce numbers of IFN- γ producing cells than supernatants of sh-mPGES-1 (PGE₂ low) tumor spheroids. Addition of autologous PGE₂ was potent enough to recover inhibitory effects of PGE₂-deficient supernatants of sh-mPGES-1 tumor spheroids (Figure 18). This experiment clearly shows that tumor-derived PGE₂ is suppressive for infiltrating CTLs. PGE₂ therefore not only acts pro-tumoral in terms of promoting tumor cell growth, but also acts as an immune suppressive barrier to protect tumors from elimination by invading CTLs.

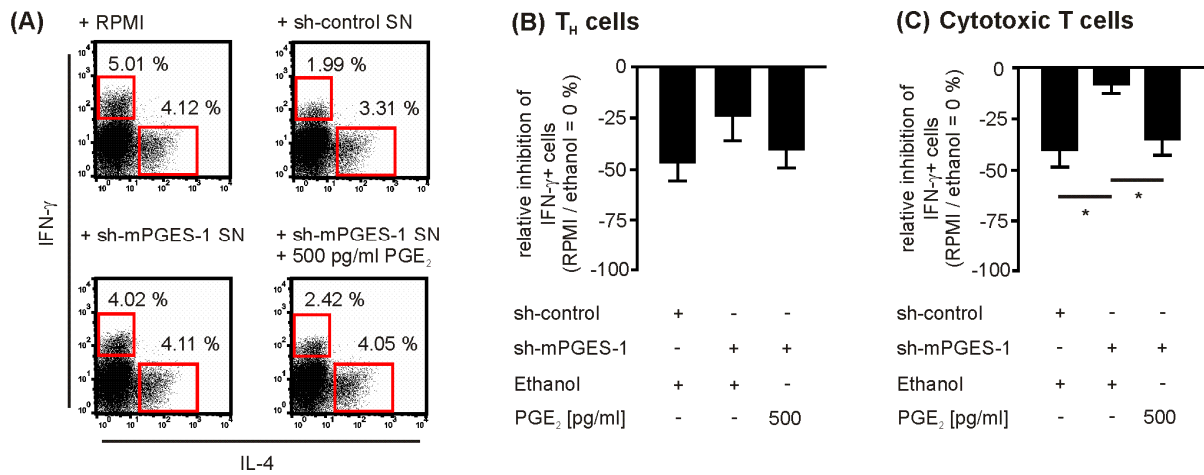


Figure 18: PGE₂ in spheroid supernatants limits IFN- γ production by activated T cells. Control (sh-control) or mPGES-1 knockdown (sh-mPGES-1) DU145 human prostate cancer cells were grown as spheroids for 10 days, growth medium was changed and supernatants were collected after additional three days. The solvent control (ethanol) or 500 pg/ml PGE₂ were added to spheroid supernatants before further use. 1×10^6 primary human pre-activated T cells were repetitively treated with 100 μ l spheroid supernatants or growth medium, each day for a period of five days. Percentage of IFN- γ ⁺ and IL-4⁺ cells was determined using intracellular staining and flow cytometry (gating strategy in Supplemental Figure 3). (A) Representative dot plots of all CD3⁺ T cells are shown. (B,C) Relative numbers of IFN- γ ⁺ T cells of (B) CD4⁺ TH cells or (C) CD8⁺ cytotoxic T cells were normalized to RPMI treated T cells (0 % inhibition). Data are means \pm SEM of T cells from five independent donors. Asterisks indicate significant differences between experimental groups (*, $p \leq 0.05$, **, $p \leq 0.01$, ***, $p \leq 0.001$).

5.2 Role of PGE₂ in immunoediting

In order to reject tumors, APcells such as DCs and macrophages prime TAA-sensitive CTLs to recognize and kill tumor cells expressing TAA (3.2). As countermeasures, tumors disrupt CTL activation by secreting immune suppressive PGE₂ as shown in chapter 5.1.7 (Figure 18). However, prior to priming of CTLs, PGE₂ may already interfere with immune activation by inactivating APcells. PGE₂ drives differentiation of DCs into myeloid-derived suppressor cells (MDSCs), a phagocyte cell type occurring with high abundance in tumors and capable of turning activated T cells into regulatory T cells (41,93). Additionally, PGE₂ impairs the ability of macrophages and DCs to induce anti-tumoral T_H1 responses by inhibition of the T_H1 cytokine IL-12 (79,95). To assess the impact of PGE₂ on shaping immune cell functions especially that of APcells, two different model approaches were chosen. First, human PBMC / breast cancer spheroid cocultures were used to monitor immune cell / tumor interactions in vitro, to define conditions that are required to mount an anti-tumoral response, and to confirm well-characterized signature markers such as CD80/CD86 expression on APcells or GrB expression in CTLs as measures of an induced anti-tumoral response. Second, the overall impact of mPGES-1 for cancer development was investigated by comparing data from the human 3D model with a mouse model, where the polyoma middle T oncogene (PyMT) was expressed under the control of the mouse mammary tumor virus (MMTV) promoter, inducing spontaneous mammary tumors.

5.2.1 Human PBMCs cocultured with MCF-7 tumor spheroids require activation to maintain allogenic responses

Spontaneous allogenic responses are possible when immune cells are facing foreign MHC molecules e.g. foreign non-self cells from another donor. Approximately 1-10 % of the whole T cell population may be alloreactive (134). Surprisingly, co-culturing PBMCs with MCF-7 spheroids alone did not result in effective reduction of spheroid sizes, indicating that no allo-response was induced. However, addition of lipopolysaccharide (LPS) or anti-CD3/anti-CD28 activation beads, i.e. immune activation, reduced tumor spheroid sizes (Figure 19). In the absence of PBMCs, tumor spheroid sizes were not affected by LPS (data not shown).

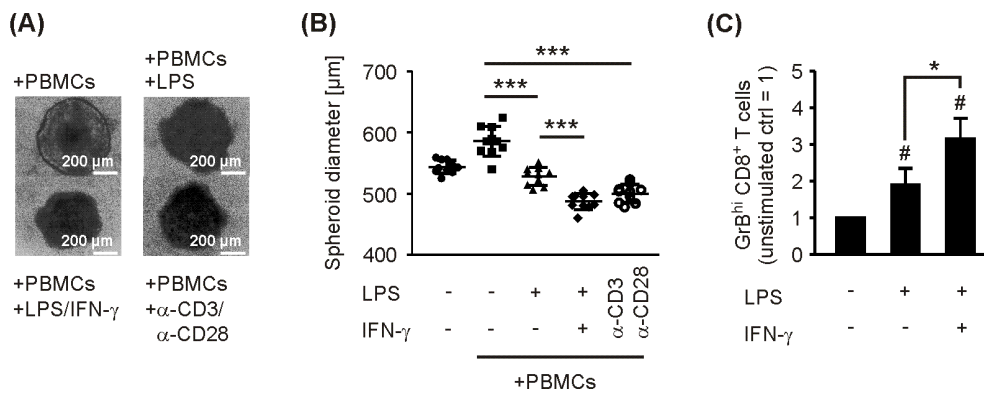


Figure 19: PBMCs require activation to restrict tumor spheroid sizes and to induce GrB^{hi} CTLs. PBMCs were pre-stimulated for 30 min as indicated and cocultured with MCF-7 tumor spheroids for two days. Spheroid sizes were assessed by microscopy. (A) Photographs of spheroid PBMC cocultures are shown and (B) diameters of at least nine tumor spheroids are displayed. Data are representatives of three independent experiments. (C) Normalized ratio of GrB^{hi} T cells after two days of coculture is displayed. Data are means \pm SD of four independent donors. Asterisks indicate significant differences between experimental groups (*, $p \leq 0.05$, **, $p \leq 0.01$, ***, $p \leq 0.001$). Diamonds indicate significant differences between experimental groups and the control group in a one-sample t-test (#, $p \leq 0.05$, ##, $p \leq 0.01$, ###, $p \leq 0.001$).

Addition of IFN- γ further strengthened the potency of LPS to induce anti-tumoral activity of PBMCs, since spheroid sizes were further reduced (Figure 19). Concomitantly, LPS increased numbers of granzyme B high (GrB^{hi}) cytotoxic T lymphocytes (CTLs), and addition of IFN- γ further elevated numbers of GrB^{hi} CTLs (Figure 19 and Figure 20). The fact that the cytotoxic response against the tumor correlated with the enhanced ability of PBMCs to reduce tumor spheroid sizes after LPS/IFN- γ activation indicates that human PBMCs require T_H1 activation to initiate an anti-tumoral response even in a MHC mismatched setting.

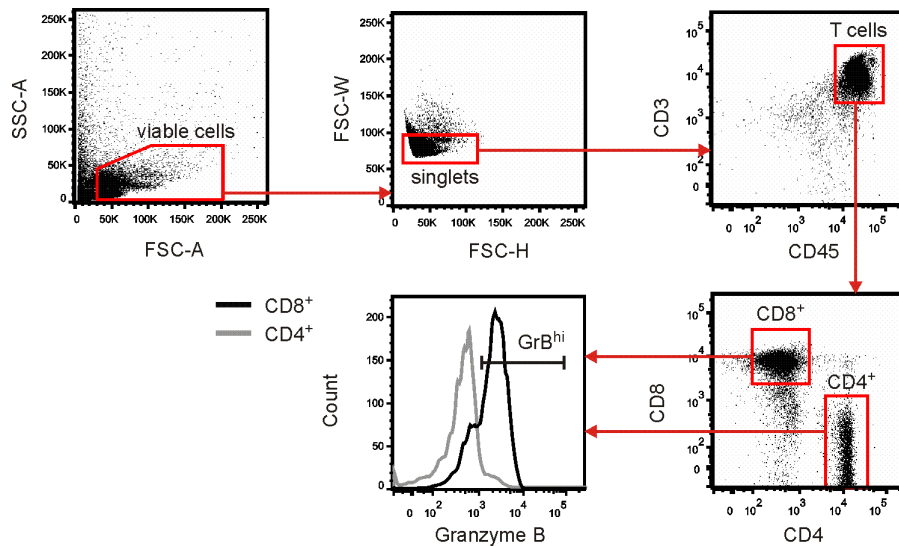


Figure 20: Gating strategy for parallel discrimination of different T cell subsets and intracellular detection of their respective Granzyme B expression. PBMCs were isolated from PBMC MCF-7 spheroid cocultures as described in Materials and Methods. First, viable cells were discriminated by gating $SSC-A^{low} FSC-A^{int}$. Cell doublets were discriminated by gating $FSC-W^{low}, FSC-H^{int}$ to define single cells. Single cells were classified as T cells ($CD45^{+}CD3^{+}$), T_H cells ($CD45^{+}CD3^{+}CD4^{+}$) and cytotoxic T lymphocytes ($CD45^{+}CD3^{+}CD8^{+}$). Granzyme B was stained in T cell subsets to determine the functionality of respective T cell subsets.

5.2.2 LPS or LPS/IFN- γ upregulate CD80 expression of $CD14^{+}CD11c^{+}$ phagocytes to induce GrB^{hi} CTLs

During antigen presentation, antigen-sensitive CTLs require activation by APCs to express GrB, which is triggered by binding of the costimulatory molecules CD80/CD86 on APCs to CD28 on T cells (135). LPS-activated $CD14^{+}CD11c^{+}$ phagocytes expressed significantly higher levels of inflammatory macrophage/DC marker CD80, and again addition of IFN- γ further strengthened CD80 expression. In contrast, CD86 expression was not significantly altered after LPS or LPS/IFN- γ challenge, whereas expression of the anti-inflammatory marker CD206 was significantly reduced in parallel (Figure 21, Figure 22), indicating that activation evokes an inflammatory phagocyte phenotype.

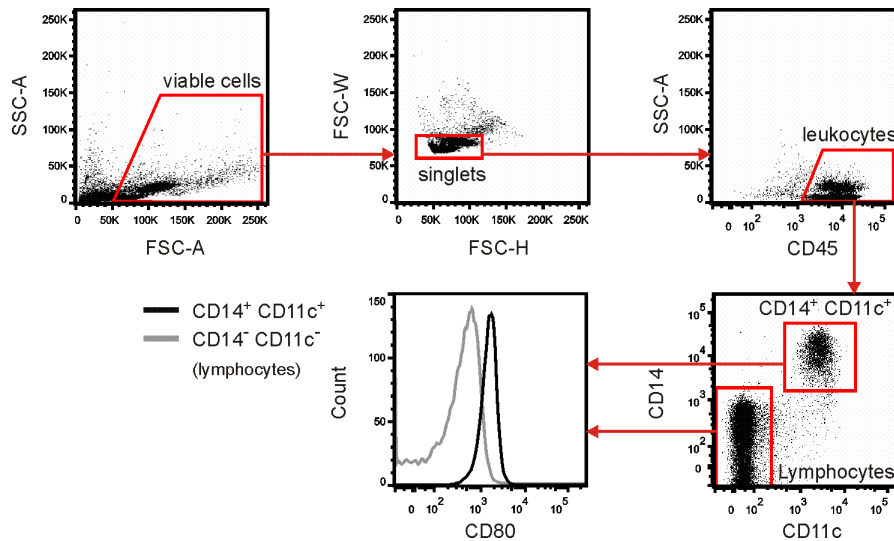


Figure 21: Gating strategy to detect CD14⁺CD11c⁺ phagocytes. PBMCs were isolated from PBMC MCF-7 spheroid cocultures as described in Materials and Methods. First, viable cells were discriminated by gating SSC-A^{low} FSC-A^{int}. Cell doublets were discriminated by gating FSC-W^{low}, FSC-H^{int} to define single cells. Single cells were classified as leukocytes (CD45⁺SSC^{low}), CD45⁺CD14⁺CD11c⁺ phagocytes and CD45⁺CD14⁺CD11c⁻ lymphocytes. Extracellular CD80, CD86, and CD206 were stained to characterize polarization of CD14⁺ CD11c⁺ phagocytes.

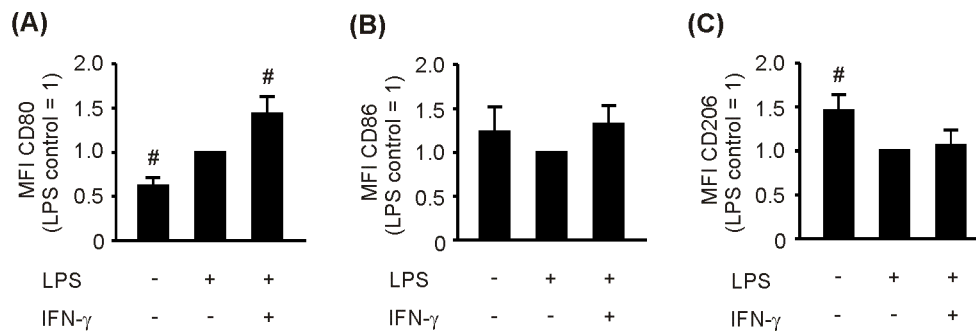


Figure 22: LPS or LPS/IFN- γ activation induces CD80 and inhibits CD206 expression on CD14⁺ CD11c⁺ phagocytes. PBMCs were pre-stimulated for 30 min as indicated and cocultured with MCF-7 tumor spheroids for two days. Normalized (A) CD80, (B) CD86, and (C) CD206 expression of CD14⁺ CD11c⁺ phagocytes is displayed. Data are means \pm SD of four independent donors. Asterisks indicate significant differences between experimental groups (*, $p \leq 0.05$, **, $p \leq 0.01$, ***, $p \leq 0.001$). Diamonds indicate significant differences between experimental groups and the control group in a one-sample t-test (#, $p \leq 0.05$, ##, $p \leq 0.01$, ###, $p \leq 0.001$).

To test whether CD80 expression on phagocytes was a prerequisite for CTL activation, interception with CD80 using an anti-CD80 antibody under activating conditions (LPS/IFN- γ) was expected to diminish numbers of GrB^{hi} expressing CTLs and prevent tumor spheroid killing. Indeed, use of the CD80-intercepting antibody efficiently blunted numbers of GrB^{hi} CTLs and abolished tumor spheroid killing,

whereas a CD86-intercepting antibody and the isotype control neither affected GrB^{hi} CTLs numbers nor tumor spheroid size reduction (Figure 23).

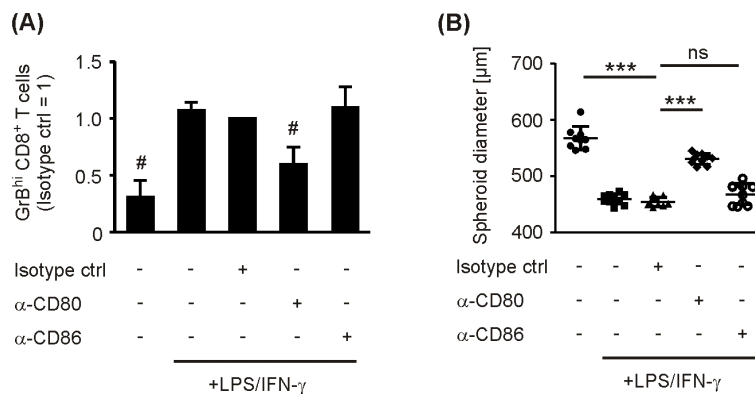


Figure 23: CD80 expression is needed for induction of GrB^{hi} CTLs and tumor spheroid killing. PBMCs were pre-stimulated for 30 min as indicated and cocultured with MCF-7 tumor spheroids for two days. (A) Normalized ratio of GrB^{hi} CTLs after two days of coculture is displayed. Data are means \pm SD of four independent donors. (B) Diameters of at least nine tumor spheroids are displayed. Data are representatives of three independent experiments. Asterisks indicate significant differences between experimental groups (*, $p \leq 0.05$, **, $p \leq 0.01$, ***, $p \leq 0.001$). Diamonds indicate significant differences between experimental groups and the control group in a one-sample t-test (#, $p \leq 0.05$, ##, $p \leq 0.01$, ###, $p \leq 0.001$).

5.2.3 Activation of PBMCs with LPS triggers COX-2/mPGES-1-derived PGE₂

After characterizing the in vitro tumor killing model, the role of PGE₂ in modulating the immune response was assessed. In earlier chapters of this work, it was shown that 3D aggregation of DU145 prostate cancer cells triggers expression of PGE₂ synthesizing enzymes by upregulation of COX-2 (5.1.3) Therefore, it was surprising that MCF-7 breast cancer cells neither upregulated COX-2 mRNA expression nor PGE₂ secretion upon spheroid formation (Figure 24). Apart from tumor cells, immune cells may be major contributors to PGE₂ production in tumors. However, coculturing of PBMCs with MCF-7 breast cancer spheroids also did not result in the production of relevant PGE₂ amounts (Figure 25), whereas LPS significantly triggered PGE₂ synthesis, indicating that an inflammatory milieu in tumors is required to provoke PGE₂ accumulation. Stimulation with LPS induced PGE₂ as well as other prostanoids such as PGF_{2α}, PGD₂, and TXB₂ (Figure 26).

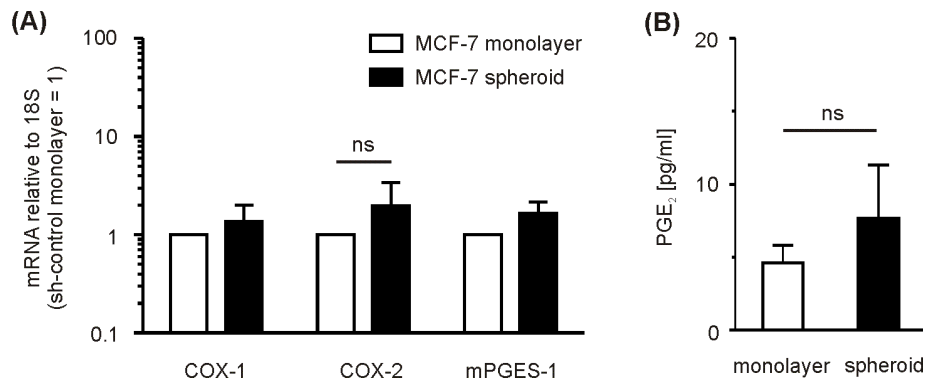


Figure 24: MCF-7 cells do not upregulate COX-2 mRNA upon spheroid formation. MCF-7 human breast cancer cells were detached and seeded on agarose to generate tumor spheroids. (A) MRNA expression of PGE₂ metabolizing enzymes in monolayer cells or five days old tumor spheroids was analyzed using qPCR and (B) PGE₂ levels in MCF-7 spheroid culture supernatants were determined by PGE₂ EIA. Data are means \pm SD of four independent experiments. Asterisks indicate significant differences between experimental groups (*, $p \leq 0.05$, **, $p \leq 0.01$, ***, $p \leq 0.001$). Diamonds indicate significant differences between experimental groups and the control group in a one-sample t-test (#, $p \leq 0.05$, ##, $p \leq 0.01$, ###, $p \leq 0.001$).

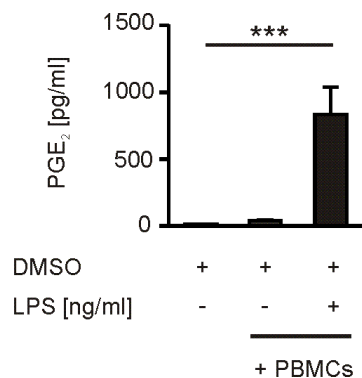


Figure 25: LPS activation of PBMCs induces PGE₂ production. PBMCs were pre-stimulated for 30 min as indicated and cocultured with MCF-7 tumor spheroids for two days. PGE₂ levels in supernatants of MCF-7 spheroid cultures or PBMC MCF-7 spheroid cocultures were measured by PGE₂ EIA. Data are means \pm SD of four independent experiments. Asterisks indicate significant differences between experimental groups (*, $p \leq 0.05$, **, $p \leq 0.01$, ***, $p \leq 0.001$).

Therefore, blocking all prostanoids with the COX-2 inhibitor celecoxib (Cxb) as opposed to selective reduction of PGE₂ by inhibiting mPGES-1 would clarify the impact of PGE₂ on LPS-induced CD80 expression. This question is relevant as it is under discussion if other prostanoids may compensate the biological function of PGE₂ in its absence. Both Cxb and C3 inhibited PGE₂ production in activated PBMC tumor spheroid cocultures. However, C3 did not affect levels of other prostanoids at all, suggesting that no shunting of arachidonic acid towards other prostanoids occurred. As CD80 expression was functionally coupled to spheroid killing, the

potency of Cxb and C3 to affect CD80 expression was compared. CD80 expression on LPS-challenged tumor-associated phagocytes was enhanced by Cxb. Although C3 selectively inhibited PGE₂ synthesis, it raised LPS-induced CD80 expression comparable to Cxb (Figure 27), suggesting PGE₂ as the major prostanoid responsible for modulating CD80 expression on tumor-associated phagocytes. Incubation of non-activated PBMC spheroid cocultures with Cxb and C3 failed to enhance levels of CD80 expression. Thus, PGE₂ inhibition modulates but does not activate CD80 expression per se. CD86 and CD206 expression were not significantly altered after Cxb or C3 incubation, indicating that blocking PGE₂ production selectively affects CD80 expression (Figure 27).

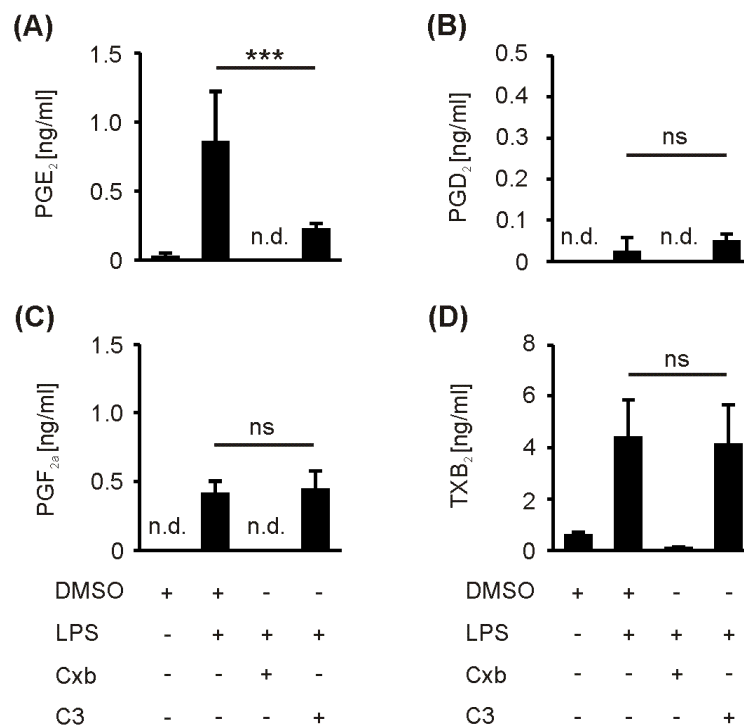


Figure 26: C3 selectively inhibits synthesis of PGE₂. PBMCs were pre-stimulated for 30 min as indicated and cocultured with MCF-7 tumor spheroids for two days. Cocultures were challenged with the COX-2 inhibitor celecoxib (Cxb) or the mPGES-1 inhibitor C3. Prostanoids (A) PGE₂, (B) PGD₂, (C) PGF_{2α}, and (D) TXB₂ in supernatants of PBMC MCF-7 spheroid cocultures were measured by LC-MS/MS. Data are means ± SD of at least four independent donors. Asterisks indicate significant differences between experimental groups (*, $p \leq 0.05$, **, $p \leq 0.01$, ***, $p \leq 0.001$).

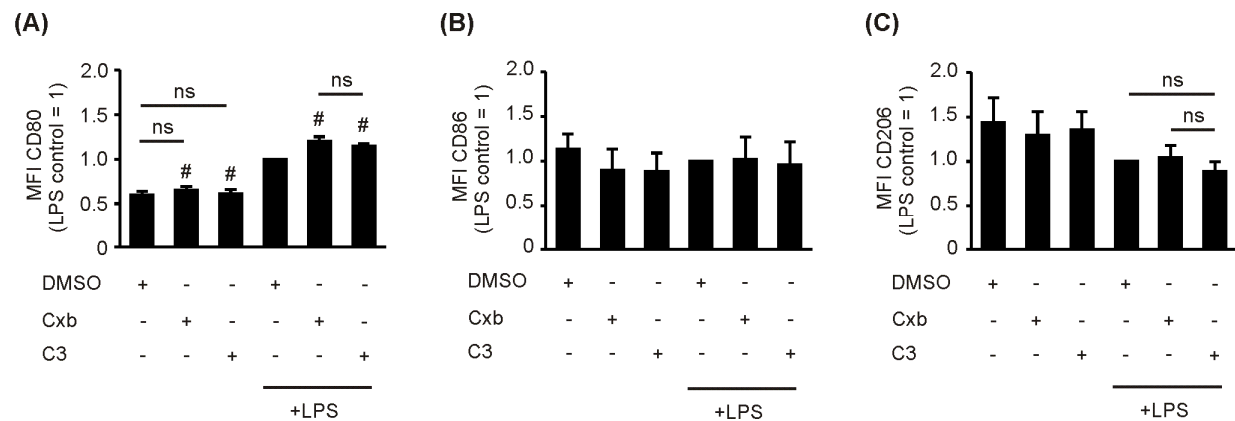


Figure 27: Inhibition of PGE₂ production enhances CD80 expression on CD14⁺ CD11c⁺ phagocytes. PBMCs were pre-stimulated for 30 min as indicated and cocultured with MCF-7 tumor spheroids for two days. Cocultures were challenged with the COX-2 inhibitor celecoxib (Cxb) or the mPGES-1 inhibitor C3. Normalized (A) CD80, (B) CD86, and (C) CD206 expression of CD14⁺ CD11c⁺ phagocytes is displayed. Data are means ± SD of at least five independent donors. Asterisks indicate significant differences between experimental groups (*, $p \leq 0.05$, **, $p \leq 0.01$, ***, $p \leq 0.001$). Diamonds indicate significant differences between experimental groups and the control group in a one-sample t-test (#, $p \leq 0.05$, ##, $p \leq 0.01$, ###, $p \leq 0.001$).

5.2.4 PGE₂ limits CD80 expression by activated CD14⁺ CD11c⁺ phagocytes via EP2 signaling and accumulation of cAMP

Depletion of PGE₂ in LPS-stimulated cocultures using C3 was used as a standard set-up in the following experiments. Substitution of authentic PGE₂ significantly inhibited LPS/C3-triggered CD80 expression at concentrations of 100 pg/ml, but did not affect CD86 expression (Figure 28). Surprisingly, CD206 expression was also inhibited by PGE₂ at 1 µg/ml (Figure 28). As discussed in chapter 3.4.1, PGE₂ signals via the PGE₂ receptors EP1-4, for which selective agonists are available. Application of the EP2 agonist butaprost, but not the EP4 agonist cay10580 or the EP1/3 agonist sulprostone, suppressed expression of LPS/C3-induced CD80 (Figure 29). EP2 activation did not affect CD86 expression on phagocytes but significantly reduced CD206 expression (Figure 29). EP2 and EP4 cause intracellular cAMP accumulation, which is simultaneously degraded by phosphodiesterase-4 (PDE4). Application of the PDE4 inhibitor rolipram enhances intracellular accumulation of cAMP and significantly reduced LPS/C3-triggered CD80 expression (Figure 29). Again, CD86 expression did not correlate with CD80 expression but CD206 followed a similar regulation pattern as CD80 (Figure 29).

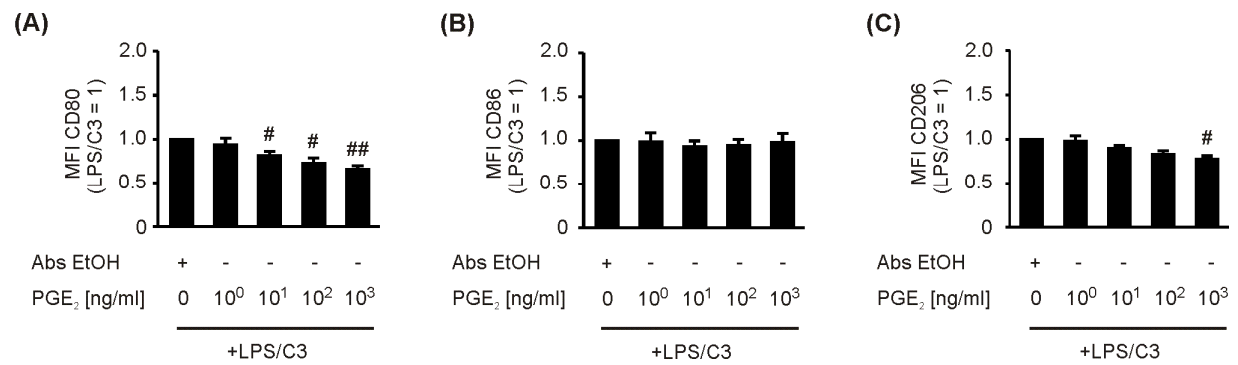


Figure 28: PGE₂ inhibits CD80 and CD206 expression on CD14⁺ CD11c⁺ phagocytes. PBMCs were pre-stimulated for 30 min as indicated and cocultured with MCF-7 tumor spheroids for two days. Cocultures were dose-dependently challenged with authentic PGE₂. Normalized (A) CD80, (B) CD86, and (C) CD206 expression of CD14⁺ CD11c⁺ phagocytes is displayed. Data are means ± SD of at least four independent donors. Asterisks indicate significant differences between experimental groups (*, p ≤ 0.05, **, p ≤ 0.01, ***, p ≤ 0.001). Diamonds indicate significant differences between experimental groups and the control group in a one-sample t-test (#, p ≤ 0.05, ##, p ≤ 0.01, ###, p ≤ 0.001).

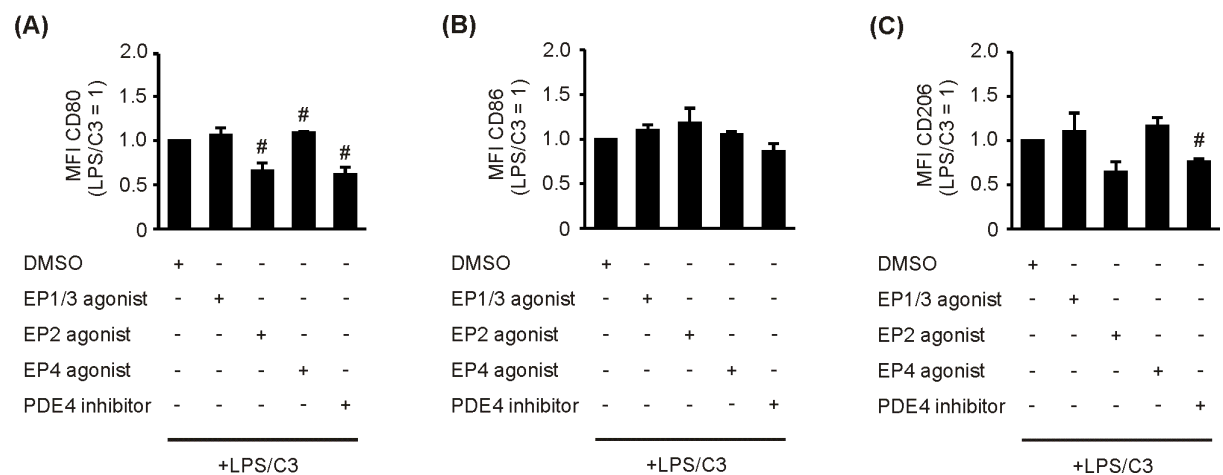


Figure 29: EP2 signaling and upregulation of cAMP CD80 and CD206 expression on CD14⁺ CD11c⁺ phagocytes. PBMCs were pre-stimulated for 30 min as indicated and cocultured with MCF-7 tumor spheroids for two days. Cocultures were dose-dependently challenged with the EP1/3 agonist sulprostone, the EP2 agonist butaprost, the EP4 agonist cay10580 and the PDE4 inhibitor rolipram. Normalized (A) CD80, (B) CD86, and (C) CD206 expression of CD14⁺ CD11c⁺ phagocytes is displayed. Data are means ± SD of at least five independent donors. Asterisks indicate significant differences between experimental groups (*, p ≤ 0.05, **, p ≤ 0.01, ***, p ≤ 0.001). Diamonds indicate significant differences between experimental groups and the control group in a one-sample t-test (#, p ≤ 0.05, ##, p ≤ 0.01, ###, p ≤ 0.001).

Taken together, LPS/C3-induced CD80 expression is suppressed by EP2 signaling and upregulation of intracellular cAMP in tumor-associated human phagocytes. In

parallel, activation of the EP2/cAMP-pathway also reduced expression of the anti-inflammatory macrophage marker CD206.

5.2.5 mPGES-1-deficiency delays tumor development in vivo

To recapitulate the tumor killing parameters observed in the human in vitro setting in a breast cancer model in vivo, mPGES-1-deficient mice were crossed into the PyMT background. Female PyMT mice are prone to develop spontaneous breast cancer at the local site of their mammary glands (19). Tumors were first observed in 8 week old female PyMT mice and tumor development was monitored until sacrifice. The deficiency of mPGES-1 delayed tumor development in PyMT mice, reducing numbers of tumor burdened mammary glands per mouse compared to wildtype PyMT mice 16 weeks after birth (Figure 30). 20 week old mice were sacrificed and screened for their respective tumor sizes and expression of COX mRNA in these tumors. Loss of mPGES-1 significantly reduced tumor mass (Figure 30). Interestingly, the distribution of different sized tumors in mPGES-1-deficient PyMT mice was not abnormal compared to wildtype PyMT mice, since PyMT mice deficient in mPGES-1 developed lower numbers of small (≤ 0.5 cm), medium (0.5 – 1 cm) and big (> 1 cm) tumors (Figure 30b).

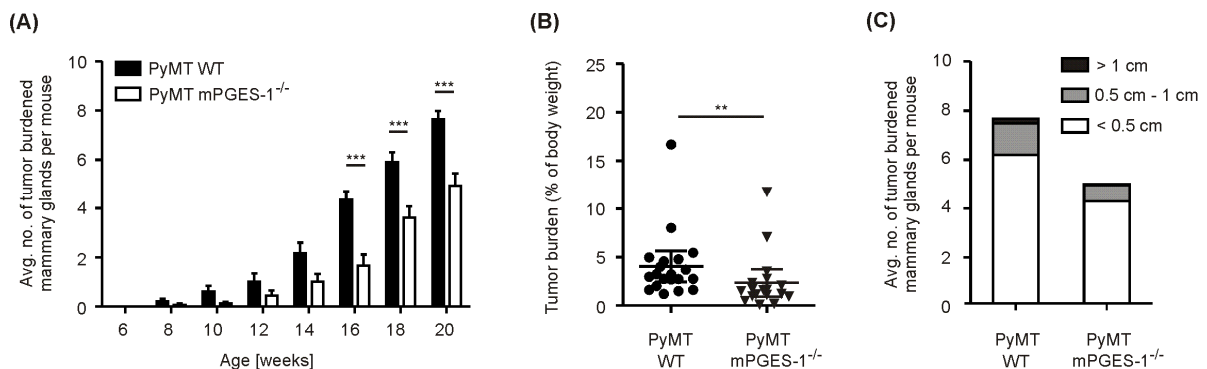


Figure 30: mPGES-1-deficiency impairs PyMT tumor growth. (A) The average number of tumor burdened mammary glands per mouse is displayed. (B-C) PyMT mice were sacrificed 20 weeks after birth. (B) Tumor burden was calculated out of the total tumor mass divided by total body mass. Mann-Whitney t-test was performed due to non-parametric distribution of mouse tumor burden analyzed with the Shapiro-Wilk normality test. (C) Tumors were categorized and their respective numbers are displayed. Data are means \pm SD of 20 wildtype mice and 18 knockout mice. Asterisks indicate significant differences between experimental groups (*, $p \leq 0.05$, **, $p \leq 0.01$, ***, $p \leq 0.001$).

Importantly, both COX-1 and COX-2 mRNA were significantly expressed in PyMT tumors, independent of the mPGES-1 status (Figure 31), indicating that prostaglandin synthesis might per se occur in PyMT tumors.

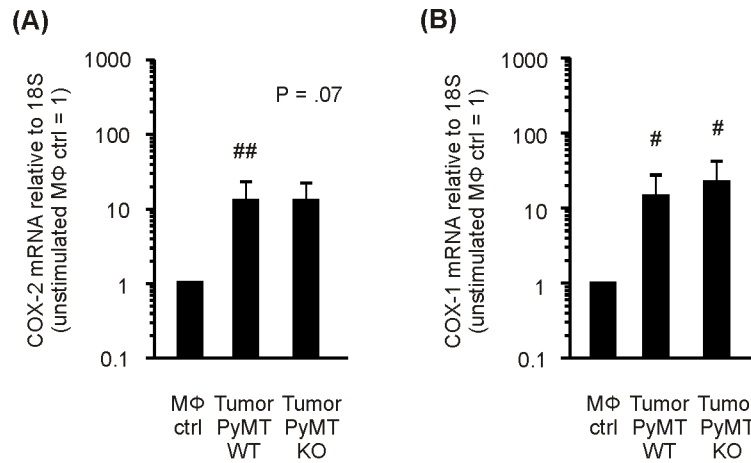


Figure 31: COX mRNA is expressed in PyMT tumors. PyMT mice were sacrificed 20 weeks after birth. mRNA expression of (A) COX-2 and (B) COX-1 in PyMT tumors and unstimulated BMDM was analyzed using qPCR. Data are means \pm SD of at least four donors. Asterisks indicate significant differences between experimental groups (*, $p \leq 0.05$, **, $p \leq 0.01$, ***, $p \leq 0.001$). Diamonds indicate significant differences between experimental groups and the control group in a one-sample t-test (#, $p \leq 0.05$, ##, $p \leq 0.01$, ###, $p \leq 0.001$).

5.2.6 Numbers of CD11c⁺ TAMs are increased in tumors of mPGES-1 knockout PyMT mice

Single cell suspensions of PyMT tumors were analyzed by polychromatic FACS to characterize tumor infiltrating leukocyte populations and to correlate reduced tumor outgrowth with a different immune status in the tumors. The majority of tumor infiltrating cells was of myeloid origin such as monocytes, neutrophils, or tumor-associated macrophages (TAMs). CD11c single positive DCs scarcely exist in PyMT tumors, whereas the majority of phagocytes coexpress the macrophage marker F4/80 and the DC marker CD11c, reported to be markers for tumor-associated macrophages infiltrating PyMT tumors (136). In general, tumor-associated macrophages promote tumor growth and their abundance at the tumor site is often associated with bad prognosis in breast cancer patients (33). Surprisingly, numbers of F4/80⁺ CD11c⁺ phagocytes were increased in mPGES-1^{-/-} PyMT tumors (Figure 32). Thus, the usual correlation between breast tumor growth and the number of tumor-infiltrating phagocytes was not reflected in the mPGES-1^{-/-} PyMT system. In

concordance with the *in vitro* observations, altered polarization of F4/80⁺ CD11c⁺ phagocytes in mPGES-1^{-/-} tumors might explain the observed differences in tumor growth.

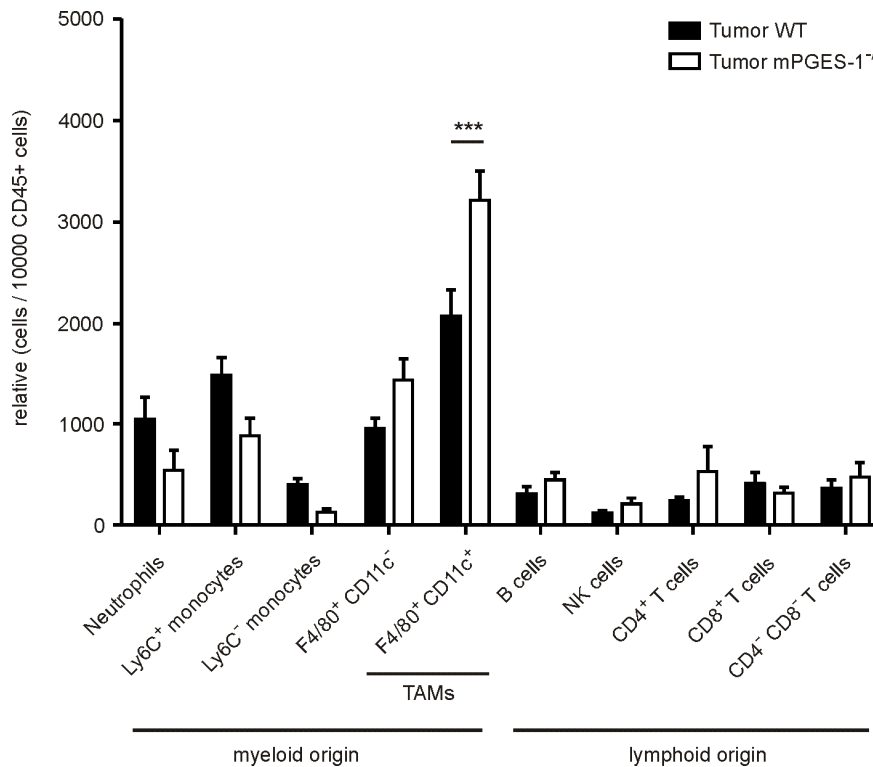


Figure 32: mPGES-1-deficiency increases the abundance of F4/80⁺ CD11c⁺ phagocytes in PyMT tumors. PyMT mice were sacrificed 20 weeks after birth. Immune cell subsets are determined by flow cytometry. Data are means \pm SEM of 11 wildtype mice and 9 knockout mice. Asterisks indicate significant differences between experimental groups (*, $p \leq 0.05$, **, $p \leq 0.01$, ***, $p \leq 0.001$).

Therefore F4/80⁺ CD11c⁺ phagocyte polarization in tumors as compared to macrophage populations in the spleen of PyMT mice was assessed using flow cytometry (Figure 33, Figure 34). However, alterations in CD80, CD86, and CD206 expression were not affected by mPGES-1-deficiency in F4/80⁺ CD11c⁺ phagocytes in tumor or spleen (Figure 34). Importantly, the overall levels of CD80 and CD86 expressed by F4/80⁺ CD11c⁺ phagocytes equaled levels found in non-activated BMDM (Figure 35). These findings imply that tumor-associated F4/80⁺ CD11c⁺ phagocytes are massively deactivated at the tumor site, independent of the presence of PGE₂. The situation might be similar to non-activated PBMCs infiltrating 3D human spheroids, where an activating stimulus is required to show a modulating role of PGE₂ in anti-tumor immunity. Interestingly, not only an activating stimulus per se, but also the tumor environment might be necessary to observe immune modulating

effects of PGE₂ since BMDM from wildtype or mPGES-1^{-/-} mice did not show alterations in CD80 or CD86 induction after stimulation with LPS/IFN- γ despite of their characteristic prostanoid profiles (Figure 35, Figure 36).

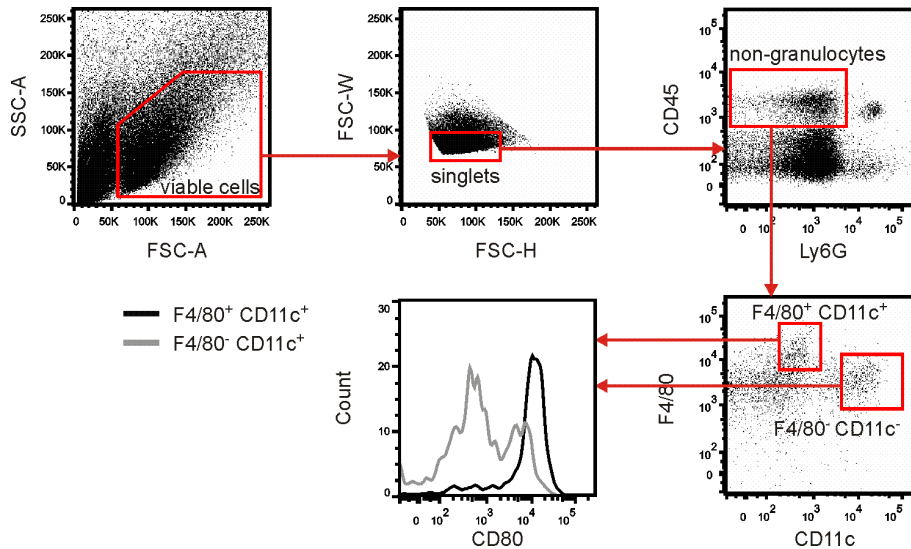


Figure 33: Gating strategy for discrimination of F4/80⁺ CD11c⁺ phagocytes in PyMT breast tumors and detection of their respective polarization markers. PyMT mice were sacrificed 20 weeks after birth and tumor suspension cells were isolated from PyMT breast tumors as described in Materials and Methods. First, viable cells were discriminated by gating SSC-A^{low} FSC-A^{int}. Cell doublets were discriminated by gating FSC-W^{low}, FSC-H^{int} to define single cells. Single cells were classified as leukocytes (CD45⁺Ly6G^{low}), CD45⁺F4/80⁺CD11c^{int} TAM-like phagocytes, and CD45⁺F4/80^{int}CD11c⁺ classical DCs. Extracellular CD80, CD86, and CD206 were stained to characterize polarization of F4/80⁺ CD11c^{int} phagocytes.

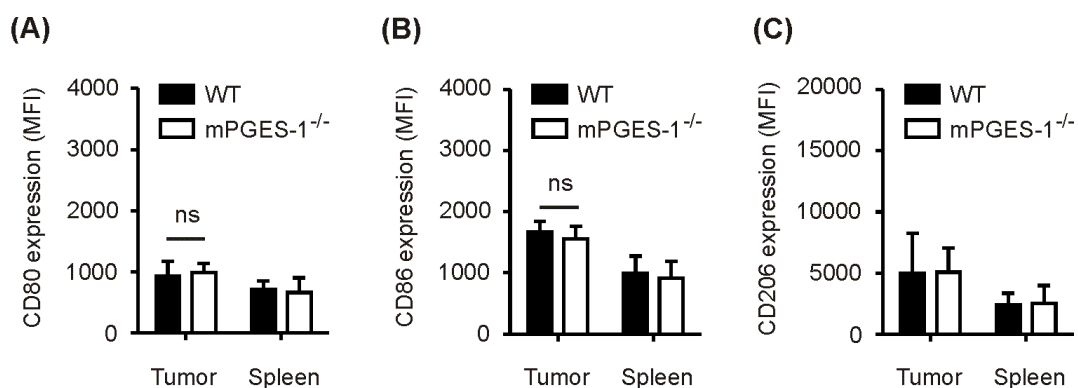


Figure 34: Polarization markers of F4/80⁺ CD11c⁺ macrophages in tumors and spleen of PyMT mice. (A) CD80, (B) CD86, and (C) CD206 expression of F4/80⁺ CD11c⁺ phagocytes in tumor and spleen tissue are displayed. Data are means \pm SD of at least six independent donors. Asterisks indicate significant differences between experimental groups (*, $p \leq 0.05$, **, $p \leq 0.01$, ***, $p \leq 0.001$).

In conclusion, selective immune modulating effects of PGE₂ might be most apparent in a set-up that comprises both inflammatory (LPS/IFN- γ) as well as anti-inflammatory (breast tumor microenvironment) components. Future experiments are required to test this hypothesis, e.g. in a setting of immunogenic chemotherapy.

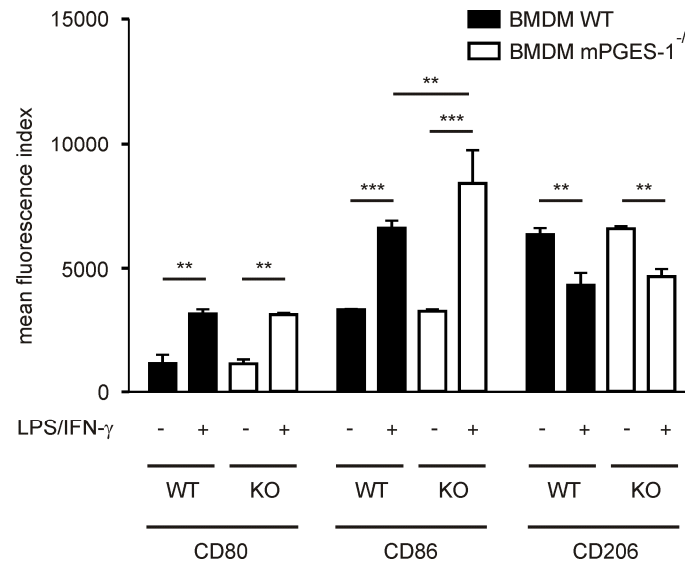


Figure 35: mPGES-1-deficiency does not enhance CD80 expression of BMDM. CD80, CD86, and CD206 expression of F4/80⁺ CD11c⁺ phagocytes after 48h of cultivation is displayed. Data are means \pm SD of at least four independent donors. Asterisks indicate significant differences between experimental groups (*, p \leq 0.05, **, p \leq 0.01, ***, p \leq 0.001).

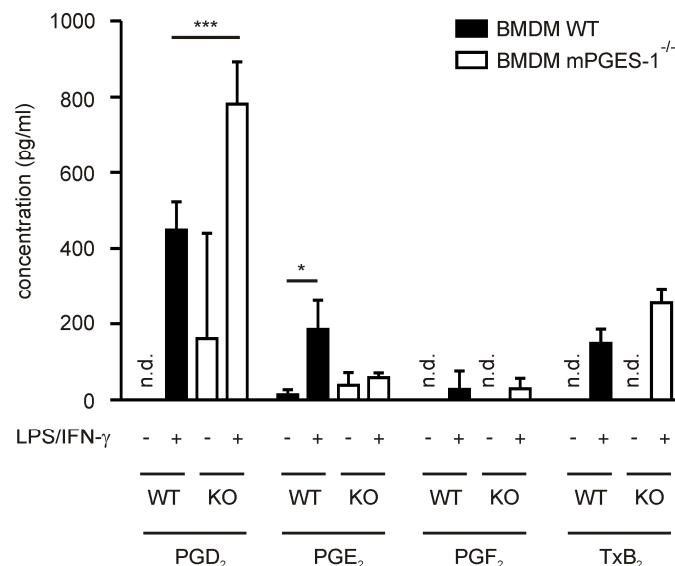


Figure 36: BMDM shift prostaglandin profile. BMDM of WT or mPGES-1 KO mice were challenged with LPS/IFN- γ or left untreated for 24h and the prostanoid profile in BMDM culture supernatants were measured by LC-MS/MS. Data are means \pm SD of at least four independent donors. Asterisks indicate significant differences between experimental groups (*, p \leq 0.05, **, p \leq 0.01, ***, p \leq 0.001).

6 Discussion

6.1 Autologous PGE₂ production by prostate cancer tumor spheroids

Since its discovery, PGE₂ has been depicted as an inflammatory agent in the literature, but in reality it also possesses anti-inflammatory properties (77,79), which makes its impact on tumorigenesis even more intriguing. One question of this work was whether mPGES-1-derived PGE₂ may contribute to prostate cancer cell growth, especially in environments, which do not primarily arise out of inflammatory stimuli. Surprisingly, a growth handicap of sh-mPGES-1-transfected DU145 cells grown in monolayer was not observed (5.1.1), which could be explained as a consequence of minimum detectable amounts of intracellular COX-2 and extracellular PGE₂ found in monolayer cultures (5.1.2), rendering the expression of mPGES-1 obsolete. Upon spheroid formation, DU145 cells are destined to face cell aggregation-induced cell stress (as a consequence of the oxygen and nutrient gradients and supply-deprived areas within tumor spheroids), which triggered COX-2 expression as the rate-limiting step for PGE₂ synthesis. In contrast, mPGES-1 expression impacts the growth of human prostate cancer cells grown as MCTS, because mPGES-1 needs COX-2 to fuel production of PGH₂ in order to convert PGH₂ to PGE₂, which means that mPGES-1 expression is only relevant in the presence of COX-2. Knockdown of mPGES-1 significantly repressed the percentage of viable cells and increased the percentage of necrotic cells in MCTS thereby impairing spheroid growth (5.1.6). Thus, these data suggest a model where necrosis-dependent induction of COX-2 and concomitant PGE₂ secretion protects living bystander cells from harmful necrotic cell-derived mediators. In the absence of PGE₂ secretion due to mPGES-1 knockdown, a stress cascade is triggered, which results in delayed tumor growth.

6.2 Pharmacological inhibition of PGE₂ synthesis

Pharmacological inhibition of spheroid growth with celecoxib or DMC (5.1.4) proved to be difficult, since availability of pharmacological agents for inner cell layers of MCTS underlies diffusion kinetics, which are ill-defined so far and are deemed responsible for resulting in higher working concentrations of inhibitors used than

common IC₅₀-values would suggest (137-138). Increasing the concentration of celecoxib beyond 50 μ M not only blocks COX-2 activity but also reduces Akt activity in a COX-2-independent manner (139). Thus, off-target effects might explain the inhibitory effect of 10 μ M celecoxib on cell growth of monolayer sh-control transfected DU145 cells, while knockdown of mPGES-1 did not impair growth of monolayer DU145 cells (5.1.4). The relevance of PGE₂ in monolayer cell cultures is likely restricted by its low abundance as compared to the high levels of PGE₂ measured in MCTS, bringing forth COX-2-independent effects of celecoxib. Additionally, celecoxib did not affect the growth of mPGES-1-deficient monolayer DU145 cells either, implicating a crosstalk of COX-2-dependent and -independent effects of celecoxib. Inhibition of mPGES-1 using DMC only impaired tumor growth of MCTS, but had no significant effect on growth of monolayer cells, emphasizing the essential role of COX-2/mPGES-1-derived autocrine PGE₂ for MCTS growth.

6.3 Necrotic cells induced COX-2 expression in DU145 cells

Previous studies have suggested that apoptotic cells stabilize COX-2 mRNA in macrophages through a S1P-dependent mechanism (140). A high percentage of apoptotic (active caspase3⁺) cells in MCTS was observed (5.1.6), correlating with elevated COX-2 in MCTS. However, the necrotic shift induced by applying the pan-caspase inhibitor Z-VAD-FMK was accompanied by further COX-2 mRNA induction and accumulation of extracellular PGE₂ (5.1.6). Also, co-culturing sh-control DU145 cells with isolated necrotic cells led to COX-2-derived PGE₂ production, although the increase of COX-2 mRNA did not match those levels abundant in MCTS cells. Hence, additional unknown environmental cues cannot be ruled out, which may promote COX-2 mRNA induction in MCTS. An alternative and more feasible explanation emphasizes that heat-triggered necrosis does not fully recapitulate necrosis in three dimensional tumor aggregates. Additionally, monolayer cells may be less susceptible to stress signals due to enhanced survival signaling through planar adhesion to cell culture dish surfaces. Given the limitations of monolayer cell-necrotic cell cocultures in accurately mimicking 3D environments, technical difficulties exist in describing mechanisms by which the presence of necrotic cell subsets in MCTS translates into such profound changes in COX-2 expression of tumor cells.

Nevertheless, these data confirm that necrotic cells are potent in inducing COX-2 expression and take part in enhancing COX-2 levels during spheroid formation.

The mode of tumor cell death is decisive in triggering specific immune responses. This currently wide-spread and accepted view envisions necrotic cells to be major inducers of inflammation, whereas apoptotic cells terminate inflammation (31). Modern anti-tumor therapy tends to include combinations of therapeutic agents to treat, for instance, pancreatic or colorectal cancer (141-142). Especially coupling of the properties of NSAIDS with those of apoptosis-triggering agents shows promise for cancer therapy (143), even though many NSAIDS such as celecoxib already possess intrinsic COX-2-independent pro-apoptotic effects (144). Still, some investigators raised the question whether inhibition of tumor apoptosis rather than inducing apoptosis *per se* would be beneficial for patient survival (106), since tumor repopulation at irradiated tumor sites was mediated by apoptotic cells in an active caspase3-dependent manner, triggering PLA₂ activity and release of PGE₂ (70,111). These data implicate that prevention of apoptosis does not solve this dilemma, since shifting of cells towards necrosis induced COX-2 expression to an even greater extent. Indeed, a protective role of caspases against necrosis upon cell stress has been suggested by investigators as inhibition of caspase 8 in the presence of apoptotic stimuli leads to programmed necrosis or necroptosis (133,145). In my experiments, use of the apoptosis inhibitor Z-VAD-FMK failed to prevent cells from undergoing cell death and further enhanced COX-2-driven protective mechanisms (5.1.6). However, using the necroptosis inhibitor Nec-1 impaired spheroid formation-induced COX-2 mRNA, suggesting a potential involvement of necroptosis, thereby supporting past reports of Z-VAD-FMK to shift apoptosis towards necroptosis after death receptor-triggered stimuli (146). In fact, the meaning of cell death in MCTS, reflecting physiological situations in tumors, may be an inevitable process. For this reason, the question was addressed, whether COX-2 mRNA induction and PGE₂ accumulation may be a general consequence of cell stress and cell death, protecting the collective tissue population from further damage. Therefore, since cell death in general seems to favor PGE₂ production either way, inhibiting PGE₂-synthesizing or signaling pathways appears to be more attractive from a therapeutic point of view. MPGES-1-derived PGE₂ did not only promote MCTS growth but also inhibited the potential of T cells to produce T_H1 inflammation-inducing IFN- γ (Figure 18). Similar

observations were made in vitro in other reports, where PGE₂ shifted T_H1 towards T_H2-type responses (79).

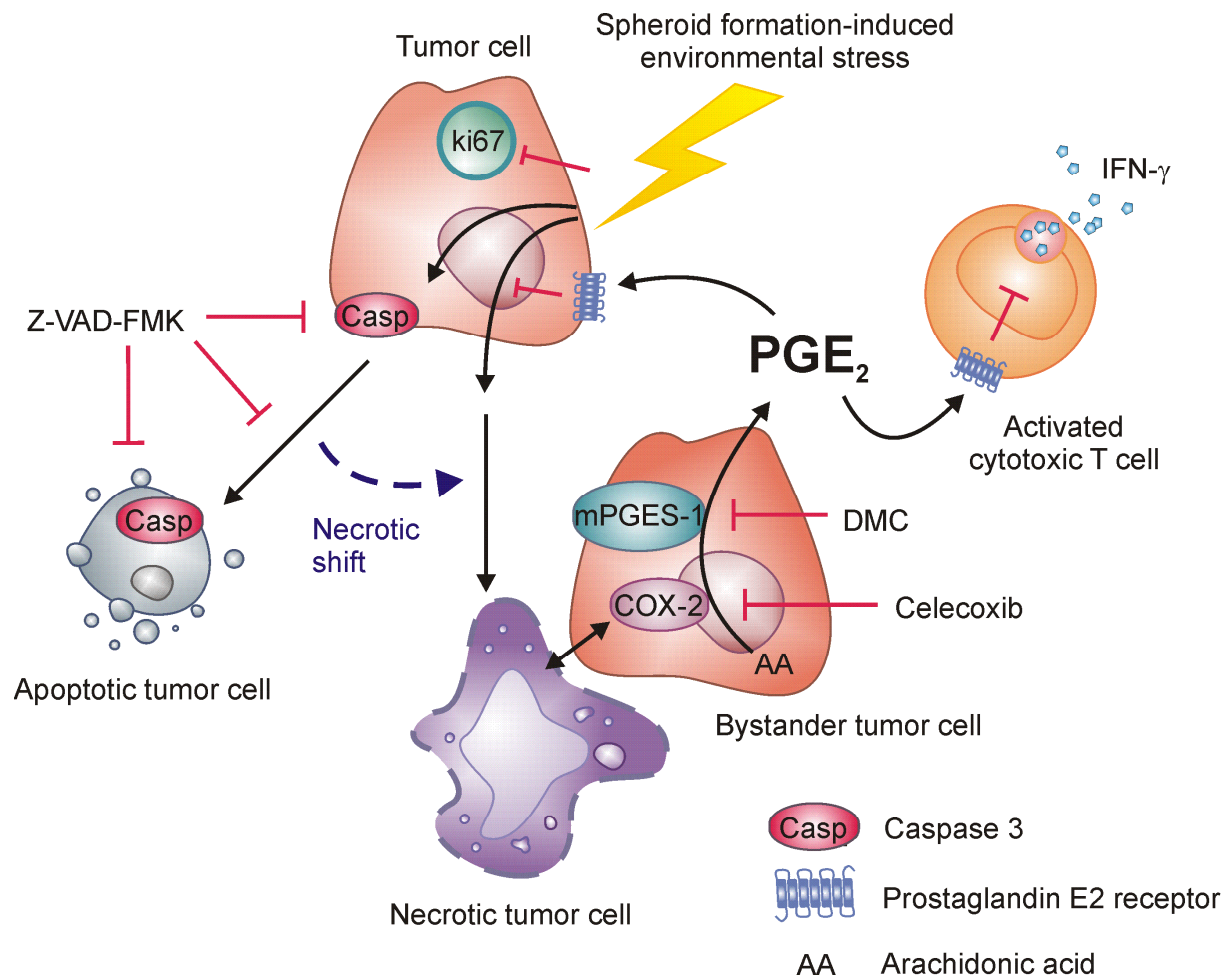


Figure 37: Overview: Stress-induced necrotic cells upregulate COX-2 and PGE₂ in DU145 tumor spheroids. Spheroid formation-induced environmental stress forces tumor cells to undergo apoptosis and/or necrosis. Inhibition of caspases with Z-VAD-FMK prevents apoptosis in MCTS, but favors necrotic cell formation, which in turn induces the PGE₂ synthesizing enzyme COX-2 in nearby cells. Inhibition of COX-2 or its downstream enzyme mPGES-1 impairs formation of PGE₂ and stalls growth of MCTS. Finally, apart from tumor growth, mPGES-1-derived PGE₂ also inhibits activated cytotoxic T cells.

However, the role of PGE₂ as an immune suppressor was challenged, since its inhibitory effect on T_H1 responses was observed rather in vitro than in vivo (147). In vivo, application of EP4 antagonists suppressed T_H1/T_H17-driven experimental autoimmune encephalomyelitis (EAE) and contact hypersensitivity (CHS). Furthermore, IFN-γ production of naïve T cells could be enhanced by PGE₂ although at extremely high concentrations of costimulators (148). These findings together with the data presented in this thesis denote that PGE₂ may induce or terminate

inflammation, dependent on the abundance of cofactors or concentration of PGE₂. MCTS did not produce measurable amounts of immunostimulatory cytokines (data not shown), indicating a different milieu as under inflammatory conditions, when PGE₂ likely suppresses immunity. Taken together, necrosis promotes PGE₂ production in prostate cancer spheroids, which in turn acts as an immune suppressor on activated T cells, conflicting with the general paradigm where necrosis is seen as an immunogenic version of cell death.

6.4 Cell line-dependent PGE₂ production

DU145 tumor spheroids are able to produce PGE₂ due to their ability to upregulate COX-2 in response to spheroid formation-induced cell stress (e.g. in the presence of necrotic cells), whereas other prostate cancer cell lines PC3 and LNCap were also capable of inducing COX-2 expression during cell aggregation (5.1.3). In breast cancer cell lines, MCF-7 cells did not regulate COX-2 expression upon spheroid formation (5.2.3), whereas T47D cells induced both COX-2 and mPGES-1 in parallel experiments (data not shown). A possible explanation for this discrepancy is the p53 status in different cancer cell lines (149). P53⁺ cell lines upregulate COX-2 in response to cell stress, whereas p53 null cell lines do not regulate COX-2 under the same conditions (150). Estradiol is required for p53 mRNA expression in MCF-7 cells and was not used for culturing MCF-7 cells in this study (151). Due to these culture conditions, the lack of estradiol-induced p53 expression may explain why spheroid formation did not provoke COX-2 induction in MCF-7 cells.

6.5 Therapy-induced PGE₂

6.5.1 Phagocyte activation and prostanoid production

PGE₂ synthesis may occur under different circumstances. In prostate cancer cells, tumor spheroid formation and necrosis induced COX-2 mRNA expression and PGE₂ production without inflammatory stimuli. Interestingly, COX-2 expression and PGE₂ production was not induced in MCF-7 spheroids and these tumor spheroids also failed to trigger PGE₂ synthesis of PBMCs in cocultures (5.2.3). LPS-activated PBMCs were shown to be more cytotoxic, but activation-triggered PGE₂ production

restricted inflammatory phagocyte activation in a negative feedback fashion (5.2.3). Despite the fact that PGE₂ synthesis is triggered by inflammatory stimuli as a result of rapid upregulation of COX-2, the underlying production kinetics of PGE₂ are mostly limited by availability of mPGES-1, which does not always correlate with the expression levels of COX-2. Importantly, COX-2 and mPGES-1 are often coexpressed in cancer tissues, but their expression in phagocytes in vitro follows separate time kinetics in response to inflammatory stimuli. COX-2 protein expression already peaks at 8 hours after initial stimulation of cells, leading to overall prostaglandin production, whereas selective PGE₂ production is favored at later stages when mPGES-1 protein expression reaches its maximum at 24 hours after initial stimulation of cells with LPS (14,152). Along with COX-2, expression of pro-inflammatory cytokines such as TNF- α , IL-6, or IL-23 usually peaks several hours after initial stimulation and declines when PGE₂ starts to accumulate (data not shown). Indeed, very recently it was reported that PGE₂ suppresses expression of TNF- α in an EP2/EP4-dependent manner and in turn favors expression of IL-6 and IL-10 (99). However, COX-2-derived PGE₂ has initially been classified as an inflammatory mediator and the use of NSAIDs inhibiting COX-2 inhibits inflammation. Thus, PGE₂ may have very diverse roles in inflammation depending on its spatial availability, its concentration and especially how it is balanced by the presence of other prostanoids, cytokines and cell-contact-mediated activation signals. Poloso et al. observed that PGE₂ enhances expression of inflammatory cytokines at very low doses, whereas high doses of PGE₂ are considered to be rather suppressive (153). Hence, early activation of COX-2 and synthesis of prostaglandins may promote inflammation, but with increasing time, upregulation of mPGES-1 expression and selective synthesis of PGE₂ terminates inflammation.

6.5.2 Shaping of phagocyte function by PGE₂

Activation of phagocyte populations can be facilitated by TLR stimulation, which literally 'stimulated' the development and FDA approval of the TLR2/TLR4 agonist *Bacillus Calmette-Guérin* (BCG), the TLR2/TLR4 agonist monophosphoryl lipid A (MPL) and the TLR9 agonist imiquimod as anti-tumor agents (52). In vitro, coculture of immune cells with MCF-7 tumor spheroids did not provoke an allogenic immune response, as non-activated PBMCs were unable to mediate tumor spheroid killing.

This was due to minimal activation of PBMCs, which demanded TLR4 activation to upregulate CD80 expression by phagocytes and to increase the numbers of GrB^{hi} CTLs. As shown in 5.2.2, CD80 was not only verified as a signature marker but also as a functional requisite for immune activation in this model system. CD80 interception with anti-CD80 antibody reduced the numbers of GrB^{hi} CTLs and prevented tumor spheroid killing as compared to the isotype control. Early on, it was suggested that the expression of CD80 and CD86 is differentially regulated and therefore their functionality embraced during different stages of T cell activation (154). Vaccination of CT26 tumor-bearing mice with recombinant vaccinia virus (rVV) expressing CD80 and model antigen enhanced survival of mice towards vaccination with rVV encoding the model antigen only, whereas rVV expressing CD86 and model antigen was less effective in enhancing anti-tumoral effects as CD80-expressing rVV (39). Interestingly, CD86 expression was not regulated by LPS treatment in the in vitro PBMC spheroid coculture system and inhibition of CD86 neither changed GrB^{hi} CTL numbers, nor rescued tumor spheroid sizes (5.2.2). Since an immune activating role of CD86 could not be verified in the in vitro coculture model, these data are different from the study of Ziller et al. 2002, which indicated that blocking CD80/CD86 in combination with CD40-CD40L-interaction fully abrogates an immune response in C57Bl/6 mice (40). It is possible that besides CD14⁺ CD11c⁺ phagocytes, other phagocyte subtypes are more dominant in regulating CD86 expression in response to LPS. Human plasma differentiated CD14⁺ CD11c⁺ macrophages upregulated CD80 but not CD86, whereas a minor population of CD14⁻ CD11c⁺ cells selectively upregulated CD86 upon LPS stimulation (data not shown). In the PBMC spheroid coculture system, the CD14⁻ CD11c⁺ phagocyte population was irrelevant since CD14 was ubiquitously expressed by all phagocytes. Activation of phagocytes provokes anti-tumoral responses, but intriguingly also induces inflammation, which in turn favors pro-tumoral signaling pathways (12). PGE₂ is such a pro-tumoral inflammatory mediator triggered by NF-κB activation. It accompanies secretion of inflammatory cytokines such as TNF-α and IL-6 and mediates the fine-tuning of their release (99). In the PBMC spheroid coculture model, inhibition of mPGES-1 by C3 selectively inhibited PGE₂ production but did not provoke prostanoid shunting as previously observed in LPS/C3-stimulated mouse peritoneal macrophages (155). Either selective inhibition of PGE₂ with C3 or inhibition of total prostanoid production with Cxb enhanced CD80 expressed on spheroid-infiltrating phagocytes, indicating

that PGE₂ is the relevant prostanoid responsible for modulating CD80 expression. Addition of exogenous PGE₂, the EP2 receptor agonist butaprost, or the PDE4 inhibitor rolipram revealed that the PGE₂/EP2/cAMP pathway impaired both CD80 and CD206 expression on phagocytes, indicating that PGE₂ signaling disrupts polarization of phagocytes in general (Figure 38).

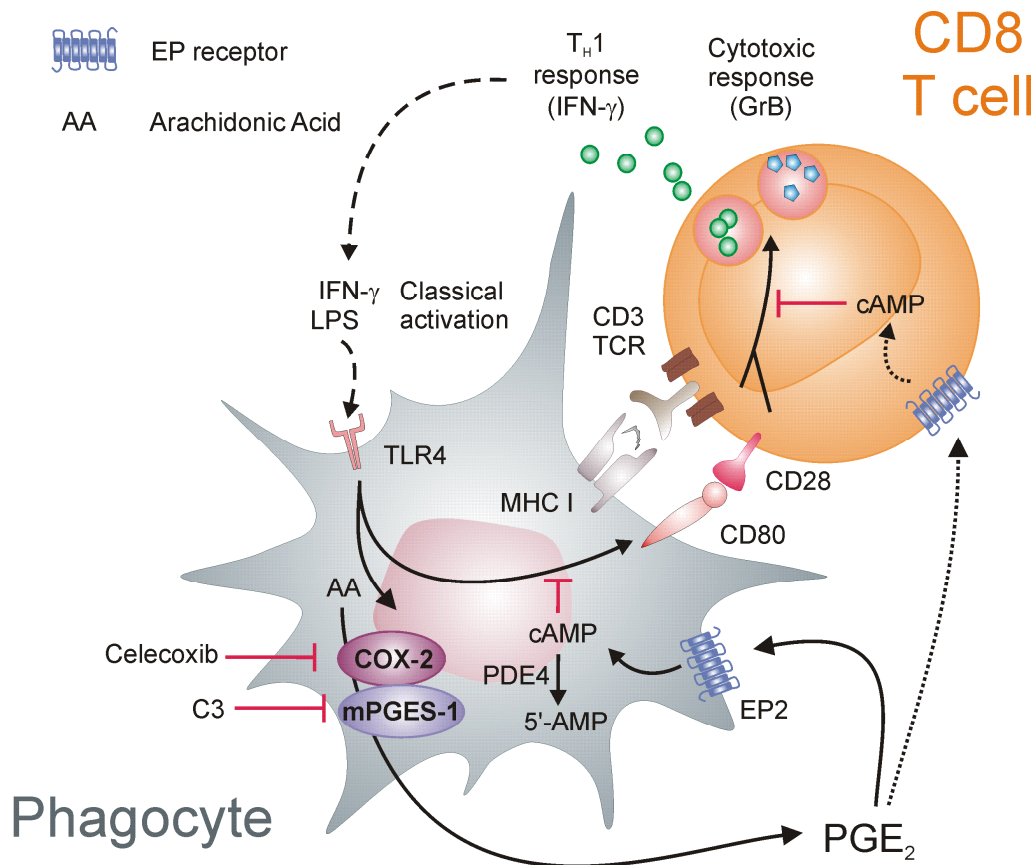


Figure 38: PGE₂ suppresses CD80 expression of tumor-associated phagocytes to inhibit the anti-tumor response. T_H1 activation via TLR4 induces CD80 expression of tumor-associated phagocytes, activation of CD8 T cells and their differentiation into GrB expressing CTLs, and promotes a feed forward loop for the anti-tumoral T_H1 response. In parallel, classical activation triggers PGE₂ synthesis by COX-2/mPGES-1, and suppresses CD80 expression. Inhibition of COX-2/mPGES-1-derived PGE₂ by celecoxib or C3 further increases CD80 expression, whereas addition of PGE₂, the EP2 agonist butaprost or cAMP-inducing PDE4 inhibitor rolipram suppresses CD80 expression on phagocytes.

In line with these findings, PGE₂ was described to possess potent anti-inflammatory properties in numerous inflammation models, acting through EP2/EP4 to elevate intracellular cAMP and to terminate macrophage activation by inhibiting inflammatory macrophage function as well as suppressing the generation of inflammatory cytokines (84-85). This study shows that besides known features such as tumor cell growth promotion (5.1.1), T cell inhibition (5.1.7) and angiogenesis formation (107),

mPGES-1-derived PGE₂ is a negative regulator of CD80-mediated immune activation (chapter 5.1.1 and 5.1.7). Despite their characteristic prostanoid profiles, CD80 and CD206 expression of mPGES-1-deficient BMDMs did not differ from wildtype BMDMs. Related to these findings, Monrad et al. showed that in GM-CSF/IL-4-differentiated bone marrow-derived dendritic cells (BMDCs), mPGES-1-deficiency did not alter levels of CD80 and CD86 after LPS/IFN- γ challenge, whereas Kubo et al. reported that EP2/cAMP signaling rather enhanced CD80 and CD86 expression in TNF- α -differentiated BMDCs (156-157). In BMDMs, it was shown that LPS-triggered CD40 expression could be inhibited by addition of PGE₂, whereas CD80 expression remained unaffected and CD86 was induced (158). However, PGE₂ inhibited CpG-induced CD80 expression and IFN- α secretion in human plasmacytoid dendritic cells (pDCs) via EP2 and EP4 signaling (92). These findings stress that regulation of costimulatory molecules in monocultures of BM-derived cells heavily depends on cell type, stimulus and protocols used for cell differentiation. In general mPGES-1-deficiency may not alter functional outcomes in phagocyte monocultures. Therefore, monoculture models may be feasible to discuss the induction of signaling molecules such as CD80/CD86, but their fine-tuning often relies on more complex interactions e.g. crosstalk of different cell types and/or the presence of tumor environmental factors, which are only available in tumor spheroid immune cell cocultures or animal tumor models. Hence, the involvement of bystander regulatory T cells cannot be excluded in regulating CD80 and CD206 expression of phagocytes in a PGE₂/EP2/cAMP-dependent manner. Indeed, cAMP promotes the expression of the transcriptional inhibitor inducible cAMP early repressor (ICER), needed for regulatory T cell function (159). It is also possible that in the presence of PGE₂, a yet unknown factor in the PBMC spheroid coculture model participates in the regulation of CD80 expression on CD14⁺ CD11c⁺ phagocytes. Possible candidates are hypoxia, hyaluronic acid or apoptotic tumor cells (160-162). Unfortunately, a spheroid-forming mouse breast cancer cell line was not available, which would have enabled the direct transition of the findings in the human in vitro coculture system to the mouse system.

In MMTV/PyMT mice, the observed delayed breast cancer development was due to loss of mPGES-1. In line with these findings, deletion of mPGES-1 reduced mammary tumorigenesis, aromatase activity, and angiogenesis in a MMTV/NDL (neu deletion mutant) breast cancer model overexpressing Her2/neu (163). Immunosuppressive features of mPGES-1 may add to classical causes for tumor

outgrowth such as tumor cell growth and angiogenesis. Thus, it is interesting how mPGES-1 affects tumor invasion of phagocytes and the shaping of these cells into inflammatory or anti-inflammatory phenotypes. Initially, an increased number of tumor infiltrating phagocytes was detected in PyMT tumors of mPGES-1-deficient mice, which per se conflicts with the paradigm that a high abundance of tumor-associated macrophages at the tumor site is regularly associated with bad prognosis in breast cancer patients (33). Further characterization of F4/80⁺ CD11c⁺ phagocytes revealed that CD80 expression on these cells was not affected by mPGES-1-deficiency and overall CD80 expression levels of tumor-infiltrating phagocytes equaled CD80 expressed on unstimulated BMDMs. This supports the notion that deficiency in mPGES-1 and thus inducible PGE₂ alone is insufficient to lift immune suppression from PyMT tumors when tumors are already established. A transition of the CD80 regulating features of mPGES-1-derived PGE₂ from the in vitro coculture tumor model to the in vivo mouse tumor model is only possible, when expression of CD80 on F4/80⁺ CD11c⁺ phagocytes is enhanced under immune-activated conditions, which shall be the focus of future studies.

6.6 Role of dead cells in immune activation

Local inflammation and immune activation are highly associated, but often inflammation does not necessarily result in effective anti-tumoral responses, even if immune activation is partially effective. This may happen when tumor microenvironmental factors add up to dampen immune activation and instead maintain potential anti-tumoral immune cells to reside at the tumor site in a minimally activated state. The underlying mechanism can be manifold and cannot be simplified or reduced to one single factor. Instead the interplay of multiple microenvironmental factors such as hypoxia, nutrient deprivation, lack of growth factors constantly 'fuel' a pool of dying tumor cells (29). Dendritic cells, after incorporating dying cells, differentiate into tumor-induced DCs and are potent in preventing activation of anti-tumoral effector cells or suppression of already activated T cells by direct cell-contact-based mechanisms or release of soluble factors (164). As a general paradigm, the clearance of dead cells is believed to regulate the nature of an immune response. In contrast to the literature, a role of necrotic cells as immune stimulators could not be confirmed in this study, since necrotic cells induced PGE₂ in prostate

cancer, which instead suppressed CTLs (5.1.7) (165). In addition, tumor spheroids are already composed of a great deal of dead cells- either necrotic or apoptotic. Coculture of tumor spheroids with PBMCs enables phagocytes infiltrating a tumor spheroid to face dead cells, whose clearance would shape the immunological phenotype. In my experiments, the proportion of necrotic cells in MCF-7 tumor spheroids did not result in measurable production of inflammatory cytokines (data not shown) or PGE₂ (5.2.3), indicating that the presence of necrotic cells in MCF-7 tumor spheroids alone is not sufficient to trigger an inflammatory response. Cocultivation of DU145 tumor spheroids with PBMCs also failed to yield measurable inflammatory cytokine amounts (data not shown), confirming the limited role of necrotic cells for NFκB activation in the PBMC / spheroid coculture model. In this regard, the presence of necrotic cells alone may be insufficient to trigger NF-κB and inflammatory responses, but requires necrosis-associated release of DAMPs such as high mobility box group 1 (HMGB-1) for consequent activation of TLR4/NF-κB (165). Necrotic cells of HMGB-1-deficient cell lines are hypothesized to be silently cleared without TLR4 activation, whereas apoptotic cells may restrict the strength of an inflammatory response (166). Therefore, the paradigm in which uptake of dead cells would shape immune responses should be reviewed in future experiments by coculturing activated phagocytes with either necrotic, apoptotic or viable cells of various tumor cell lines to determine whether the inflammatory response is altered by phagocytosis of dead cells in terms of cytokine release by phagocytes and their costimulatory molecule expression profile.

6.7 Therapeutic perspectives of PGE₂ inhibition

When all the pieces are put together, the answers to the question why tumors develop in such a predictable fashion are mirrored by the actions of PGE₂. Since PGE₂ production is triggered under both inflammatory and anti-inflammatory conditions, its tumor-favoring features are ubiquitously present in the tumor microenvironment and in the long run help to enforce a state of chronic inflammation: Insufficient immune activation fails to kill the tumor and in turn fuels the induction of cell-stress-related or activation-induced PGE₂. Accumulated PGE₂ induces tumor cell proliferation, angiogenesis, or protects the tumor against incoming T cell responses. This mix of inflammatory and immune suppressive signaling maintains a state of

prolonged inconsequential immune activation and favors wound-healing conditions, which again evokes additional synthesis of PGE₂ (Figure 39). Under anti-inflammatory conditions, PGE₂ maintains a state of increased cell stress by fueling tumor cell proliferation, which again creates more cell stress and short-circuits the process (Figure 39).

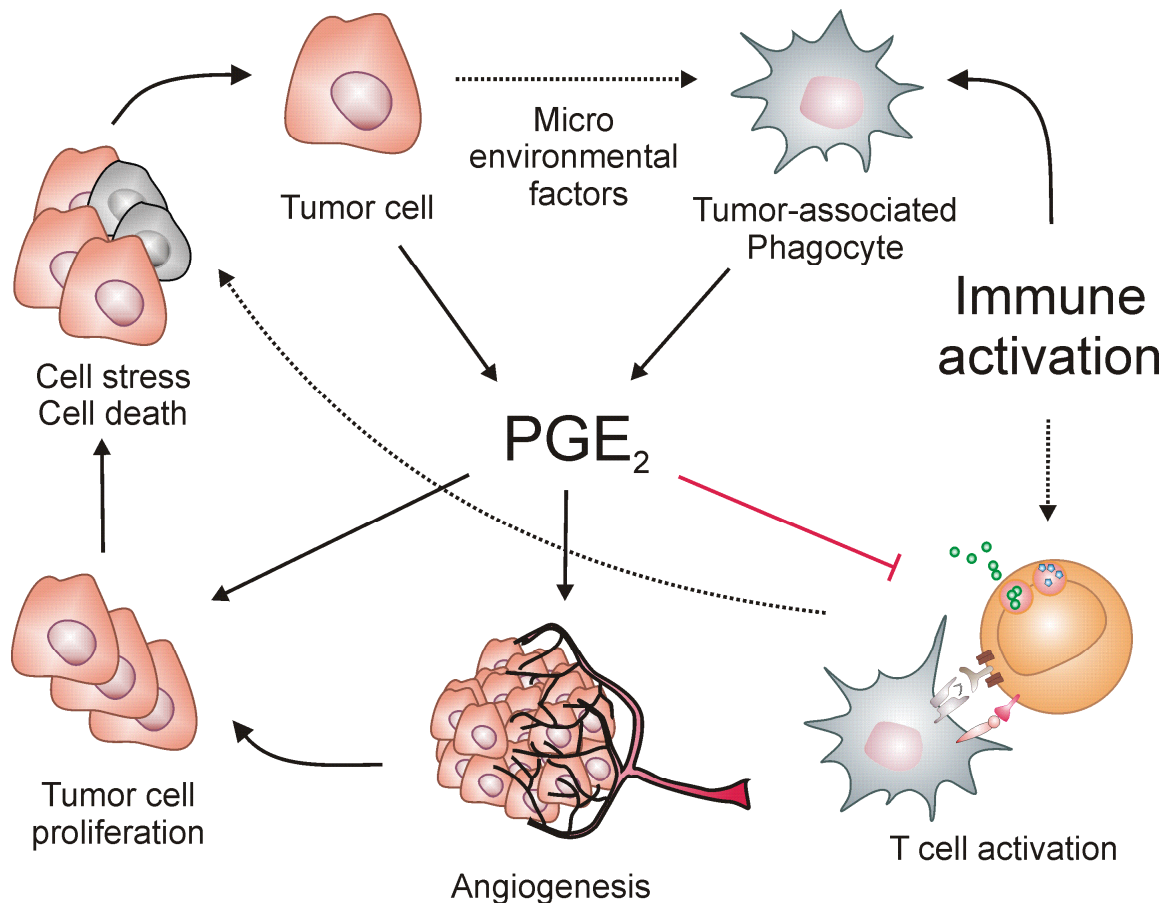


Figure 39: PGE₂ favors tumor growth by enforcing a chronic inflammatory microenvironment. PGE₂ production can be stress-triggered in tumor cells or induced in tumor-associated phagocytes by immune activation. During the anti-tumoral response PGE₂ acts as a negative feedback to inhibit T cell activation and in turn favors angiogenesis and tumor cell growth. The characteristic cell stress- or cell death-loaded tumor microenvironment is maintained by enhanced tumor cell proliferation or CTL-driven tissue damage, which evokes wound-healing and immune regulating mechanisms, jamming infiltrated phagocytes at the local tumor site. Tumor microenvironmental factors add up to dampen tumor-associated phagocyte activation, which aid the tumor with their immune suppressive capacities. Inefficient tumor killing also creates an environment of a long-lasting but inconsequential immune response due to a mix of abundant pro- and anti-inflammatory signals, a typical trait of chronic inflammation.

Hence, inhibition of PGE₂ may be suitable to shut-down multiple tumor-favoring processes such as tumor cell growth, angiogenesis, and immune suppression. In

respect of immune therapeutic approaches (3.2.3), TLR agonists have emerged as adjuvant components of tumor vaccination strategies to reactivate TAA-sensitive T cell responses. However, these agents also induce PGE₂ production and may promote wound-healing and angiogenesis when applied under-dosed. The cancer vaccine L-BLP25 also known as Stimuvax®, contains the TLR2/4 agonistic component MPL, and failed to meet primarily endpoints in Phase III trials of non small cell lung carcinoma (NSCLC) patients recently, but instead improved survival in combination with low-dose chemotherapeutic cyclophosphamide, which is able to lift suppressive functions of regulatory T cells (167-168). In my experiments, TLR4 activation was sufficient to trigger MCF-7 spheroid killing by PBMCs. However, when using T47D breast cancer spheroids for PBMC / spheroid cocultures, LPS stimulation was ineffective in activating PBMCs, but instead promoted tumor spheroid growth (data not shown), indicating that TLR4 activation leads to different immunological outcomes depending on the cell line used. In fact, T47D cells upregulate COX-2 and mPGES-1 expression upon spheroid formation and per se produce high levels of immune suppressive PGE₂ (data not shown), which may add to the therapy-inflicted PGE₂ and terminate immune activation or promote tumor spheroid growth to a stronger extent than in PBMC / MCF-7 spheroid cocultures. Hence, selective PGE₂ inhibition may improve TLR activation-based therapeutics, since TLR agonists may not lack efficiency in general but their original anti-tumoral mode of action is rather restricted by negative feedback mechanisms of the inflammatory mediator PGE₂. Indeed, recently PGE₂ inhibition has been suggested to improve immune therapeutic approaches by restricting generation of inflammation-induced MDSCs, which are responsible for generation of regulatory T cells at the tumor site (93,169-170). The COX-2 inhibitors celecoxib (celebrex®) and etoricoxib (arcoxia®) blunt prostanoid production and thus PGE₂ and their use has been clinically approved for the treatment of inflammatory autoimmune diseases such as rheumatoid arthritis or morbus bechterew but not for treating cancer. The tendency to disrupt the thromboxane/prostacyclin balance is associated with increase in cardiovascular risks limiting their range of indications (171), even though the efficacy of COX-2 inhibitors has been demonstrated in the therapy of different cancer types including lung, breast, prostate and colon cancers (114). The down-stream enzyme of COX-2, mPGES-1 may serve as a potential target for selective inhibition of PGE₂. MPGES-1 inhibitors are currently tested in Phase 1 trials (LY3023703- start June 2012). Hence,

selective inhibition of PGE₂ may highly improve immunotherapeutic approaches in general and should also be considered as a supplement to conventional cancer therapies or as an agent for long-term relapse-prevention in cancer patients recovering from surgery.

7 Literature

1. Bissell, M.J., *et al.* (2011) Why don't we get more cancer? A proposed role of the microenvironment in restraining cancer progression. *Nat Med*, **17**, 320-9.
2. Egeblad, M., *et al.* (2010) Tumors as organs: complex tissues that interface with the entire organism. *Dev Cell*, **18**, 884-901.
3. Alexandrov, L.B., *et al.* (2013) Signatures of mutational processes in human cancer. *Nature*, **500**, 415-21.
4. Stratton, M.R., *et al.* (2009) The cancer genome. *Nature*, **458**, 719-24.
5. Casas-Selves, M., *et al.* (2011) How cancer shapes evolution, and how evolution shapes cancer. *Evolution (N Y)*, **4**, 624-634.
6. Hanahan, D., *et al.* (2011) Hallmarks of cancer: the next generation. *Cell*, **144**, 646-74.
7. Bussard, K.M., *et al.* (2012) Human breast cancer cells are redirected to mammary epithelial cells upon interaction with the regenerating mammary gland microenvironment in-vivo. *PLoS One*, **7**, e49221.
8. Grivennikov, S.I., *et al.* (2010) Immunity, inflammation, and cancer. *Cell*, **140**, 883-99.
9. Marx, J. (2008) Cancer biology. All in the stroma: cancer's Cosa Nostra. *Science*, **320**, 38-41.
10. Junttila, M.R., *et al.* (2013) Influence of tumour micro-environment heterogeneity on therapeutic response. *Nature*, **501**, 346-54.
11. Galon, J., *et al.* (2012) Cancer classification using the Immunoscore: a worldwide task force. *J Transl Med*, **10**, 205.
12. Colotta, F., *et al.* (2009) Cancer-related inflammation, the seventh hallmark of cancer: links to genetic instability. *Carcinogenesis*, **30**, 1073-81.
13. Balkwill, F.R., *et al.* (2012) Cancer-related inflammation: Common themes and therapeutic opportunities. *Semin Cancer Biol*, **22**, 33-40.
14. Xiao, C.X., *et al.* (2013) Distribution of bone-marrow-derived endothelial and immune cells in a murine colitis-associated colorectal cancer model. *PLoS One*, **8**, e73666.
15. Hemminki, K., *et al.* (2012) Effect of autoimmune diseases on risk and survival in female cancers. *Gynecol Oncol*, **127**, 180-5.
16. Chen, D.S., *et al.* (2013) Oncology meets immunology: the cancer-immunity cycle. *Immunity*, **39**, 1-10.
17. Richmond, A., *et al.* (2008) Mouse xenograft models vs GEM models for human cancer therapeutics. *Dis Model Mech*, **1**, 78-82.
18. Fantozzi, A., *et al.* (2006) Mouse models of breast cancer metastasis. *Breast Cancer Res*, **8**, 212.
19. Lin, E.Y., *et al.* (2003) Progression to malignancy in the polyoma middle T oncoprotein mouse breast cancer model provides a reliable model for human diseases. *Am J Pathol*, **163**, 2113-26.
20. Feder-Mengus, C., *et al.* (2008) New dimensions in tumor immunology: what does 3D culture reveal? *Trends Mol Med*, **14**, 333-40.
21. Nyga, A., *et al.* (2011) 3D tumour models: novel in vitro approaches to cancer studies. *J Cell Commun Signal*, **5**, 239-48.
22. Ivascu, A., *et al.* (2007) Diversity of cell-mediated adhesions in breast cancer spheroids. *Int J Oncol*, **31**, 1403-13.
23. Carlsson, J., *et al.* (1984) Liquid-overlay culture of cellular spheroids. *Recent Results Cancer Res*, **95**, 1-23.

24. Timmins, N.E., *et al.* (2004) Hanging-drop multicellular spheroids as a model of tumour angiogenesis. *Angiogenesis*, **7**, 97-103.
25. Ho, W.Y., *et al.* (2012) Development of multicellular tumor spheroid (MCTS) culture from breast cancer cell and a high throughput screening method using the MTT assay. *PLoS One*, **7**, e44640.
26. Akira, S., *et al.* (2006) Pathogen recognition and innate immunity. *Cell*, **124**, 783-801.
27. Lundin, J.I., *et al.* (2009) Endotoxin and cancer. *Environ Health Perspect*, **117**, 1344-50.
28. Karin, M. (2009) NF-kappaB as a critical link between inflammation and cancer. *Cold Spring Harb Perspect Biol*, **1**, a000141.
29. Kuraishy, A., *et al.* (2011) Tumor promotion via injury- and death-induced inflammation. *Immunity*, **35**, 467-77.
30. Schreiber, R.D., *et al.* (2011) Cancer immunoediting: integrating immunity's roles in cancer suppression and promotion. *Science*, **331**, 1565-70.
31. Peter, C., *et al.* (2010) Dangerous attraction: phagocyte recruitment and danger signals of apoptotic and necrotic cells. *Apoptosis*, **15**, 1007-28.
32. Sato, Y., *et al.* (2009) Cancer Cells Expressing Toll-like Receptors and the Tumor Microenvironment. *Cancer Microenviron*, **2 Suppl 1**, 205-14.
33. Laoui, D., *et al.* (2011) Mononuclear phagocyte heterogeneity in cancer: different subsets and activation states reaching out at the tumor site. *Immunobiology*, **216**, 1192-202.
34. Guth, A.M., *et al.* (2012) Depletion of phagocytic myeloid cells triggers spontaneous T cell- and NK cell-dependent antitumor activity. *Oncoimmunology*, **1**, 1248-1257.
35. Zhu, J., *et al.* (2010) Differentiation of effector CD4 T cell populations (*). *Annu Rev Immunol*, **28**, 445-89.
36. Williams, M.A., *et al.* (2007) Effector and memory CTL differentiation. *Annu Rev Immunol*, **25**, 171-92.
37. Seder, R.A., *et al.* (1994) CD28-mediated costimulation of interleukin 2 (IL-2) production plays a critical role in T cell priming for IL-4 and interferon gamma production. *J Exp Med*, **179**, 299-304.
38. Mouchacca, P., *et al.* (2013) Visualization of cytolytic T cell differentiation and granule exocytosis with T cells from mice expressing active fluorescent granzyme B. *PLoS One*, **8**, e67239.
39. Chamberlain, R.S., *et al.* (1996) Costimulation enhances the active immunotherapy effect of recombinant anticancer vaccines. *Cancer Res*, **56**, 2832-6.
40. Ziller, C., *et al.* (2002) Transient blocking of both B7.1 (CD80) and B7.2 (CD86) in addition to CD40-CD40L interaction fully abrogates the immune response following systemic injection of adenovirus vector. *Gene Ther*, **9**, 537-46.
41. Lindau, D., *et al.* (2013) The immunosuppressive tumour network: myeloid-derived suppressor cells, regulatory T cells and natural killer T cells. *Immunology*, **138**, 105-15.
42. Yang, R., *et al.* (2006) CD80 in immune suppression by mouse ovarian carcinoma-associated Gr-1+CD11b+ myeloid cells. *Cancer Res*, **66**, 6807-15.
43. Zou, W., *et al.* (2008) Inhibitory B7-family molecules in the tumour microenvironment. *Nat Rev Immunol*, **8**, 467-77.
44. Mellman, I., *et al.* (2011) Cancer immunotherapy comes of age. *Nature*, **480**, 480-9.

45. Grosso, J.F., *et al.* (2013) CTLA-4 blockade in tumor models: an overview of preclinical and translational research. *Cancer Immun*, **13**, 5.
46. Suntharalingam, G., *et al.* (2006) Cytokine storm in a phase 1 trial of the anti-CD28 monoclonal antibody TGN1412. *N Engl J Med*, **355**, 1018-28.
47. Topalian, S.L., *et al.* (2012) Safety, activity, and immune correlates of anti-PD-1 antibody in cancer. *N Engl J Med*, **366**, 2443-54.
48. Morgan, R.A., *et al.* (2010) Case report of a serious adverse event following the administration of T cells transduced with a chimeric antigen receptor recognizing ERBB2. *Mol Ther*, **18**, 843-51.
49. Kantoff, P.W., *et al.* (2010) Sipuleucel-T immunotherapy for castration-resistant prostate cancer. *N Engl J Med*, **363**, 411-22.
50. Walter, S., *et al.* (2012) Multi-peptide immune response to cancer vaccine IMA901 after single-dose cyclophosphamide associates with longer patient survival. *Nat Med*, **18**, 1254-61.
51. Le, D.T., *et al.* (2012) Regulatory T-cell modulation using cyclophosphamide in vaccine approaches: a current perspective. *Cancer Res*, **72**, 3439-44.
52. Vacchelli, E., *et al.* (2013) Trial Watch: Toll-like receptor agonists for cancer therapy. *Oncoimmunology*, **2**, e25238.
53. Wurz, G.T., *et al.* (2013) Antitumor effects of L-BLP25 Antigen-Specific tumor immunotherapy in a novel human MUC1 transgenic lung cancer mouse model. *J Transl Med*, **11**, 64.
54. Balsinde, J., *et al.* (2002) Phospholipase A(2) regulation of arachidonic acid mobilization. *FEBS Lett*, **531**, 2-6.
55. Habenicht, A.J., *et al.* (1985) Human platelet-derived growth factor stimulates prostaglandin synthesis by activation and by rapid de novo synthesis of cyclooxygenase. *J Clin Invest*, **75**, 1381-7.
56. Tanioka, T., *et al.* (2000) Molecular identification of cytosolic prostaglandin E2 synthase that is functionally coupled with cyclooxygenase-1 in immediate prostaglandin E2 biosynthesis. *J Biol Chem*, **275**, 32775-82.
57. Jakobsson, P.J., *et al.* (1999) Identification of human prostaglandin E synthase: a microsomal, glutathione-dependent, inducible enzyme, constituting a potential novel drug target. *Proc Natl Acad Sci U S A*, **96**, 7220-5.
58. Tanikawa, N., *et al.* (2002) Identification and characterization of a novel type of membrane-associated prostaglandin E synthase. *Biochem Biophys Res Commun*, **291**, 884-9.
59. Spencer, A.G., *et al.* (1998) Subcellular localization of prostaglandin endoperoxide H synthases-1 and -2 by immunoelectron microscopy. *J Biol Chem*, **273**, 9886-93.
60. Murakami, M., *et al.* (2000) Regulation of prostaglandin E2 biosynthesis by inducible membrane-associated prostaglandin E2 synthase that acts in concert with cyclooxygenase-2. *J Biol Chem*, **275**, 32783-92.
61. Murakami, M., *et al.* (2003) Cellular prostaglandin E2 production by membrane-bound prostaglandin E synthase-2 via both cyclooxygenases-1 and -2. *J Biol Chem*, **278**, 37937-47.
62. Ensor, C.M., *et al.* (1995) 15-Hydroxyprostaglandin dehydrogenase. *J Lipid Mediat Cell Signal*, **12**, 313-9.
63. Uematsu, S., *et al.* (2002) Lipopolysaccharide-dependent prostaglandin E(2) production is regulated by the glutathione-dependent prostaglandin E(2) synthase gene induced by the Toll-like receptor 4/MyD88/NF-IL6 pathway. *J Immunol*, **168**, 5811-6.

64. Casos, K., *et al.* (2011) Tumor cells induce COX-2 and mPGES-1 expression in microvascular endothelial cells mainly by means of IL-1 receptor activation. *Microvasc Res*, **81**, 261-8.
65. Bezugla, Y., *et al.* (2006) COX-1 and COX-2 contribute differentially to the LPS-induced release of PGE2 and TxA2 in liver macrophages. *Prostaglandins Other Lipid Mediat*, **79**, 93-100.
66. de Oliveira, A.C., *et al.* (2008) Regulation of prostaglandin E2 synthase expression in activated primary rat microglia: evidence for uncoupled regulation of mPGES-1 and COX-2. *Glia*, **56**, 844-55.
67. Harding, P., *et al.* (2006) Transforming growth factor beta regulates cyclooxygenase-2 in glomerular mesangial cells. *Kidney Int*, **69**, 1578-85.
68. Kaidi, A., *et al.* (2006) Direct transcriptional up-regulation of cyclooxygenase-2 by hypoxia-inducible factor (HIF)-1 promotes colorectal tumor cell survival and enhances HIF-1 transcriptional activity during hypoxia. *Cancer Res*, **66**, 6683-91.
69. Roberts, H.R., *et al.* (2011) Colon tumour cells increase PGE(2) by regulating COX-2 and 15-PGDH to promote survival during the microenvironmental stress of glucose deprivation. *Carcinogenesis*, **32**, 1741-7.
70. Li, F., *et al.* (2010) Apoptotic cells activate the "phoenix rising" pathway to promote wound healing and tissue regeneration. *Sci Signal*, **3**, ra13.
71. Greenhough, A., *et al.* (2009) The COX-2/PGE2 pathway: key roles in the hallmarks of cancer and adaptation to the tumour microenvironment. *Carcinogenesis*, **30**, 377-86.
72. Sakata, D., *et al.* (2010) Emerging roles of prostanoids in T cell-mediated immunity. *IUBMB Life*, **62**, 591-6.
73. Hata, A.N., *et al.* (2004) Pharmacology and signaling of prostaglandin receptors: multiple roles in inflammation and immune modulation. *Pharmacol Ther*, **103**, 147-66.
74. Watabe, A., *et al.* (1993) Cloning and expression of cDNA for a mouse EP1 subtype of prostaglandin E receptor. *J Biol Chem*, **268**, 20175-8.
75. Honda, A., *et al.* (1993) Prostaglandin E2 stimulates cyclic AMP-mediated hyaluronan synthesis in rabbit pericardial mesothelial cells. *Biochem J*, **292 (Pt 2)**, 497-502.
76. Israel, D.D., *et al.* (2009) EP(3) prostanoid receptor isoforms utilize distinct mechanisms to regulate ERK 1/2 activation. *Biochim Biophys Acta*, **1791**, 238-45.
77. Wang, D., *et al.* (2010) Eicosanoids and cancer. *Nat Rev Cancer*, **10**, 181-93.
78. Wang, D., *et al.* (2010) The role of COX-2 in intestinal inflammation and colorectal cancer. *Oncogene*, **29**, 781-8.
79. Kalinski, P. (2012) Regulation of immune responses by prostaglandin E2. *J Immunol*, **188**, 21-8.
80. Trebino, C.E., *et al.* (2003) Impaired inflammatory and pain responses in mice lacking an inducible prostaglandin E synthase. *Proc Natl Acad Sci U S A*, **100**, 9044-9.
81. Serhan, C.N., *et al.* (2005) Resolution of inflammation: the beginning programs the end. *Nat Immunol*, **6**, 1191-7.
82. Ratcliffe, M.J., *et al.* (2007) Activation of E-prostanoid4 and E-prostanoid2 receptors inhibits TNF-alpha release from human alveolar macrophages. *Eur Respir J*, **29**, 986-94.

83. Nemeth, K., *et al.* (2009) Bone marrow stromal cells attenuate sepsis via prostaglandin E(2)-dependent reprogramming of host macrophages to increase their interleukin-10 production. *Nat Med*, **15**, 42-9.
84. Brenneis, C., *et al.* (2011) Anti-inflammatory role of microsomal prostaglandin E synthase-1 in a model of neuroinflammation. *J Biol Chem*, **286**, 2331-42.
85. Peters-Golden, M. (2009) Putting on the brakes: cyclic AMP as a multipronged controller of macrophage function. *Sci Signal*, **2**, pe37.
86. Quan, Y., *et al.* (2013) EP2 receptor signaling pathways regulate classical activation of microglia. *J Biol Chem*, **288**, 9293-302.
87. Akaogi, J., *et al.* (2004) Prostaglandin E2 receptors EP2 and EP4 are up-regulated in peritoneal macrophages and joints of pristane-treated mice and modulate TNF-alpha and IL-6 production. *J Leukoc Biol*, **76**, 227-36.
88. Wall, E.A., *et al.* (2009) Suppression of LPS-induced TNF-alpha production in macrophages by cAMP is mediated by PKA-AKAP95-p105. *Sci Signal*, **2**, ra28.
89. Zaslona, Z., *et al.* (2012) Prostaglandin E2 restrains macrophage maturation via E prostanoid receptor 2/protein kinase A signaling. *Blood*, **119**, 2358-67.
90. Bystrom, J., *et al.* (2008) Resolution-phase macrophages possess a unique inflammatory phenotype that is controlled by cAMP. *Blood*, **112**, 4117-27.
91. Sombroek, C.C., *et al.* (2002) Prostanoids play a major role in the primary tumor-induced inhibition of dendritic cell differentiation. *J Immunol*, **168**, 4333-43.
92. Fabricius, D., *et al.* (2010) Prostaglandin E2 inhibits IFN-alpha secretion and Th1 costimulation by human plasmacytoid dendritic cells via E-prostanoid 2 and E-prostanoid 4 receptor engagement. *J Immunol*, **184**, 677-84.
93. Obermajer, N., *et al.* (2011) Positive feedback between PGE2 and COX2 redirects the differentiation of human dendritic cells toward stable myeloid-derived suppressor cells. *Blood*, **118**, 5498-505.
94. Obermajer, N., *et al.* (2011) PGE(2)-induced CXCL12 production and CXCR4 expression controls the accumulation of human MDSCs in ovarian cancer environment. *Cancer Res*, **71**, 7463-70.
95. Heusinkveld, M., *et al.* (2011) M2 macrophages induced by prostaglandin E2 and IL-6 from cervical carcinoma are switched to activated M1 macrophages by CD4+ Th1 cells. *J Immunol*, **187**, 1157-65.
96. Yang, L., *et al.* (2003) Cancer-associated immunodeficiency and dendritic cell abnormalities mediated by the prostaglandin EP2 receptor. *J Clin Invest*, **111**, 727-35.
97. Qian, B.Z., *et al.* (2010) Macrophage diversity enhances tumor progression and metastasis. *Cell*, **141**, 39-51.
98. Mantovani, A., *et al.* (2008) Cancer-related inflammation. *Nature*, **454**, 436-44.
99. Treffkorn, L., *et al.* (2004) PGE2 exerts its effect on the LPS-induced release of TNF-alpha, ET-1, IL-1alpha, IL-6 and IL-10 via the EP2 and EP4 receptor in rat liver macrophages. *Prostaglandins Other Lipid Mediat*, **74**, 113-23.
100. Kambayashi, T., *et al.* (2001) cAMP-elevating agents suppress dendritic cell function. *J Leukoc Biol*, **70**, 903-10.
101. Eisengart, C.A., *et al.* (2000) Prostaglandins regulate melanoma-induced cytokine production in macrophages. *Cell Immunol*, **204**, 143-9.
102. Duff, M., *et al.* (2003) Cyclooxygenase-2 inhibition improves macrophage function in melanoma and increases the antineoplastic activity of interferon gamma. *Ann Surg Oncol*, **10**, 305-13.

103. Bianchini, F., *et al.* (2007) Expression of cyclo-oxygenase-2 in macrophages associated with cutaneous melanoma at different stages of progression. *Prostaglandins Other Lipid Mediat*, **83**, 320-8.
104. Nakano, Y., *et al.* (2006) Induction of macrophagic prostaglandin E2 synthesis by glioma cells. *J Neurosurg*, **104**, 574-82.
105. Ravichandran, K.S. (2011) Beginnings of a good apoptotic meal: the find-me and eat-me signaling pathways. *Immunity*, **35**, 445-55.
106. Gregory, C.D., *et al.* (2011) Cell death in the neighbourhood: direct microenvironmental effects of apoptosis in normal and neoplastic tissues. *J Pathol*, **223**, 177-94.
107. Brecht, K., *et al.* (2011) Macrophages programmed by apoptotic cells promote angiogenesis via prostaglandin E2. *FASEB J*, **25**, 2408-17.
108. Medeiros, A.I., *et al.* (2009) Efferocytosis impairs pulmonary macrophage and lung antibacterial function via PGE2/EP2 signaling. *J Exp Med*, **206**, 61-8.
109. Weigert, A., *et al.* (2006) Apoptotic cells promote macrophage survival by releasing the antiapoptotic mediator sphingosine-1-phosphate. *Blood*, **108**, 1635-42.
110. Weigert, A., *et al.* (2010) Cleavage of sphingosine kinase 2 by caspase-1 provokes its release from apoptotic cells. *Blood*, **115**, 3531-40.
111. Huang, Q., *et al.* (2011) Caspase 3-mediated stimulation of tumor cell repopulation during cancer radiotherapy. *Nat Med*, **17**, 860-6.
112. Sha, W., *et al.* (2012) The multi-faceted roles of prostaglandin E(2) in cancer-infiltrating mononuclear phagocyte biology. *Immunobiology*, **217**, 1225-32.
113. Karnezis, T., *et al.* (2012) VEGF-D promotes tumor metastasis by regulating prostaglandins produced by the collecting lymphatic endothelium. *Cancer Cell*, **21**, 181-95.
114. Harris, R.E. (2009) Cyclooxygenase-2 (cox-2) blockade in the chemoprevention of cancers of the colon, breast, prostate, and lung. *Inflammopharmacology*, **17**, 55-67.
115. Chan, A.T., *et al.* (2012) Are we ready to recommend aspirin for cancer prevention? *Lancet*, **379**, 1569-71.
116. Sasaki, Y., *et al.* (2011) Microsomal prostaglandin E synthase-1 is involved in multiple steps of colon carcinogenesis. *Oncogene*, **31**, 2943-2952.
117. Scher, J.U., *et al.* (2005) 15d-PGJ2: the anti-inflammatory prostaglandin? *Clin Immunol*, **114**, 100-9.
118. Ban, J.O., *et al.* (2010) Suppression of NF-kappaB and GSK-3beta is involved in colon cancer cell growth inhibition by the PPAR agonist troglitazone. *Chem Biol Interact*, **188**, 75-85.
119. Scher, J.U., *et al.* (2009) The anti-inflammatory effects of prostaglandins. *J Investig Med*, **57**, 703-8.
120. Samuelsson, B., *et al.* (2007) Membrane prostaglandin E synthase-1: a novel therapeutic target. *Pharmacol Rev*, **59**, 207-24.
121. Hanaka, H., *et al.* (2009) Microsomal prostaglandin E synthase 1 determines tumor growth in vivo of prostate and lung cancer cells. *Proc Natl Acad Sci U S A*, **106**, 18757-62.
122. Wang, D., *et al.* (2004) Prostaglandin E(2) promotes colorectal adenoma growth via transactivation of the nuclear peroxisome proliferator-activated receptor delta. *Cancer Cell*, **6**, 285-95.
123. Elander, N., *et al.* (2008) Genetic deletion of mPGES-1 accelerates intestinal tumorigenesis in APC(Min/+) mice. *Biochem Biophys Res Commun*, **372**, 249-53.

124. Elander, N., *et al.* (2009) Association between adenomatosis polyposis coli functional status and microsomal prostaglandin E synthase-1 expression in colorectal cancer. *Mol Carcinog*, **48**, 401-7.
125. Nakanishi, M., *et al.* (2008) Genetic deletion of mPGES-1 suppresses intestinal tumorigenesis. *Cancer Res*, **68**, 3251-9.
126. Oshima, H., *et al.* (2004) Hyperplastic gastric tumors induced by activated macrophages in COX-2/mPGES-1 transgenic mice. *EMBO J*, **23**, 1669-78.
127. Kamei, D., *et al.* (2010) Microsomal prostaglandin E synthase-1 in both cancer cells and hosts contributes to tumour growth, invasion and metastasis. *Biochem J*, **425**, 361-71.
128. Kamata, H., *et al.* (2010) mPGES-1-expressing bone marrow-derived cells enhance tumor growth and angiogenesis in mice. *Biomed Pharmacother*, **64**, 409-16.
129. Sekar, D., *et al.* (2012) Apoptotic tumor cells induce IL-27 release from human DCs to activate Treg cells that express CD69 and attenuate cytotoxicity. *Eur J Immunol*, **42**, 1585-98.
130. Linke, B., *et al.* (2009) Toponomics analysis of drug-induced changes in arachidonic acid-dependent signaling pathways during spinal nociceptive processing. *J Proteome Res*, **8**, 4851-9.
131. Bage, T., *et al.* (2010) Signal pathways JNK and NF-kappaB, identified by global gene expression profiling, are involved in regulation of TNFalpha-induced mPGES-1 and COX-2 expression in gingival fibroblasts. *BMC Genomics*, **11**, 241.
132. Freire-de-Lima, C.G., *et al.* (2006) Apoptotic cells, through transforming growth factor-beta, coordinately induce anti-inflammatory and suppress pro-inflammatory eicosanoid and NO synthesis in murine macrophages. *J Biol Chem*, **281**, 38376-84.
133. Galluzzi, L., *et al.* (2008) Necroptosis: a specialized pathway of programmed necrosis. *Cell*, **135**, 1161-3.
134. Fabre, J.W. (2001) The allogeneic response and tumor immunity. *Nat Med*, **7**, 649-52.
135. Medina, M.A., *et al.* (2012) Granzyme B- and Fas ligand-mediated cytotoxic function induced by mitogenic CD28 stimulation of human memory CD4+ T cells. *J Leukoc Biol*, **91**, 759-71.
136. Sharda, D.R., *et al.* (2011) Regulation of macrophage arginase expression and tumor growth by the Ron receptor tyrosine kinase. *J Immunol*, **187**, 2181-92.
137. Karlsson, H., *et al.* (2012) Loss of cancer drug activity in colon cancer HCT-116 cells during spheroid formation in a new 3-D spheroid cell culture system. *Exp Cell Res*, **318**, 1577-85.
138. Lee, J., *et al.* (2009) In vitro toxicity testing of nanoparticles in 3D cell culture. *Small*, **5**, 1213-21.
139. Beales, I.L., *et al.* (2010) Microsomal prostaglandin E synthase-1 inhibition blocks proliferation and enhances apoptosis in oesophageal adenocarcinoma cells without affecting endothelial prostacyclin production. *Int J Cancer*, **126**, 2247-55.
140. Johann, A.M., *et al.* (2008) Apoptotic cell-derived sphingosine-1-phosphate promotes HuR-dependent cyclooxygenase-2 mRNA stabilization and protein expression. *J Immunol*, **180**, 1239-48.

141. Jalving, M., *et al.* (2005) Review article: the potential of combinational regimen with non-steroidal anti-inflammatory drugs in the chemoprevention of colorectal cancer. *Aliment Pharmacol Ther*, **21**, 321-39.
142. Shi, S., *et al.* (2012) Combinational therapy: new hope for pancreatic cancer? *Cancer Lett*, **317**, 127-35.
143. Michael, M.S., *et al.* (2003) Inhibition of cyclooxygenase-2 and activation of peroxisome proliferator-activated receptor-gamma synergistically induces apoptosis and inhibits growth of human breast cancer cells. *Int J Mol Med*, **11**, 733-6.
144. Grosch, S., *et al.* (2006) Cyclooxygenase-2 (COX-2)-independent anticarcinogenic effects of selective COX-2 inhibitors. *J Natl Cancer Inst*, **98**, 736-47.
145. Kreuzaler, P., *et al.* (2012) Killing a cancer: what are the alternatives? *Nat Rev Cancer*, **12**, 411-24.
146. Dong, K., *et al.* (2011) Targeting death receptor induced apoptosis and necroptosis: a novel therapeutic strategy to prevent neuronal damage in retinal detachment. *Med Hypotheses*, **77**, 144-6.
147. Sakata, D., *et al.* (2010) Prostaglandin E2, an immunoactivator. *J Pharmacol Sci*, **112**, 1-5.
148. Yao, C., *et al.* (2009) Prostaglandin E2-EP4 signaling promotes immune inflammation through Th1 cell differentiation and Th17 cell expansion. *Nat Med*, **15**, 633-40.
149. Berglind, H., *et al.* (2008) Analysis of p53 mutation status in human cancer cell lines: a paradigm for cell line cross-contamination. *Cancer Biol Ther*, **7**, 699-708.
150. Han, J.A., *et al.* (2002) P53-mediated induction of Cox-2 counteracts p53- or genotoxic stress-induced apoptosis. *EMBO J*, **21**, 5635-44.
151. Qin, C., *et al.* (2002) Estrogen up-regulation of p53 gene expression in MCF-7 breast cancer cells is mediated by calmodulin kinase IV-dependent activation of a nuclear factor kappaB/CCAAT-binding transcription factor-1 complex. *Mol Endocrinol*, **16**, 1793-809.
152. Diaz-Munoz, M.D., *et al.* (2012) Involvement of PGE2 and cyclic AMP signaling pathway in the up-regulation of COX-2 and mPGES-1 expression in LPS -activated macrophages. *Biochem J*, **443**, 451-61.
153. Poloso, N.J., *et al.* (2013) PGE2 differentially regulates monocyte-derived dendritic cell cytokine responses depending on receptor usage (EP2/EP4). *Mol Immunol*, **54**, 284-95.
154. Nunes, J.A., *et al.* (1996) Signal transduction by CD28 costimulatory receptor on T cells. B7-1 and B7-2 regulation of tyrosine kinase adaptor molecules. *J Biol Chem*, **271**, 1591-8.
155. Leclerc, P., *et al.* (2013) Characterization of a human and murine mPGES-1 inhibitor and comparison to mPGES-1 genetic deletion in mouse models of inflammation. *Prostaglandins Other Lipid Mediat*, **107**, 26-34.
156. Monrad, S.U., *et al.* (2011) Genetic deletion of mPGES-1 abolishes PGE2 production in murine dendritic cells and alters the cytokine profile, but does not affect maturation or migration. *Prostaglandins Leukot Essent Fatty Acids*, **84**, 113-21.
157. Kubo, S., *et al.* (2004) E-prostanoid (EP)2/EP4 receptor-dependent maturation of human monocyte-derived dendritic cells and induction of helper T2 polarization. *J Pharmacol Exp Ther*, **309**, 1213-20.

158. Sa-Nunes, A., *et al.* (2007) Prostaglandin E2 is a major inhibitor of dendritic cell maturation and function in *Ixodes scapularis* saliva. *J Immunol*, **179**, 1497-505.
159. Bodor, J., *et al.* (2012) Cyclic AMP underpins suppression by regulatory T cells. *Eur J Immunol*, **42**, 1375-84.
160. Bosseto, M.C., *et al.* (2010) Hypoxia modulates phenotype, inflammatory response, and leishmanial infection of human dendritic cells. *APMIS*, **118**, 108-14.
161. Park, J., *et al.* (2012) Differential functional effects of biomaterials on dendritic cell maturation. *Acta Biomater*, **8**, 3606-17.
162. Gleisner, M.A., *et al.* (2011) Delivery of alloantigens via apoptotic cells generates dendritic cells with an immature tolerogenic phenotype. *Transplant Proc*, **43**, 2325-33.
163. Howe, L.R., *et al.* (2013) Genetic deletion of microsomal prostaglandin E synthase-1 suppresses mouse mammary tumor growth and angiogenesis. *Prostaglandins Other Lipid Mediat*, **106**, 99-105.
164. Kim, R., *et al.* (2006) Functional roles of immature dendritic cells in impaired immunity of solid tumour and their targeted strategies for provoking tumour immunity. *Clin Exp Immunol*, **146**, 189-96.
165. Vakkila, J., *et al.* (2004) Inflammation and necrosis promote tumour growth. *Nat Rev Immunol*, **4**, 641-8.
166. Yamazaki, T., *et al.* (2013) Defective immunogenic cell death of HMGB1-deficient tumors: compensatory therapy with TLR4 agonists. *Cell Death Differ*.
167. Kroemer, G., *et al.* (2013) Victories and deceptions in tumor immunology: Stimuvax. *Oncoimmunology*, **2**, e23687.
168. Wu, Y.L., *et al.* (2011) INSPIRE: A phase III study of the BLP25 liposome vaccine (L-BLP25) in Asian patients with unresectable stage III non-small cell lung cancer. *BMC Cancer*, **11**, 430.
169. Veltman, J.D., *et al.* (2010) COX-2 inhibition improves immunotherapy and is associated with decreased numbers of myeloid-derived suppressor cells in mesothelioma. Celecoxib influences MDSC function. *BMC Cancer*, **10**, 464.
170. Lee, S.Y., *et al.* (2009) The immune tolerance of cancer is mediated by IDO that is inhibited by COX-2 inhibitors through regulatory T cells. *J Immunother*, **32**, 22-8.
171. Catella-Lawson, F., *et al.* (2001) Cyclooxygenase inhibitors and the antiplatelet effects of aspirin. *N Engl J Med*, **345**, 1809-17.

8 Publications

1. **Sha W**, Brune B, Weigert A. The multi-faceted roles of prostaglandin E(2) in cancer-infiltrating mononuclear phagocyte biology. *Immunobiology* 2012, 217(12):1225-32.
2. Weigert A, Weichand B, Sekar D, **Sha W**, Hahn C, Mora J, Ley S, Essler S, Dehne N, Brune B. HIF-1alpha is a negative regulator of plasmacytoid DC development in vitro and in vivo. *Blood* 2012, 120(15):3001-6.
3. **Sha W**, Olesch C, Hanaka H, Radmark O, Weigert A, Brune B. Necrosis in DU145 prostate cancer spheroids induces COX-2/mPGES-1-derived PGE2 to promote tumor growth and to inhibit T cell activation. *Int J Cancer* 2013, 133(7):1578-88.
4. Milke L, Schulz K, Weigert A, **Sha W**, Schmid T, Brune B. Depletion of tristetraprolin in breast cancer cells increases interleukin-16 expression and promotes tumor infiltration with monocytes/macrophages. *Carcinogenesis* 2013, 34(4):850-7.
5. **Sha W**, Olesch C, Angioni C, Sha LK, Patrignani P, Jakobsson PJ, Grösch S, Geisslinger G, von Knethen A, Weigert A, Brune B. MPGES-1-derived PGE₂ suppresses CD80 expression on tumor-associated phagocytes to inhibit anti-tumor responses. *Carcinogenesis* (submitted).

9 Acknowledgements

I have met many wonderful people on my journey of developing into a scientist and the person I am today. Without their support I would not have been able to walk this path. It is to them that I owe my deepest gratitude:

Prof. Dr. B. Brüne for making things possible: He enabled me to start my PhD in the first place and helped me to mature as a scientist with his wisdom, knowledge, discipline and dedication. His excellent guidance and critical comments really set the high standard and kept me committed to the tasks we set for this study.

PD. Dr. A. Weigert for just everything he does: His often genius ideas and his positive mindset is a blessing for everyone in the laboratory. He motivated and inspired me in many frustrating situations and helped me to unravel dozens of unexpected and fascinating findings.

Prof. Dr. D. Steinhilber and Dr. B. Held for running FIRST and HKG and for giving me the opportunity to realize that working on a PhD thesis is so much more than just earning a title: The grad school allowed me to build a network of fellow scientists; many of them have become trusted and loyal friends over the past years. Working with them really motivated me to go beyond my limit and to perform better.

Everyone from the Institute of Biochemistry I and the natural science grad schools of the Goethe-University for supporting my work and creating the friendly environment I needed for prospering.

All my friends, known and new, for the inspiring, funny, motivating and just wonderful moments we shared together. Hard times in science are just less tormenting when I know that I can count on them.

Most of all, I want to thank my wife Lisa and our whole family to whom I dedicate my thesis, for their boundless love and everlasting support.

10 Curriculum Vitae

Name: Weixiao Sha
Date of birth: 20.03.1984
Place of birth: Beijing, PR China
Nationality: German
Marital status: Married
Address: Karlstrasse 36, 63263 Neu-Isenburg
Cell: (+49)157-30137575
Mail: sha.weixiao@gmail.com

2003 Abitur Karolinen Gymnasium, Frankenthal, Germany
2003 – 2004 Military service 10th Armored Division Sigmaringen, Germany
2004 – 2010 Diploma in Biomedical Chemistry, Johannes Gutenberg-University Mainz
2010 – 2013 Frankfurt International Research School for Translational Medicine (FIRST), Dr. Hans Kröner Graduate School (HKG) stipend
2010 – PhD Research student, Institute of Biochemistry I (Prof. Bernhard Brüne), Faculty of Medicine, Johann Wolfgang Goethe-University, Frankfurt am Main

11 Ehrenwörtliche Erklärung

Ich erkläre ehrenwörtlich, dass ich die dem Fachbereich Biologie, Chemie und Pharmazie der Johann Wolfgang Goethe-Universität Frankfurt am Main zur Promotionsprüfung eingereichte Arbeit mit dem Titel

“Formation of PGE₂ in the tumor microenvironment and its impact on tumorigenesis”

im Institut für Biochemie I – Pathobiochemie unter Betreuung und Anleitung von Prof. Dr. Bernhard Brüne ohne sonstige Hilfe selbst durchgeführt und bei der Abfassung der Arbeit keine anderen als die in der Dissertation angeführten Hilfsmittel benutzt habe.

Ich habe bisher an keiner in- oder ausländischen Universität ein Gesuch um Zulassung zur Promotion eingereicht. Die vorliegende Arbeit wurde bisher nicht als Dissertation eingereicht.

Teile der vorliegenden Arbeit wurden in den folgenden Publikationsorganen veröffentlicht:

Sha et al. Immunobiology 2012, 217(12):1225-32 (PMID: 22727331)

Sha et al. Int J Cancer 2013, 133(7):1578-88 (PMID: 23536473)

Sha et al. Carcinogenesis (submitted 11th Dec. 2013).

Frankfurt am Main, den